UNIVERSITY OF MANITOBA

REMODELING AND REGULATION OF CARDIAC COLLAGEN DURING THE DEVELOPMENT OF HEART FAILURE DUE TO MYOCARDIAL INFARCTION

A DISSERTATION SUBMITTED TO
THE FACULTY OF GRADUATE STUDIES
OF THE UNIVERSITY OF MANITOBA

IN PARTIAL FULFILLMENT OF THE REQUIREMENTS FOR THE

DEGREE OF
DOCTOR OF PHILOSOPHY

BY
HAISONG JU

DEPARTMENT OF PHYSIOLOGY
FACULTY OF MEDICINE

FEBRUARY 1998

National Library of Canada
Acquisitions and Bibliographic Services
395 Wellington Street
Ottawa ON K1A 0N4
Canada

Bibliothèque nationale du Canada
Acquisitions et services bibliographiques
395, rue Wellington
Ottawa ON K1A 0N4
Canada

Your file Votre référence

Our file Notre référence

The author has granted a non-exclusive licence allowing the National Library of Canada to reproduce, loan, distribute or sell copies of this thesis in microform, paper or electronic formats.

The author retains ownership of the copyright in this thesis. Neither the thesis nor substantial extracts from it may be printed or otherwise reproduced without the author's permission.

L'auteur a accordé une licence non exclusive permettant à la Bibliothèque nationale du Canada de reproduire, prêter, distribuer ou vendre des copies de cette thèse sous la forme de microfiche/film, de reproduction sur papier ou sur format électronique.

L'auteur conserve la propriété du droit d'auteur qui protège cette thèse. Ni la thèse ni des extraits substantiels de celle-ci ne doivent être imprimés ou autrement reproduits sans son autorisation.

0-612-31995-4

Canada

THE UNIVERSITY OF MANITOBA

FACULTY OF GRADUATE STUDIES

*****

COPYRIGHT PERMISSION PAGE

REMODELING AND REGULATION OF CARDIAC COLLAGEN DURING THE DEVELOPMENT OF HEART FAILURE DUE TO MYOCARDIAL INFARCTION

BY

HAISONG JU

A Thesis/Practicum submitted to the Faculty of Graduate Studies of The University of Manitoba in partial fulfillment of the requirements of the degree of

DOCTOR OF PHILOSOPHY

Haisong Ju ©1998

Permission has been granted to the Library of The University of Manitoba to lend or sell copies of this thesis/practicum, to the National Library of Canada to microfilm this thesis and to lend or sell copies of the film, and to Dissertations Abstracts International to publish an abstract of this thesis/practicum.

The author reserves other publication rights, and neither this thesis/practicum nor extensive extracts from it may be printed or otherwise reproduced without the author's written permission.

CONTENTS

ACKNOWLEDGMENTS

I would like to express my gratitude to those who have helped me to fulfill my Ph.D. program. I must first acknowledge my advisor Dr. Ian M.C. Dixon. I really appreciate his kind personality, dedication in science, and scientific perspective. His paternal care of my daily life and patient guidance of my English usage, computer skills and overall scientific training has strongly bolstered my enthusiasm in research and greatly sharpened my intellect throughout the years. The excellent opportunity and freedom of doing his type of research also stimulated my spirit and cemented myself confidence in science. Without his exceptional supervision and tender care, the accomplishment of this thesis would have been impossible.

Special thanks are offered to my advisory committee members, including Drs. N.S. Dhalla, P.K. Singal, and V. Panagia, for their guidance. Their critical comments as well as encouragement on my research greatly helped to keep me on the right track. Likewise, I would like to thank Drs. R.E. Beamish, A. Junaid, and E. Kardami for their generous help and friendship.

Many thanks should be given to all the members of my laboratory and my friends for their everlasting and solid support and sincere friendship. I have to admit that I have enjoyed and benefited very much from every minute of being with them both in science and in life. Among these smart people, special space should be given to: Tracy Scammell-La Fleur, Jianming Hao, Nicole L. Reid, Davinder S. Jassal, Paramjit S. Tappia, Xueliang Liu, Jingwei Wang, Xi Wang, Xiaobing Guo, Qiming Shao, Bradley W. Doble, Robert R. Fandrich, and David Wilson.

I wish to express my gratitude to University of Manitoba for providing me with a Graduate Fellowship and Manitoba Health Research Council for providing me with a studentship.

Finally, I dedicate this thesis to my wife, Shufang, who has devoted the deepest love in the world to me. Her understanding and support have been essential, as she is a constant well of wisdom, happiness and energy. My gratitude is bestowed upon my lovely son, Robert, whose first cries, toddling steps and baby talk have taught me what the life should be and how to meet its challenges. In totality, I feel like that I have been conferred a Ph.D. degree in life.

LIST OF FIGURES

LIST OF TABLES

LIST OF ABBREVIATIONS

ACE, angiotensin converting enzyme

Ang II, angiotensin II

ANP, atrial natriuretic peptide

AT_1 receptor, angiotensin II type I receptor

AT_2 receptor, angiotensin II type II receptor

BCA, bicinchoninic acid

CDK, cyclin-dependent kinase

CHF, congestive heart failure

DAG, diacylglycerol

DEPC, diethyl pyrocarbonate

$\pm dP/dt_{max}$, the maximum rate of isovolumic pressure development or decay

ECM, extracellular matrix

ELISA, enzyme-linked immunoabsorbant assay

ET, endothelin

GAPDH, glyceraldehyde-3-phosphate dehydrogenase

HRP, horseradish peroxidase

IP_3, inositol 1,4,5-trisphosphate

Jak, Janus kinase

LV, left ventricular/left ventricle

LVEDP, left ventricular end-diastolic pressure

LVSP, left ventricular systolic pressure

β-MHC, β-myosin heavy chain

MI, myocardial infarction

MMP, matrix metalloproteinase

MOPS, 3-[N-morpholino]propanesulfonic acid

PBS, phosphate-buffered saline

PIP_2, phosphatidylinositol 4, 5-bisphosphate

PKC, protein kinase C

PLC-β, phospholipase C-β

PVDF, polyvinylidene difluoride

RAS, renin angiotensin system

RV, right ventricular/right ventricle

STAT, signal transducers and activators of transcription

TβRI, TGF-β receptor type I

TβRII, TGF-β receptor type II

TBS-T, Tris-buffered saline with 0.1% Tween-20

TGF-β, transforming growth factor-β

TIMP, tissue inhibitor of metalloproteinase

t-PA, tissue plasminogen activator

u-PA, urokinase plasminogen activator

VSMC, vascular smooth muscle cell

ABSTRACT

Cardiac fibrosis may contribute to the development of congestive heart failure (CHF) due to myocardial infarction (MI). In order to investigate cardiac collagen remodeling in post-MI hearts, we addressed the time-dependent collagen remodeling at the levels of mRNA and protein in noninfarcted left ventricular (LV) and right ventricular (RV) myocardium after ligation of the left coronary artery in rats. We also assessed the activity of different myocardial matrix metalloproteinases (MMPs) using zymography to study collagen degradation. Furthermore, we assessed the passive stiffness of RV from experimental hearts. We observed that the mRNA abundance of types I and III collagen was increased 3 days after MI in both viable LV and RV tissues, peaked at 1 and 2 weeks, and maintained at relatively high levels in 4 and 8 weeks post-MI hearts. These findings correlated with increased immunofluorescent staining patterns of different collagen species in the surviving cardiac interstitium from 2, 4, and 8 weeks experimental groups. RV stiffness was significantly increased in the 8 weeks experimental group when compared to control values. MMP-2 activity was increased in viable LV at 2, 4 and 8 weeks and at 2 weeks in the experimental RV when compared to control values, whereas MMP-1 activity was increased only in scar tissue. These results indicated that cardiac collagen remodeling is characterized by increased collagen synthesis and this alteration is sustained during the chronic phase of MI.

To investigate the role of Ang II in cardiac collagen synthesis, MI rats were treated with losartan (15 mg/kg/day), an Ang II type I (AT_1) receptor blocker. Immunofluorescent staining and 4-hydroxyproline assays confirmed that losartan treatment attenuates fibrosis in experimental hearts. Northern analysis revealed that

losartan treatment of 1, 2, or 4 week experimental groups had no effect on collagen mRNA abundance compared to untreated post-MI rats. On the other hand, immunoreactive prolyl 4-hydroxlase concentration was significantly decreased in the post-MI group treated with losartan. Determination of cardiac mass and cardiac function revealed that losartan treatment attenuated cardiac hypertrophy and improved LV function in experimental animals. These results indicated that the attenuation of cardiac fibrosis by losartan in post-MI heart may be effected at the suppression of prolyl 4-hydroxylase.

We investigated $G_{q\alpha}$ at protein and mRNA abundance levels in myocardium subsequent to MI (8 weeks). To investigate the functional significance of $G_{q\alpha}$ in post-MI hearts, we examined the levels of phospholipase-β (PLC-β) proteins and PLC-β activity, inositol 1,4,5-trisphosphate (IP_3) accumulation and protein kinase C (PKC) activity in experimental hearts. Immunofluorescent staining indicated elevated $G_{q\alpha}$ expression in the scar and border tissues. Western analysis also confirmed significant upregulation of $G_{q\alpha}$ proteins in these regions compared to controls. Northern analysis revealed that the ratios of $G_{q\alpha}$/GAPDH mRNA abundance in both scar and viable tissues from experimental hearts were significantly increased compared to controls. Increased expression of PLC-β1 and PLC-β3 proteins was apparent in the scar and viable tissues after MI compared to controls, and was associated with increased PLC-β1 activity in experimental hearts. Furthermore, cardiac IP_3 and total PKC activity were significantly increased in the border and scar tissues when compared to control values. Upregulation of the $G_{q\alpha}$/PLC-β pathway was observed in the viable, border and scar tissues in post-MI hearts. $G_{q\alpha}$ and PLC-β may play important roles in scar remodeling as well as in cardiac

hypertrophy and the developing fibrosis of the surviving tissue in post-MI rat heart. It is suggested that the $G_{q\alpha}$/PLC-β pathway may provide a possible novel target for altering post infarct remodeling.

The alteration and significance of transforming growth factor-β (TGF-β) signaling in heart failure after MI remain unexplored. Cardiac TGF-β1, TGF-β receptor type I (TβRI) and type II (TβRII), and Smad protein (downstream effectors) levels were investigated in the chronic phase (8 weeks) of MI. Both TGF-β1 mRNA abundance and protein were significantly increased in scar and border tissues when compared to viable tissue and sham-operated rats. Increased active TGF-β1 was noted in viable and border tissues when compared to sham-operated animals. TβRI (53 kDa) protein was significantly reduced in the scar, while the 75 kDa and 110 kDa isoforms of TβRII was unchanged and significantly increased in scar samples, respectively. Cardiac Smad2 and 4 proteins were significantly increased in border and scar tissues compared to sham-operated rats. Immunofluorescent studies localized Smad protein accumulation in the nuclei of cells in scar tissue. Concentrations of TGF-β1-inducible cyclin-dependent kinase (CDK) inhibitors, p15 and p21 were increased in border and scar regions compared to control values. Increased active TGF-β1 with attendant elevation of Smad proteins in post-MI hearts suggests an involvement of this cytokine in ongoing remodeling of scar and viable regions. Increased p15 and p21 levels support the hypothesis that activation of the TGF-β pathway may lead to the inhibition of the cardiac fibroblast proliferation in the chronic phase of scar remodeling. Thus, pharmacological modulation of the TGF-β signaling pathway may provide novel targets for manipulating post-infarct remodeling.

Chapter 1. General Introduction and Statement of the Problem

MI results from occlusion of the coronary artery and is recognized as a major health issue in industrialized nations.[1] This is because of the high mortality of MI due to acute ischemic insult or subsequent heart failure. MI has been identified as one of the major causes of heart failure in North America.[2] MI results in complex time-dependent alterations of ventricular architecture involving both the infarcted and noninfarcted zones and these changes are collectively referred to as "ventricular remodeling".[3] After a large MI, ventricular remodeling is characterized by the development of cardiac hypertrophy, interstitial fibrosis of remnant myocardium (i.e. excessive deposition of collagen), as well as chamber dilatation and sphericalization.[2] As ventricular remodeling may profoundly affect ventricular function and is associated with the onset of heart failure, an understanding of the remodeling process and its regulation is crucial for the efficacious treatment of heart failure.[3,4] Recently, collagen remodeling after MI has attracted considerable attention, while the information directly addressing this issue is limited.[5-7] After MI, fibrosis occurs not only in the necrotic tissues (infarct zone), but also in the viable tissue (noninfarcted LV region) and in RV.[8-10] It has been well documented that cardiac collagen is an important determining factor for passive cardiac stiffness, and that excessive collagen accumulation may contribute to increased myocardial stiffness.[11-15] The accumulation of interstitial collagen also leads to disruption of electrical coupling among myocytes, reduced capillary density, and increased diffusion distance for oxygen, which may lead to increase of metabolic stress or even overt ischemia with increased incidence of myocyte apoptosis.[16-18] Thus the occurrence of cardiac fibrosis in viable myocardium after MI may result in an impairment of cardiac function leading to the development of CHF.

Although both clinical and experimental studies have documented the occurrence of cardiac fibrosis after MI, there is only limited information regarding to the regulation of cardiac collagen remodeling after MI.[6] Thus an understanding of the molecular mechanisms that underlie cardiac fibrosis and scar remodeling is warranted. As the net collagen concentration depends on the dynamic balance of collagen synthesis and degradation, we have undertaken an effort to investigate collagen synthesis at mRNA and posttranslational levels as well as collagen removal in post-MI rat heart. It is also known that angiotensin II (Ang II) and transforming growth factor-β (TGF-β) have regulatory effects on the proliferation of fibroblasts and collagen metabolism *in vitro*.[19-22] However, very limited information is available regarding to the regulatory role of Ang II and TGF-β in cardiac fibrosis and scar remodeling after MI. The effect of Ang II in collagen remodeling was investigated at protein, mRNA, and posttranslational levels by administration of an AT_1 receptor antagonist (losartan) in post-MI rats. The major signaling pathway mediated by Ang II occurs via the activation of $G_{q\alpha}$ protein.[23,24] Activated $G_{q\alpha}$ is known to stimulate phospholipase C-β (PLC-β) which will produce inositol 1,4,5-trisphosphate (IP_3), and subsequent activate protein kinase C (PKC).[25] However, the status of signaling mediated by AT_1 receptor in post-MI hearts remains unexplored, and specific information addressing the status of $G_{q\alpha}$ expression and function in heart failure is currently lacking. We hypothesize that $G_{q\alpha}$ is upregulated in post-MI hearts and is involved in the ongoing alteration of scar tissue as well as in the development of myocyte hypertrophy and fibrosis of surviving myocardium. To test this hypothesis, we investigated myocardial $G_{q\alpha}$ by protein quantification and localization as well as by detection of mRNA abundance in the ventricular myocardium remote to the site of infarction as well as in border and scar regions of failing hearts subsequent to MI. To examine the functional significance of $G_{q\alpha}$ in post-

MI hearts, we addressed the protein level and activity of PLC-β (downstream effector), IP_3 accumulation and PKC activity in experimental hearts.

TGF-β has been implicated in many fibrotic disorders including glomerulonephritis, cirrhosis, lung fibrosis and vascular restenosis.[26] As yet there is only limited information regarding the role of TGF-β in cardiac fibrosis and hypertrophy.[27-29] Recently, a major advance in TGF-β signaling has been the identification of Smad proteins as downstream effectors of TGF-β.[30] On activation, these proteins translocate to nuclei and initiate gene transcription in response to TGF-β binding to its receptors, designated as type I (TβRI) and type II (TβRII).[31,32] The alteration and significance of cardiac TβRI, TβRII, and Smad proteins in heart failure post-MI is unknown. We hypothesize that TGF-β is involved in the development of fibrosis of surviving myocardium and in the continued remodeling of scar tissue in post-MI hearts. To test our hypothesis, we investigated cardiac TGF-β1, TβRI (ALK-5), and TβRII protein levels and localization in noninfarcted left ventricular (LV) tissue from sham animals, viable LV remote to infarct, border and scar tissues of failing hearts subsequent to MI. In order to examine the functional significance of altered TGF-β1 in post-MI hearts, we also addressed the expression patterns of the downstream effectors of TGF-β receptors, including Smad proteins and cyclin-dependent kinase (CDK) inhibitors p15 and p21, in control myocardium, noninfarcted tissue, scar and border tissue.

Chapter 2. Review of Literature

2.1. Extracellular Matrix

A substantial amount of spatial volume in any given organ is occupied by the extracellular matrix (ECM) which is defined as a complex network of macromolecules that serve to form physical connections among major constitutive cells. In most organs, major ECM macromolecules are synthesized and secreted by fibroblasts.[33] Major ECM components include **i)** fibrous proteins i.e., structural collagens and elastin as well as cell adhesive or anti-adhesive molecules including fibronectin, vitronectin, laminin; and **ii)** proteoglycans, a class of molecules with a small core protein linked to array of extensive glycosaminoglycans side-chains.[33,34] In the heart, nonmyocytes reside in the cardiac interstitium and occupy ~25% of the total tissue space but may account for the two-thirds of the total cell population.[35] Cardiac fibroblasts, endothelial cells and vascular smooth muscle cells (VSMCs) are the major cardiac nonmyocytes. Fibroblasts are the predominant cell type among nonmyocytes.[36] As collagen is a determinant factor of myocardial structure and function, the structure and function of cardiac collagen, its synthesis and degradation, collagen remodeling and regulation as well as the possible role of collagen in the development of heart failure is reviewed.

2.2. Structure and Function of Cardiac Collagen

2.2.1. Collagen subtypes and structure

A total of five different types of collagen are present in heart tissue, including collagen types I, III, IV, V and VI.[37,38] Cardiac collagen is a relatively insoluble macromolecules when compared to that isolated from other tissues. This attribute is likely due to abundant inter- and intramolecular covalent cross-links among mature collagen molecules.[39] Collagen type I is a heterotrimer containing two α_1 (I) and one α_2 (I) chains;

while collagen type III is a homotrimer of three α_1 (III) chains. Fibrillar collagen types I and III are the most abundant forms of cardiac collagen and represent more than 90% of this class of proteins within the myocardium.[40] Fibrillar collagen type I normally aggregates into relatively thick fibers (50-150 nm in diameter), whereas type III collagen aggregates to form fine network in the interstitium.[36,37] Type I collagen has the approximate tensile strength of steel and accounts for ~75% of total collagen in the adult myocardium; type III collagen is more resilient than type I collagen.[35]

2.2.2. The functions of cardiac collagen

Experimental evidence provides support for the hypothesis that cardiac collagen plays a vital role in the maintenance of myocardial structure and in beat-to-beat cardiac function.[41] Collagen aggregates form fibrous tethers which serve to support and align cardiac myocytes, blood vessels, and lymphatic vessels and thereby maintain myocardial stiffness as well as the geometry of ventricular chambers.[41] Fibrillar collagen is also known to contribute to the transduction of force generated by myocytes, prevention of muscle fiber slippage, as well as protection of myocytes from overstretching.[41] As the ventricular walls of the heart are continuously subjected to repeated mechanical stresses, structural rigidity is required. It is known that loss of cardiac collagen in ischemic region such as after acute infarction is associated with rupturing of ventricular walls. Collagen fibers have been suggested to store energy during systole (under compression), and thereby plays a role in the relengthening of myocytes during the relaxation and early filling phases of the cardiac cycle.[42] Collagen struts attach to specific sites immediately lateral to the Z band where they bind integrin proteins on the sarcolemma membrane of myocytes.[43] Integrin links to the contractile apparatus through several cytoskeletal proteins such as talin, vinculin, and α-actinin.[44] Finally, collagen types IV, V and VI are present in relatively low abundance and together make up ~10% of total cardiac collagen component.[37] Collagen type IV is located in the basement membrane where it forms a crucial structural component and plays a regulatory role in molecular transport and cell adhesion.[37,40] Collagen type V is now known

to co-exist with type IV in the basement membrane and is interspersed with types I and III in the cardiac interstitium.[37] Type VI collagen is found in the cardiac interstitium where it is associated with other fibrillar collagen types and appears to coat the surface of collagen fibers.[37]

2.3. Collagen Synthesis and Degradation

2.3.1. Synthesis of collagen

Collagen synthesis involves a number of transcriptional and posttranslational steps.[45] Individual collagen polypeptide chains are synthesized on membrane-bound ribosomes and transported into the lumen of the rough endoplasmic reticulum (ER) as larger precursors, referred to as pro-α chains.[34] Selected proline and lysine residues are hydroxylated by prolyl 4-hydroxylase and lysyl hydroxylase, respectively, to form hydroxyproline and hydroxylysine in ER lumen.[34] Hydroxylation of the pro-α chain facilitates the formation of stable triple-stranded helical procollagen molecules and their subsequent secretion. Under-hydroxylated procollagen is highly unstable, is unable to form triple helices, and is therefore susceptible to degradation inside the cell.[37] Mature collagen molecules are produced by the cleavage of propeptides by specific proteolytic enzymes. Collagen molecules undergo further assembly in the extracellular space to form much larger collagen fibrils. These fibrils are strengthened by covalent cross-linking among lysine residues of constituent collagen molecules and will aggregate to form collagen fiber.[37] Posttranslational regulation of collagen is an important mechanism for myocardium collagen remodeling.[46,47]

2.3.2. Degradation and removal of collagen

Net collagen concentration in the heart depends upon a balance between collagen synthesis and collagen degradation. ECM components, including collagens, may be degraded by matrix metalloproteinases (MMPs) which are a family of Zn^{2+}- and Ca^{2+}-dependent enzymes;[48] at least fifteen secreted MMPs and membrane type MMPs (MT-MMP) have been identified.[49] These proteins have been classified into two groups based on

substrate preference and structural features and were listed as follow: classic type including collagenase (MMP-1, MMP-8, MMP-13), stromelysins (MMP-3, MMP-7 and MMP-10), gelatinases (MMP-2 and MMP-9), elastase (MMP-12), and novel type including (MMP-11, MT-MMP1-3 or MMP-14).[50] For example, rate-limiting degradation of mature fibrillar collagen types I and III may be initiated by MMP-1, MMP-8, and MMP-13, whereas MMP-2 may degrade collagen type IV. Stromelysins catalyze the disruption of various ECM members such as fibronectin, laminin, elastin, proteoglycans, collagen types III and IV.[51] The activity of MMP is regulated at three levels: transcription, activation of the latent proenzyme and inhibition of proteolytic activity.[51] Under normal physiological conditions, MMPs are present in a latent form and they can be activated by serine proteinases such as plasmin and urokinase plasminogen activator (u-PA).[51] A family of naturally occurring specific factors, namely tissue inhibitors of metalloproteinase (TIMPs), tightly controls the activation of MMPs. Four members of this family have been identified and referred to as TIMP-1, TIMP-2, TIMP-3, and TIMP-4.[51,52] TIMP-1 has relatively high affinity for the active forms of collagenase, stromelysin and gelatinase; the noncovalent binding TIMP-1 to the target MMPs is irreversible. Of the various MMPs and their inhibitor, it is known that MMP-1, MMP-2, MMP-9, TIMP-1, TIMP-3, and TIMP-4 are expressed in heart.[52-56] TIMP-4 has been found to be highly expressed in heart indicating a role in cardiac collagen remodeling.[52,57] The precise role and regulation of MMPs and TIMPs in myocardium under physiological and pathological condition is far from clear.

2.4. Collagen Remodeling and Heart Failure after Myocardial Infarction

The remodeling of noninfarcted cardiac tissue includes the appearance of ventricular hypertrophy and interstitial fibrosis and loss of normal ventricular geometry followed by the development of heart failure. The role of collagen in the remodeling of both scar and viable cardiac tissues after MI has been increasingly recognize as an important factor in heart failure during recent years.[6,7,58]

2.4.1. Early remodeling of collagen after myocardial infarction

In the rat model of MI, total collagen content in the infarct zone is known to decrease by 25% - 50% one to three h after the induction of MI when compared with noninfarcted myocardium.[59] Results from a electronic microscopic study indicate that collagen fibrils and elastic fibers are rapidly broken down in acute ischemic conditions.[60] Cardiac interstitial collagenase, elastase, and cathepsin G activities are significantly increased in infarcted tissue compared with noninfarcted control values, and these findings suggest that the increased activities of collagenase and other neutral proteinases may be responsible for these changes.[55,59,61] It is held that the acute loss of cardiac matrix may lead to myocyte slippage causing thinning and dilatation of the necrotic region (infarct expansion), and even rupture of the myocardium.[11,62] Infarct expansion may impair heart function by increase of ventricular volume in the early post-MI phase thereby reducing the normal effectiveness of the cardiac functional mechanism and a time-dependent secondary changes in the noninfarcted tissue.[2,3]

2.4.2. The chronic phase of collagen remodeling after myocardial infarction

Cardiac interstitial fibrosis, present in chronic phase of MI, is becoming recognized as a hallmark of this pathological state. Collagen deposition in the infarct zone is progressively increased from one to six weeks after the induction of MI.[10] Cardiac collagen is also found to be increased in the myocardium from patients with coronary artery disease.[63,64] Results from our laboratory indicate that total collagen concentration in viable LV and RV, as determined by 4-hydroxyproline measurement, was increased at 2, 4, and 8 weeks after MI.[8] Moreover, others have shown that the mRNA abundances of collagen types I, III, and IV, as well as fibronectin are all increased in viable myocardium after MI.[58,65] It is known that the stability and functionality of collagen are dependent not only on the total

amount of collagen but also on the degree of covalent cross-linkage and organization among fibrils. A recent description of the degree of cross-linking of collagen fibrils as assessed by hydroxylysylpyridinoline (HP) assay, indicates that cross-linkage was increased in viable free wall, but was unchanged in cardiac septum after infarction.[66] HP is the major lysine aldehyde-derived, non-reducible collagen cross-linkage in myocardium and the concentration of trivalent HP is directly proportional to the tensile strength of constitutive collagen.[67]

It has been well documented that cardiac collagen is an important determinant factor influencing cardiac muscle passive stiffness and that excessive collagen accumulation may contribute to abnormal (increased) myocardial stiffness.[11-14] Further work has revealed that increased myocardial stiffness may also be a consequence of an enhanced collagen cross-linking.[68] Increased stiffness was found in papillary muscle from post-MI hearts and depression of normal cardiac contractility was associated with an increase in myocardial collagen content.[15] The accumulation of collagen proteins may also leads to morphologic and functional separation of myocytes.[16] Enlarged interstitium due to excessive deposition of collagen results in the inhibition of electrical coupling of these myocytes, as well as increased diffusion distance for oxygen and all metabolic substrates.[16,17] Recent study found that the apoptotic cells are localized in collagen-encased myocytes in cardiac tissue bordering the scar.[18] This result indicate that cardiac fibrosis may contribute to the development of heart failure by the loss of myocytes through apoptotic mechanism.[18] Thus cardiac fibrosis in post-MI may result in the development of CHF through variety aforementioned mechanisms.

Recent studies have shown that MMP-1, MMP-2 and TIMP-1 are co-expressed in heart tissue.[53] The expression of these proteins in myocardium has been localized to both

cardiac fibroblasts and endothelial cells.[69] The activation of MMP plays an important role in collagen remodeling in both coronary artery disease and idiopathic dilated cardiomyopathy in humans.[70-72] Increased MMPs activities may then lead to myocyte slippage and misalignment within the myocardium, resulting in abnormalities in force production. These data support the hypothesis that abnormal turnover of collagen mediated by the increased MMPs activities may contribute to dilatation of the ventricular wall leading to the development of heart failure.

2.5. Angiotensin II in the Heart

2.5.1. RAS in cardiovascular system

Renin angiotensin system (RAS) components include renin, angiotensinogen, angiotensin converting enzyme (ACE) as well as angiotensin I (Ang I) and Ang II. Classically, the liver is a major source of angiotensinogen, which is a large plasma protein and is the only known natural substrate of renin (produced by the juxtaglomerular apparatus of the kidney).[73] Renin cleaves angiotensinogen to release the Ang I decapeptide, and this inactive precursor is immediately converted to active Ang II (an octapeptide) by ACE. ACE is a well characterized protein, and is widely acknowledged to be synthesized by endothelial cells lining the vascular system. Ang II also may be produced by ACE-independent pathway in cardiovascular system. For example, Ang II can be released by directly cleavage of angiotensinogen and AI by tissue plasminogen activator (t-PA), cathepsin G, tonin, and elastase in the vessel wall or from AI by cardiac chymase.[74] During the past several years, the existence of a local or tissue RAS system in cardiovascular system has been acknowledged, and has gained considerable attention.[75,76] This finding is supported by evidence indicating that most of components of the RAS are synthesized in cardiovascular

tissues.[76] However, the question as to whether renin is synthesized by cardiac and extrarenal vascular tissues remains controversial.[77] For the purpose of this discussion, local cardiac RAS is defined by the ability of the heart to express most RAS components leading to generation of Ang II.[75] It has since been demonstrated that Ang II is generated and released by cardiac myocytes and cardiac fibroblasts.[78,79] As the heart may use circulating renin for *in situ* synthesis of Ang II, the cardiac synthesis of this component may not be crucial for local generation of Ang II.[80] That Ang I and Ang II levels are > 100-fold higher in interstitial fluid than in plasma strongly supports the hypothesis emphasizing the role of local production in cardiac myocytes and fibroblasts.[81] Unlike the half-life of ^{125}I-Ang II in the heart *in vivo* is approximately 15 minutes, $t_{1/2}$ of Ang II in the circulation is only 30 seconds.[82] Thus the accumulation and compartmentalization of Ang II in myocardium will prevent its rapid degradation. Whether generated locally or not, Ang II may influence the myocardium in both direct and indirect manner. The direct actions of Ang II on the cardiovascular system include potent vasoconstriction, positive cardiac inotropism and positive cardiac chronotropism.[83] Indirect actions of Ang II on the heart include increasing cardiac load due to activation of the sympathetic system, and stimulation of aldosterone synthesis.[83]

2.5.2. Ang II receptors in myocardium

Cellular responses induced by Ang II are dependent upon the balanced activation of different Ang II receptors. Biochemical, pharmacological and functional studies have revealed the presence of two main subgroups which are further divided into multiple receptor subtypes.[84] Studies on binding affinities for plasma membrane receptors to nonpeptide antagonists such as losartan and PD123177 have defined the existence of AT_1 and AT_2 receptors, respectively.[85-87] To date, the majority of known physiological functions

mediated by Ang II within the cardiovascular system are carried out by Ang II binding to the AT_1 receptor.[88] The AT_1 receptor is a "typical" seven transmembrane domain membrane receptor protein. The AT_1 group of Ang II receptors is further subdivided into AT_{1A} and AT_{1B} classes.[84] Among them, the AT_{1A} and AT_{1B} isoforms contain 18-22 different amino acids yet maintain similar binding profiles for Ang II and nonpeptide antagonists (including losartan) as well as peptide AT_1 receptor antagonists.[84,88] The AT_{1A} subtype is localized mainly in vascular smooth muscle cells, hypothalamic tissue, lung, kidney, and adrenal tissues.[84,89] In the cardiovascular system, the AT_{1A} receptor is constitutively expressed in all developmental stages.[90] The AT_{1B} receptor has been described in the zona glomerulosa of the adrenal medulla, uterine, anterior pituitary, and renal tissues.[84,89] Recent work has shown that the AT_{1B} receptor contributes to the regulation of blood pressure in AT_{1A} receptor-deficient mice.[91] In rat heart, both AT_1 and AT_2 receptors density are roughly equal based on binding assay.[92] On the other hand, the ratio of AT_1 to AT_2 receptors in human heart (including myocytes and nonmyocytes) remains controversial.[93,94] In general, both neonatal and adult cardiac fibroblasts are characterized by the presence of predominant of AT_1 receptor with very low levels of the AT_2 receptor.[22,95]

Unlike the AT_1 receptor, AT_2 receptor does not undergo ligand-mediated endocytosis upon Ang II stimulation.[96] In spite of the intense scrutiny paid to the investigation of the function of the AT_2 receptor, our understanding of the precise role of this receptor in the cardiovascular system is far from clear. Nonetheless, some lines of evidence point to multiple putative functions in various tissues. These functions include i) mediation of apoptosis in PC12W and R3T3 cells;[97] ii) the inhibition of cellular proliferation in coronary endothelial cells;[98] iii) an antiproliferative effect on VSMCs in neointima after vascular injury;[99] and iv) maintenance of normal cardiovascular and central nervous system

function.[100,101] In view of some of these findings, it has been suggested that AT_2 receptor actions may oppose some of the functions mediated by the AT_1 receptor i.e., in blood pressure and growth regulation. Thus the overall observed response to Ang II in the whole organism is a balanced activation of AT_1 and AT_2 receptors.

2.5.3. Regulation of Ang II and its receptors

The mechanisms for release of Ang II in heart tissue and for the regulation of AT_1 and AT_2 receptors have been well examined during the past several years. Sadoshima *et al.* have clearly demonstrated that mechanical stretching of cardiac myocytes induces Ang II secretion from these cells *in vitro*, and have suggested that stretch-induced release of Ang II is an important mechanism for stimulating myocyte hypertrophy.[78] In cultured neonatal cardiac myocytes, elevation of Ang II receptor expression at transcriptional and posttranscriptional levels may also occur via mechanical stretching.[102] Mechanical stretching of cultured myocytes and pressure-overload *in vivo* result in the upregulation of AT_1 and AT_2 mRNA as well as receptor densities.[102,103] These studies strongly support the role of mechanical stretch i.e., abnormal hemodynamic cardiac loading, is pivotal in the development of cardiac hypertrophy. Furthermore, in canine model of RV chronic hypertrophy and failure induced by tricuspid valve avulsion and pulmonary artery constriction, a study has revealed that cardiac ACE, chymase, as well as AT_1 and AT_2 receptor mRNAs were subject to regulation by local mechanical stimuli.[104] Thus, mechanical stimulation may play an important role in the regulation of cardiac RAS. Several *in vitro* studies have shown that binding of Ang II to AT_1 receptor initiates internalization of receptor-ligand complex leading to receptor desensitization in different cell type including VSMC.[96,105-107] As only ~25% of the internalized receptors are recycled to the plasma membrane,[108] the degradation of internalized receptor may be the main mechanism by which

Ang II may regulate its receptor number. In addition, the AT_1 receptor is regulated through inhibition of transcription, whereas the AT_2 receptor is regulated mainly by decreasing its mRNA stability.[109]

2.5.4. Ang II mediated signal transduction

Ang II activation of the AT_1 receptor is characterized by the activation of a heterotrimeric of G_q proteins.[23,110-112] G_q is made up of three subunits, α, β, and γ subunits. It is suggested that the major function of α subnunit ($G_{q\alpha}$) is associated with the activation of phospholipase C-β (PLC-β),[25] whereas the βγ subunit may be involved in variety of functions including the activation of K^+ channel, PLC-β, phospholipase A_2 (PLA_2), phosphoinositide 3-kinase (PI3-kinase), and mitogen-activated protein (MAP) kinase.[113] Activation of G_q facilitates PLC-β mediated cleavage of phosphatidylinositol 4,5-bisphosphate (PIP_2) to IP_3 and 1,2 diacylglycerol (DAG). Both anti-PLC-β1 and anti-$G_{q\alpha}$ antibodies inhibit Ang II-induced inositol polyphosphate production, while anti-PLC-γ antibody had no effect. This result suggests that PLC-β is critical for Ang II signaling.[114] DAG binding is known to activate PKC which has been postulated to activate several downstream molecules including MAP kinase.[115,116] Experiments utilizing cultured cardiac myocytes and fibroblasts as well as isolated perfused hearts have demonstrated that AT_1 receptor activation is associated with stimulation of PLC-β, IP_3, and PKC.[117,118] Recent studies indicate that overexpression PKC targeted in mice heart is associated with the development of cardiac hypertrophy, fibrosis and heart failure.[119,120] These results support the hypothesis that PKC may be a causal factor in the development of heart failure. Activation of MAP kinase may play a pivotal role in coordinating external stimuli with gene

expression in the nuclei leading to cellular growth and differentiation including cardiac myocytes and fibroblasts.[24,121-124]

Ang II also has been shown to activate Src family kinase, a cytoplasmic tyrosine kinase in VSMC and myocytes.[125,126] Ang II has been shown to directly activate soluble tyrosine kinases (Janus kinase, Jak) in VSMC[127] and neonatal myocytes.[128] Activated Jak proteins may specifically phosphorylate a family of proteins known as signal transducers and activators of transcription (STAT) proteins. Ang II stimulation leads to the translocation of STAT proteins into the nucleus of VSMC.[129] Thus they play an essential role in Ang II-induced VSMC proliferation.[130] In cultured neonatal cardiac fibroblasts, Ang II induces STAT protein phosphorylation, translocation of STAT into the nucleus and the initiation of gene transcription.[131] Recent data provides evidence that the YIPP motif in AT_1 receptor physically associated with Jak2 and leads to the activation of Jak2.[132] From the preceding evidence, it is apparent that Ang II may rapidly stimulate the growth of myocardial cells involved in cardiac remodeling by the activation several signaling pathways. Further study is needed to elucidate the role of $G_{q\alpha}$ in AT_1 receptor mediated activation of cytosolic tyrosine kinase, STAT and cell cycle regulatory proteins.

The AT_2 receptor shares the seven transmembrane domain receptor protein configuration as AT_1 receptor, however has only 32% sequence homology with this protein.[133] AT_2 receptors are further subdivided into AT_{2A} and AT_{2B} classes based on distinct pharmacological characteristics which include differential binding of trimeric G proteins.[84] The signaling mediated by AT_2 receptor is not clear. Some recent evidences have been indicated that AT_2 receptors may bind to $G_i\alpha$ subunit in whole fetal tissue and VSMC.[134,135]

2.6. TGF-β in the Myocardium

TGF-β1 contributes to an array of biological functions including regulation of embryogenesis, cell differentiation and proliferation, wound repair, and synthesis of ECM component proteins as well as immunosuppression.[136,137] In mammals, three different TGF-β isoforms have been described including TGF-β1, TGF-β2, and TGF-β3; all seem to exert similar effects on target cells.[137] All three types of TGF-βs are found to be expressed in myocardium. It has been demonstrated that cardiac myocytes, endothelial cells, and fibroblasts may generate TGF-β.[138-142] However, the expression of cardiac TGF-β is mainly localized to cardiac fibroblasts.[143,144] Typically, TGF-β is secreted by the cell in biologically inactive or latent form due to binding with latency associated peptide (LAP).[145] Latent TGF-β can be activated by heating, extreme pH, urea, sodium dodecyl sulfate (SDS), plasmin, cathepsin D, and glycosidases, but the mode of physiological activation remains to be elucidated.[145] It is known that all active TGF-β isoforms are covalently linked homodimers of ~25 kDa subunit proteins. Once released from the latent complex, active TGF-β binds to ECM and accumulate in the interstitium.[136] This action may serve to protect TGF-β from degradation and might function as a long-term reservoir of this cytokine. While another ECM protein decorin has been shown to bind TGF-β and neutralize its activity.[146] Overexpression of decorin may lead to a marked inhibition of TGF-β1 induced fibrosis.[147]

2.7. TGF-β Receptors and Signaling

Affinity labeling has identified three major TGF-β receptors present in most mammalian systems and these are designated as type I (TβRI; mass 53 kDa); type II (TβRII; mass 70-100 kDa) and type III (a relatively large betaglycan of 200-400 kDa).[136] These receptor types have been localized in both cardiac myocytes and cardiac

fibroblasts.[19,148] Cardiac myocytes may have ~ 2000 TβRI binding sites and ~5000 TβRII binding sites *per* cell.[149,150] The effect of TGF-β are mediated through transmembrane TβRI and TβRII that display serine/threonine kinase activity.[32] TGF-β receptor activation occurs upon the binding of TGF-β to TβRII, which then recruits and phosphorylates TβRI.[151] Although most of aforementioned studies have been performed in epithelial cell, receptor dimerization and subsequent phosphorylation of TβRI in TGF-β signaling is known to exist in cardiac myocytes and fibroblasts.[152,153] Over the past year, it has been shown that Smad proteins serve as TGF-β signal transducers.[31,154] The phosphorylated TβRI is activated and phosphorylates the downstream target Smad2 (or Smad3) carboxy-terminal serine residues.[31,32] Phosphorylated Smad2 (and/or Smad3) then form(s) a heteromeric complex with Smad4 and this complex accumulates in the nucleus.[30,32,155,156] In the nucleus, Smad2-Smad4 complexes regulate transcriptional response by specifically interacting with DNA-binding proteins, such as forkhead active signal transducer-1 (FAST1) or by direct activation of specific genes.[157,158] Recent studies indicate that this TGF-β signaling may be inhibited by other Smad proteins such as Smad6 and Smad7.[159-161] Although it has been shown that overexpression of TβRIII results in increased responsiveness of vascular endothelial cells to TGF-β2 suggesting TβRIII may facilitate TGF-β binding,[162] the function of the TβRIII is far from clear.

2.8. Reciprocal Influence of Ang II and TGF-β in the Cardiovascular System

In vitro studies have shown that Ang II may stimulates TGF-β1 gene expression and increased TGF-β1 production in adult rat cardiac fibroblasts, myocytes, endothelial cells, and VSMCs.[139,141,142,163] For example, Chua *et al.* has demonstrated that Ang II-mediated induction of TGF-β1 occurs in a dose- and time-dependent manner in rat heart endothelial

cells.[142] Results from a different laboratory indicate that norepinephrine and Ang II may elevate steady-state levels of TGF-β1 and TGF-β2 mRNAs in VSMCs.[163] These studies have shown that the production of TGF-β induced by Ang II is PKC-dependent.[142,163] Furthermore, Ang II stimulation is associated with an accelerated rate of conversion of latent TGF-β1 to active form.[163] TGF-β may also play a role in the regulation of RAS; this hypothesis is supported by results which have shown that TGF-β1 and TGF-β2 stimulate the release of renin from cultured juxtaglomerular cells.[164] It is pointed out that these factors may exert positive feedback on each other in the failing myocardium and may take on an important causal role for the development of pathological hypertrophy involving multiple cell types.

2.9. Ang II in Myocyte Hypertrophy, Cardiac Fibrosis, and Heart Failure

2.9.1. Ang II and myocyte hypertrophy

Studies using neonatal cardiac myocytes have shown that Ang II causes an increase in protein synthesis via AT_1 receptor activation in these cells and along with the induction of "early" and "late" markers for myocyte hypertrophy.[117] This trophic effect was enhanced by the administration of AT_2 receptor antagonist suggesting AT_2 receptors may mediate an anti-growth effect in cardiac myocytes.[165,166] Ang II also increases protein synthesis in isolated adult heart via AT_1 receptor activation.[167] However, Ang II-mediated enhancement of protein synthesis in unloaded perfused adult rat heart may occur without preceding protooncogene expression.[167] Recent studies suggested that cardiac fibroblasts play an important role in Ang II-induced myocyte hypertrophy.[95,168,169] Specifically, Ang II failed to increase protein synthesis in cultured pure neonatal myocytes. However, the addition of

nonmyocyte to the myocyte culture is observed to restores Ang II-induced protein synthesis.[168] Similarly, although Ang II may stimulate protein synthesis in adult myocytes, this stimulation was significantly inhibited when bromodeoxyuridine was added to the culture to inhibit proliferation of fibroblasts.[169] Furthermore, the conditioned medium from untreated fibroblasts is seen to increase protein synthesis in both Ang II-treated and untreated myocytes.[95,169] These findings support the suggestion that the interaction between myocytes and fibroblasts for the development of myocyte hypertrophy may be triggered by Ang II.

In addition to the *in vitro* trophic effect of Ang II on myocytes, some lines of evidence also support Ang II's role in cardiac hypertrophy *in vivo*. It has been shown that chronic infusion of subpressor doses of Ang II caused ventricular hypertrophy in rat without alteration of blood pressure supporting a direct trophic effect of Ang II on the heart.[170] It is well documented that suppression of Ang II by administration of ACE inhibition is associated with the attenuation of cardiac hypertrophy in post-MI rat heart.[171-173] It has been postulated that the beneficial effect of ACE inhibitor in this regard may be caused in part by elevation of bradykinin level.[173] As it has been shown that kinins may inhibit the interstitial accumulation of collagen but do not modulate myocyte hypertrophy after MI, the inhibitory effects of ACE on myocyte hypertrophy has been suggested to be related only to the reduction of Ang II.[173] This suggestion is supported by recent findings in studies using AT_1 receptor antagonists that effectively inhibit cardiac hypertrophy without alteration of bradykinin post-MI rat.[171,174]

2.9.2. Ang II and cardiac fibrosis

Cardiac fibrosis occurs not only in the scar tissue but also the remnant or viable myocardium in post-MI heart. Recently from both *in vitro* and *in vivo* studies have

suggested that Ang II play crucial role in the development of cardiac fibrosis. In cardiac fibroblasts, the AT_1 receptor is known to participate in the induction of ECM protein component synthesis and gene expression mediating mitogenic responses.[21,117] The results from *in vivo* administration of Ang II to experimental animals have shown that Ang II is associated with increased cardiac collagen and fibronectin via AT_1 receptor activation.[175-178] Evidence from experimental studies undertaking the investigation of ACE inhibition and AT_1 blockade provide evidences that their use is associated with attenuation of cardiac fibroblast proliferation and deposition of cardiac collagen.[174,179,180] In the rat model of CHF after induction of MI (≥40% LV free wall), myocardial collagen concentration was significantly increased in viable tissue at 7, 14, 21 and 35 days post-MI.[179] These investigators found that this increase of cardiac collagen concentration was inhibited by treatment with ACE inhibitor captopril. In another study, ramipril (ACE inhibitor) is found to inhibit cardiac fibrosis without lowering blood pressure in spontaneous hypertensive rats compared to Wistar-Kyoto control.[181] These studies suggested that ACE inhibitor therapy may attenuate cardiac collagen, and that this inhibitory effects is independent of afterload reduction. The molecular mechanisms responsible for the attenuation of interstitial fibrosis by ACE inhibition remain obscure. It may be argued that ACE inhibitor treatment may potentiate an increase in the concentration of bradykinin in heart by inhibition of the kininase II enzyme (i.e. ACE).[173] In this respect, chronic treatment of infarcted hearts with AT_1 receptor antagonist is effective in partial attenuation of collagen protein deposition to a level comparable to that by ACE inhibition.[171] Thus, the efficacy of ACE inhibition may lie in the ability of these agents to suppress Ang II in the stimulation of cardiac fibroblasts and potentiate the inhibitory effect of bradykinin on collagen in post-MI heart. Therefore these

results support the hypothesis that Ang II may be a causal factor for the stimulation of cardiac fibrosis after MI in rat heart.

AT_1 receptor has been shown to be highly expressed in cardiac fibroblasts and myofibroblasts which appear at the site of infarct in 1 week post-MI hearts.[65,182] On the other hand, the expression of AT_2 receptor is known to be elevated in tissue undergoing wound repair, as well as in vascular injury and cardiac hypertrophy associated with MI,[99,183] however the role of this receptor in cardiac fibrosis is not clear. AT_1 (but not AT_2) receptor blockade is associated with attenuated cardiac collagen accumulation in post-MI heart suggesting that cardiac fibrosis is mediated by AT_1 receptor activation.[184] Furthermore, AT_2 receptor antagonism is seen to abolish the attenuation of cardiac collagen deposition mediated by AT_1 receptor antagonism, indicating that the effects of AT_1 blockade is mediated by activation of the AT_2 receptor.[184]

2.9.3. Ang II and heart failure

A number of studies support the hypothesis that Ang II is important in the onset of pathological myocyte hypertrophy, cardiac fibrosis and subsequent development of CHF in post-MI.[185] The results that support the activation of local and circulating RAS after MI are listed in Table 1.

Table 1. Activation of RAS after myocardial infarction.

First author	Species	Duration of Post-MI	Major findings
Hirsch, *et al.* (1991)[186]	rat	85 days	plasma renin and ACE activity (—), viable tissue ACE mRNA and activity (↑)
Yamagishi, *et al.* (1993)[187]	rat	21 days	Ang II in scar (↑), plasma renin and Ang II (—).
Lindpaintner, *et al.* (1993)[188]	rat	5 days	angiotensinogen and Ang I in viable tissue (↑).
Reiss, *et al.* (1993)[189]	rat	2-3 days	Cardiac Ang II receptor mRNA and density (↑).
Schunkert, *et al.* (1993)[190]	rat	6 weeks	plasma renin and Ang II (↑).
Johnston, *et al.* (1993)[191]	rat	1 month	Cardiac ACE activity (↑).
Huang, *et al.* (1994)[192]	rat	3 months	Plasma renin and ACE activity (↑), plasma angiotensinogen and Ang II (—).
Sun, *et al.* (1994)[193]	rat	2-8 weeks	ACE in viable and scar tissues (↑).
Nio, *et al.* (1995)[183]	rat	7 days	Cardiac AT_{1A} and AT_2 receptor mRNAs (↑), AT_1 and AT_2 density (↑), AT_{1B} mRNA (—).
Passier, *et al.* (1995)[194]	rat	7 and 90 days	ACE activity in infarcted tissues (↑).
Sun, *et al.* (1995)[182]	rat	1 and 4 weeks	Ang II receptor density in scar (↑).
Hokimoto, *et al.* (1996)[195]	human	years	ACE in scar and border tissues (↑).
Lefroy, *et al.* (1996)[196]	rat	7 days and 8 month	AT_1 receptor density in scar (↑).
Duncan, *et al.* (1997)[197]	rat	1-28 days	Plasma renin, ACE and Ang II (↑), RV Ang II (↑) at 7 days.

(—) No significant change, (↑) significantly increased.

Thus, ventricular remodeling in post-MI heart is now well established to be associated with the activation of RAS as shown in Table 1. Specifically, there is an increase in Ang II concentration in scar and a transient increase of Ang II in the viable tissue after MI.[187,197] Furthermore, Ang II receptor density is significantly elevated in both noninfarcted myocardium and scar.[182,183,196] For example, a 4.2-fold and 3.2-fold increase in AT_{1A} and AT_2 mRNA levels, respectively, are found in infarcted regions, while a ~2-fold increase in these mRNAs for both AT_{1a} and AT_2 receptors are observed in non-infarcted regions of the myocardium in the 7-day post MI group.[183] Similarly, cardiac Ang II and its receptors have been shown to be upregulated in rapid pacing induced heart failure in dogs and in hearts of hamster with genetic cardiomyopathy.[198,199]

The contribution of locally generated Ang II appears to be important for the development of cardiac hypertrophy and failure.[200,201] The local RAS may act in concert with circulating RAS, and the efficacy of ACE inhibitor therapy for patients with heart failure wherein the overall effect of treatment is due to inhibition of both systems. Administration of ACE inhibitors is well known to reduce afterload and preload in rat, and to cause an elevation of bradykinin, as well as to be associated with prolongation of life after MI in rat.[172,202] In two large clinical studies, long-term ACE inhibitor therapy for patients with heart failure after MI has been shown to reduce mortality regardless of the degree of LV dysfunction.[203,204] Nevertheless, ACE inhibition is unable to prevent the formation of Ang II by non-ACE pathways such as by the activation of chymase. For this reason, treatment with an AT_1 receptor antagonist such as losartan is an alternative for more complete suppression of Ang II in the cardiovascular system. Milavetz *et al.* have shown that the long-term use of losartan is efficacious in reducing mortality and in improving heart function in post-MI rats supporting the role of Ang II in the development of heart failure.[205]

Furthermore, in heart failure patients, treatment with losartan was associated with lower mortality than in those patients receiving captopril.[206] Taken together, these results strongly support the role of Ang II in the development of heart failure.

2.10. TGF-β in Cardiac Fibrosis, Myocyte Hypertrophy, and Heart Failure

In a variety of cells, TGF-β1 is known to stimulate ECM protein synthesis, including the synthesis of fibrillar collagen.[136,137] It has been demonstrated that TGF-β1 is involved in many fibrotic disorders including glomerulonephritis, cirrhosis, lung fibrosis and vascular restenosis.[26] As a potent stimulus for collagen synthesis, this cytokine may be important for the induction and development of cardiac fibrosis. In cultured cardiac fibroblasts, exposure to TGF-β1 is known to stimulate ECM production including collagen, fibronectin and proteoglycans.[20,207,208] Increased expression of TGF-β1 mRNA and protein has been demonstrated in myocytes bordering the acute infarct region in rat heart suggesting its association with the cardiac wound healing response.[27] Stimulation of cardiac collagen production by TGF-β1 indicates an beneficial to myocardial tissue repair at an early stage but this events may contribute to the development of heart failure in the late phase. It is suggested that TGF-β regulate not only cardiac collagen synthesis, but also collagen degradation by MMP. This supposition is supported by evidence that TGF-β1 attenuates the stimulatory effects of basic fibroblast growth factor (bFGF) on collagenase gene expression in human cardiac fibroblasts.[20] It has been reported that TGF-β1 elevates deposition of ECM by decreasing its degradation via inhibition of MMP-1 activity or by stimulating TIMP expression in cultured cells.[20] In addition to the direct effects of the TGF-β superfamily on MMPs and TIMPs, TGF-β1 may regulate the activation of MMPs through the inhibition of t-PA and stimulation of PA inhibitor (PAI-1) gene expression.[209] In summary, TGF-β

appears to stimulate the synthesis of ECM and inhibit its degradation and thus increasing the net production of ECM in various tissues.

It was well documented that TGF-β1 mediates growth inhibition on a variety of cell types by arresting the cell-cycle at the G1 phase,[210,211] which is known to be mediated by the induction of CDK inhibitors p15 and p21.[212,213] The effect of TGF-β1 on cardiac fibroblasts growth and differentiation is somewhat controversial and may depend on the developmental stage of these cells. Nevertheless, treatment of isolated neonatal fibroblasts with TGF-β is associated with stimulation of DNA synthesis;[214] while the pre-treatment of adult cardiac fibroblasts with TGF-β1 results in inhibition of bFGF-induced DNA synthesis.[19] Investigation from Dr. E. Kardami's laboratory using adult cardiac fibroblasts has shown that TGF-β1 may inhibit DNA synthesis in a dose-dependent manner in these cells (personal communication). Others have shown that TGF-β1 infusion into rat inhibits total DNA synthesis in myocardium.[215] As adult cardiac myocytes are known to be unable to proliferate, the inhibition of total cardiac DNA synthesis is believed due to its inhibition in nonmyocytes.

TGF-β1 is known to alter myocardial gene expression in cultured neonatal cardiac myocytes and the induction of β-myosin heavy chain (β-MHC), skeletal α-actin genes, smooth muscle α-actin, and atrial natriuretic peptide (ANP) as well as downregulation of α-MHC and sarcoplasmic reticular Ca^{2+} ATPase (SERCA2) mRNA expression have been noted.[28] These alterations mimic the changes that characteristically transpire during the development of cardiac hypertrophy and failure.[28] TGF-β1, TGF-β2 and, TGF-β3 have been shown stimulate protein synthesis in cultured neonatal cardiac myocytes in the absence of other mitogens and under serum-free conditions.[214,216] In contrast, Parker *et al.* has reported

that TGF-β1 had no effect on the growth of cultured cardiac myocytes.[217] Nevertheless, the increase of total protein synthesis in adult myocytes induced by isoproterenol was abolished by the application of a neutralizing antibody specific to TGF-β1, while the administration of TGF-β1 was associated with restoration of this hypertrophic response.[218] Unpublished work from Dr. E. Kardami's laboratory has indicated that TGF-β1 may stimulate DNA synthesis in cultured adult cardiac myocytes in a dose-dependent manner (personal communication). Although TGF-β does not induce *c-fos* expression in myocytes, it is known to potentiate norepinephrine and stretch-induced *c-fos* expression and protein synthesis in this cell.[219] On the other hand, the *in vivo* effects of TGF-β1 on cardiac myocytes are not clear. In this regard, increased cardiac expression of TGF-β mRNA is associated with the development of cardiac hypertrophy in a variety of experimental models.[220,221] In addition, TGF-β1 has been proposed to be involved in myocardial remodeling induced by hypertrophic stimuli via an autocrine/paracrine mechanism.[144,214] Recent studies have indicated that TGF-β1 protein is increased in the myocardium from pressure-overloaded experimental rat hearts and human idiopathic cardiomyopathy.[222,223] These data support the hypothesis that TGF-β may be involved in development of cardiac hypertrophy.

Chapter 3. Methods

3.1. Experimental Model

All experimental protocols for animal studies were approved by an appointed Animal Care Committee located at the University of Manitoba, following guidelines established by the Medical Research Council of Canada. MI was produced in male Sprague-Dawley rats (weighing 200-250 g) by surgical occlusion of the left coronary artery as described previously by Johns and Selye with minor modifications.[224-226] In short, after isofluorane anesthesia, the chest was opened by cutting the third and fourth ribs, and the heart was extruded through the intercostal space. The left coronary artery was ligated 2-3 mm from the origin with a suture (6-0 silk), and the heart was repositioned in the chest. Closure of the wound was accomplished using a purse-string suture. Throughout the operation, ventilation of the lungs was maintained by positive-pressure inhalation of 95% O_2 and 5% CO_2 mixed with isofluorane. Sham-operated animals were treated similarly, except that the coronary suture was not tied. The mortality of all animals operated upon in this fashion was about 45% within 48 h. The animals were sacrificed 3 days, 1 week, 2 weeks, 4 weeks, and 8 weeks after ligation and the hearts were stored in liquid nitrogen (-196°C) for further analysis. Animals from the losartan treatment study and 8 weeks groups underwent assessment of cardiac function, determination of infarct size, and subsequently the RV tissue, viable LV (non-infarcted LV free wall remote to infarct), border tissue (~ 2 mm viable tissue and ~2 mm scar tissue) and scar were used for further analysis.

In another series of experiments, post-operated animals were divided into three groups: Group 1: sham-operated animals, Group 2: MI animals, and Group 3: MI rats treated with losartan (15 mg/kg/day).[180] All losartan treatment regimens were initiated one day following coronary ligation by implanting an Alzet osmotic mini-pump (Alza Corporation,

La Jolla, CA; model 2002) and continued for 1, 2, and 4 weeks. To achieve the 4 weeks treatment, two 2-week duration osmotic mini-pumps were implanted consecutively. For comparative purposes, sham-operated controls (group 1) and MI animals were administered vehicle (0.9% saline) using the same method. After losartan or vehicle infusion, the animals underwent LV functional assessment and infarct size determination; then the viable LV and RV tissues were used to assess collagen protein profile, fibrillar collagen steady-state mRNA abundance, and immunoreactive prolyl 4-hydroxylase concentration.

3.2. Hemodynamic Measurements

Mean arterial blood pressure (MAP) and LV function of sham-operated control, MI, and MI treated with losartan groups were measured following induction of MI, as described previously.[224,227] Briefly, rats were anesthetized by intraperitoneal injection of a ketamine:xylazine mixture (100 mg/kg : 10 mg/kg). A micromanometer-tipped catheter (2-0) (Millar SPR-249) was inserted into the right carotid artery. The catheter was advanced into the aorta to determine MAP, and then further advanced to the LV chamber to record LV systolic pressure (LVSP), LV end-diastolic pressure (LVEDP), the maximum rate of isovolumic pressure development ($+dP/dt_{max}$) and the maximum rate of isovolumic pressure decay ($-dP/dt_{max}$). Hemodynamic data was computed instantaneously and displayed using a computer data acquisition workstation (Biopac, Harvard Apparatus Canada). In another series of experiments, LV function and blood pressure of control and MI animals were measured 8 weeks following induction of MI, as described previously.[224]

3.3. Infarct Size

Following heart function recordings, the LV from different groups were fixed by immersion in 10% formalin and embedded in paraffin. Six transverse slices were cut from the apex to the base. Serial sections (50 μm each) were made from each slice and mounted

and stained with Masson's trichrome. The percentage of infarcted LV was estimated after coronary ligation by planimetric techniques as described previously.[228]

3.4. Determination of Cardiac Total Collagen

Samples from different groups were ground into powder in liquid nitrogen. Then 100 mg (wet weight) cardiac tissue was dried to constant weight. Tissue samples were digested in 6 M HCl (0.12 ml/mg dry weight) for 16 h at 105°C. Hydroxyproline was measured according to the method of Chiariello *et al.*[229] A stock solution containing 40 mM of 4-hydroxyproline in 1 mM HCl was used as a standard. Collagen concentration was calculated by multiplying hydroxyproline levels by a factor of 7.46, assuming that interstitial collagen contains an average of 13.4 % hydroxyproline.[229] The data was expressed as μg collagen per mg dry tissue.

3.5. Immunofluorescence

Myocardium from sham-operated animals, viable LV remote to the infarct and RV, scar and border tissues from various times after induction of MI were immersed in OCT compound and stored frozen at -80°C. Serial cryostat sections of 7 μm thickness were mounted on gelatin-coated slides. A minimum of 6 sections from different regions of each group was processed. Sections were fixed in 4% paraformaldehyde for 15 min and then washed 6 x 5 min in 1x PBS to eliminate background caused by paraformaldehyde. Immunofluorescent staining was performed using the indirect immunofluorescent technique.[230] In brief, the tissue sections were incubated with primary antibodies overnight at 4°C. Sections were then washed 3 x 5 min in phosphate-buffered saline (PBS) and were incubated with biotinylated secondary antibody for 90 minutes at room temperature. Sections were washed 3 x 5 minutes and then incubated with FITC labeled or Texas Red labeled streptavidin. Finally, the slides were mounted and coverslipped. The results were recorded

by photography on Kodak T-MAX 400 black and white film. Quantification of resultant image data from immunofluorescent staining was performed using digital image analysis software (SigmaScan Pro).

The primary antibodies and secondary antibodies used in this study were listed. Primary antibodies are as follows: 1. Goat polyclonal anti-types I and III collagen were diluted in 1:100 (Southern Biotechnology Associates Inc, Alabama, USA). 2. Rabbit polyclonal anti-$G_{q\alpha}$ subunit (Calbiochem-Novabiochem International, San Diego, CA, USA) were diluted 1:500. 3. Polyclonal antibody against active TGF-β1 was diluted in 1:50 (Promaga Corporation, Madison, WI, USA). 4. Goat polyclonal against TβRI, TβRII, Smad2, 3 and 4 antibodies were diluted 1:50 to 1:100 (Santa Cruz Biotechnology Inc., Santa Cruz, CA, USA). Secondary antibodies are as follows: biotinylated anti-goat, anti-mouse, and anti-rabbit IgG were diluted 1:20 (Amersham Life Sciences Inc. Canada). Texas Red-labeled streptavidin and FITC-labeled streptavidin were diluted 1:20 (Amersham Life Sciences Inc. Canada). Texas Red-labeled streptavidin was used for the detection of collagen type I and FITC-labeled streptavidin was used for the detection of all other proteins. All antibodies were diluted in PBS containing 1% BSA and 0.1% sodium azide.

3.6. RNA Extraction

Total RNA was extracted from cardiac tissues by the procedure of Chomczynski and Sacchi as described previously.[231,232] Briefly, cardiac tissue was rapidly excised, the atria were removed, and the ventricular tissues was washed twice with a solution containing 10 mM 3-[N-morpholino]propanesulfonic acid (MOPS) and 10 mM sodium ethylenediaminetetraacetate (EDTA). Tissue samples were then quickly frozen and stored in liquid nitrogen (-196°C). Previously frozen ventricular tissues were ground with mortar and pestle while immersed in liquid nitrogen. Powdered samples were suspended in 4 ml

Solution D [4 M guanidinium thiocyanate, 25 mM sodium citrate (pH 7.0) 0.5% N-lauroylsarcosine, 0.1 M 2-mercaptoethanol] and subjected to mechanical homogenization (Diamed, Toronto) (3 x 10 seconds). At this point, tissue homogenates were treated with 0.1 volumes of 2 M sodium acetate (pH 4.0), equal volumes of water-saturated phenol (pH 7.4), and 0.2 volumes of chloroform-isoamyl alcohol mixture (49:1) and mixed by inversion. After the mixture was cooled on ice for an additional 15 minutes, samples were centrifuged at 6,000 x g for 20 minutes at 4°C. The RNA-containing aqueous phase was transferred to a fresh tube, mixed with an equal volume of isopropanol and placed at -20°C for 60 minutes. RNA was sedimented at 10,000 x g for 20 minutes and resuspended in solution D, and then again precipitated with an equal volume of cold isopropanol and placed at -20°C for 30 minutes. Then the ventricular RNA pellets were washed twice by repeated resuspended in 75% ethanol and sedimented. The ethanol solution was decanted and finally vacuum dried (duration of 30 seconds to 2 minutes, then visually assessed to avoid complete drying of the pellet). RNA was dissolved in diethyl pyrocarbonate (DEPC)-treated water and the concentration of nucleic acid was calculated from the absorbance at 260 nm prior to size fractionation.

3.7. Northern Blot Analysis

Steady-state levels of mRNA were determined by Northern hybridization analysis. Twenty μg of total RNA was denatured in 50% formamide, 7% formaldehyde, 20 mM MOPS (pH 7.4), 2 mM EDTA (pH 8.0), 0.1% SDS and electrophoresed in a 1% agarose/formaldehyde gel to size fractionate the mRNA transcripts. The fractionated RNA was transferred (using capillary action) on to a 0.45 μm positively charge-modified nylon filter (NYTRAN Maximum Strength Plus, Schleicher and Schuell, Keene, NH, USA) filter. After 24 hours, the filter was removed and RNA was covalently crosslinked using UV

radiation (UV Stratalinker 2400, Stratagene). Blots were prehybridized in a mixture of 50% formamide, 10x Denhardt's solution, 1% SDS, 0.2 mg/ml denatured salmon sperm DNA, 10 mM EDTA (pH 8.0), 25% "4 x RNA" solution [3 M NaCl, 0.6 M Tris-HCl (pH 7.5), 0.18 M NaH_2PO_4, 0.24 M Na_2PO_4, 0.1 M $Na_4P_2O_7$] at 42°C for 6-16 hours. Membrane was hybridized for 6 to 16 hours at 42°C in the presence of labeled probe with a specific activity > 10^9 cpm per μg DNA. The filter then was washed for certain period of time in each of the following: 2 x SSC / 0.1% SDS (first wash), 0.5 x SSC / 0.1% SDS (second wash), and 0.1 x SSC / 0.1% SDS (third wash) using an INNOVA 4000 incubator (New Brunswick Scientific, Canada) oscillating at a rate of 60 rotations per minute. After washing, the membrane was exposed to x-ray film (Kodak X-OMAT) at -80°C with two intensifying screens.

The following inserts were separated from recombinant plasmids and used as cDNA probes in Northern blot analysis: human procollagen type α1(I) (Hf 677), type α1(III) (Hf 934), TGF-β1, Gqα, and human glyceraldehyde-3-phosphate dehydrogenase (GAPDH) were obtained from the American Type Culture Collection (Rockville, MD, USA). Decorin cDNA was graciously provided by Dr. Kevin L. Dreher, United States Environmental protection Agency, Research Triangle Park, NC, USA. Rat 18S rRNA (5'-ACGGTATCAGATCGTCTTCGAACC-3') was synthesized using the Beckman Oligo 1000 DNA synthesizer.[233] The cDNA clones were prepared for hybridization to specific mRNA transcripts and subsequent autoradiography using a Random Primers DNA Labeling System (GIBCO BRL) radiolabeled α-^{32}P-dCTP. Results of autoradiographs from Northern blot analysis were quantified by densitometry (Bio-Rad imaging densitometer GS 670 Hercules, CA, USA).

3.8. Enzyme Immunoassay for Prolyl 4-Hydroxylase

Cardiac tissues from different groups were ground into powder under liquid nitrogen. Powdered tissues (20 mg/ml) were homogenized in 10 mM Tris-HCl buffer pH 7.8 containing 0.1 M NaCl, 0.1 M glycine, 0.1% Triton X-100, 20 mM EDTA, 10 mM N-ethylmaleimide, 1 mM phenylmethylsulfonyl fluoride (PMSF), 1 mM P-hydroxymercuribenzoic acid, 1 mM dithiothreitol (DTT). The homogenized samples were centrifuged 20,000 x g at 4°C for 30 minutes. The supernatants were transferred to fresh Eppendorff tubes and then used for prolyl 4-hydroxylase assay, employing an ELISA kit (Fuji Chemical Industries, Ltd. Toyama, Japan).[234] Briefly, this assay employs two monoclonal antibodies wherein the first is used as a capture antibody in solid phase and the other antibody is linked to horseradish peroxidase. Myocardial samples were diluted 1:20 in distilled water prior to the total protein concentration assay.

3.9. Protein Assay

Total protein concentration in cardiac samples was determined using the Bicinchoninic acid solution (BCA) Kit (Sigma, St. Louis USA).[235]

3.10. Zymography: Detection of Cardiac Matrix Metalloproteinase Activity

Ventricular tissues were ground with mortar and pestle while immersed in liquid nitrogen. Powdered tissues (50 mg) were suspended in 1 ml in phosphate-buffered saline (pH 7.4) containing 100 μg/ml PMSF and 2 μg/ml leupeptin and incubated at 4°C with continuous agitation for 20 h to extract MMPs. The samples were then centrifuged at 10,000 rpm, 4°C for 10 minutes. The resulting supernatant was used for total protein assay and zymographic analysis. Total protein was determined using the BCA protein assay kit. Cardiac MMP activities were detected by zymography.[236] Gelatin (final concentration 1 mg/ml) was added to the gel made with standard 7.5% SDS-polyacrylamide and this gel was

subjected to electrophoresis. Gelatin was deemed to be a suitable substrate because it is readily cleaved by connective tissue-degrading enzymes and incorporates well into polyacrylamide gels. Thirty μg of protein was loaded per lane without reduction or boiling (to maintain the activity of MMPs), and samples were run at 15 mA/gel. After electrophoresis, gels were washed two times (15 minutes/wash) in 25 mM glycine (pH 8.3) containing 2.5% Triton X-100 with gentle shaking at 4°C in order to eliminate SDS. Gels were rinsed and incubated at 37°C for 18 h in substrate buffer (50 mM Tris-HCl, pH 8.0, 5 mM Ca_2Cl). After incubation, gels were stained in 0.05% coomassie brilliant blue R-250 for 30 minutes, and then destained in acetic acid and methanol. Gels were then dried and scanned using a CCD camera densitometer (Bio-Rad imaging densitometer GS 670) for relative lytic activity.

3.11. Passive Pressure-Volume Relationship in Right Ventricle

Myocardial stiffness was determined according to the methods as described by Raya *et al.*[237] Briefly, rat hearts from both sham-operated and MI groups were subjected to Langendorff perfusion with Krebs-Henseleit solution. A latex balloon, attached to a stiff plastic tube, was inserted into the RV via the tricuspid valve. The other end of the tube was connected to a pressure transducer and a 1 ml syringe via a three way stopcock. After 15 minutes equilibration, the heart was arrested by perfusion with a 15 mM potassium Krebs-Henseleit solution. The volume of the balloon was adjusted to reduce the pressure to -5 mmHg. Steady state RV pressure was recorded during increments in balloon volume (10 μl) until the pressure increased to 50 mmHg. The data was computed in real time and analyzed using a dedicated IBM PC with AcqKnowledge (version 3.0) software (Biopac, Harvard Apparatus Canada).

3.12. Western Blot Analysis

$G_{q\alpha}$, PLC-β1, PLC-β3, TβRI, TβRII, Smad2, Smad4, p15 and p21 were detected using Western blot analysis. Cardiac tissues from sham-operated LV, viable LV, border area and scar were homogenized in 100 mM Tris (pH 7.4) containing 1 mM EDTA, 1 mM PMSF, 4 μM leupeptin, 1 μM pepstatin A, and 0.3 μM aprotinin. Samples were sonicated for 3 x 5 seconds. Crude membrane and cytosolic fraction was isolated according to the method of Gettys *et al.*[238] Briefly, samples were centrifuged for 3000 x g at 4°C for 10 minutes to remove unbroken cells and nuclei. The supernatant was further subjected to centrifugation for 48,000 x g for 20 minutes at 4°C. The subsequent crude membrane pellet was resuspended in the homogenizing buffer. For total cardiac Smad proteins assay, myocardium was homogenized with above buffer containing 0.1% Triton X-100. This homogenate was sonicated for 5 x 5 seconds to disrupt nuclear membrane. The homogenate was allowed to lyse for 15 min on ice to further disrupt nuclear membrane. After centrifugation at 10,000 x g for 20 min at 4°C, the resultant supernatant was used for Smad proteins assay. Total protein concentration of membrane fractions was measured using the BCA method.[235] Prestained high or low molecular weight markers (Bio-Rad, Hercules CA, USA) and twenty μg proteins from samples were separated on 10% ($G_{q\alpha}$, TβRI, TβRII, Smad2, and Smad4), 6% (PLC-β1 and PLC-β3), and 12% (p15 and p21) SDS-PAGE. Separated proteins were transferred on to 0.45 μm polyvinylidene difluoride (PVDF) membrane. PVDF membrane was blocked overnight at 4°C or at room temperature for 1 h in Tris-buffered saline with 0.1% Tween-20 (TBS-T) containing 5%-8% skim milk. After washing with TBS-T solution, membranes were probed with primary antibodies for 1 h at room temperature. After washing, membrane was incubated with HRP-labeled secondary antibodies for 1 h at room temperature. The target proteins were detected and visualized by

enhanced chemiluminescence (ECL) or ECL "Plus" according to the manufacturer's instruction (Amersham Life Science Inc. Canada). Specific bands from autoradiographs derived from Western blots were quantified using a CCD camera imaging densitometer (Bio-Rad GS 670, Hercules, CA, USA).

Primary antibodies used in the current set of studies were as follows: 1. Rabbit antibody against $G_{q\alpha}$ was diluted in 1:1000 (Calbiochem-Novabiochem International, San Diego, CA, USA). 2. Rabbit polyclonal antibodies against PLC-β1, PLC-β3, TβRI, and TβRII, as well as goat polyclonal antibodies against Smad2, Smad4, p15 and p21 were diluted in 1:250-1:500 (Santa Cruz Biotechnology, Inc., Santa Cruz, CA, USA). The primary antibodies were diluted in TBS-T containing up to 5% skim milk. Secondary antibodies were as follows: Horseradish peroxidase (HRP)-labeled anti-rabbit IgG and anti-goat IgG were diluted in 1:10,000. Secondary antibodies were diluted with TBS-T containing up to 1% skim milk.

3.13. Immunoprecipitation of Cardiac PLC-β1 and Assay for PLC-β1 Activity

Crude cardiac membrane proteins were extracted using buffer containing 1% w/v Na-cholate, 50 mM HEPES (pH 7.2), 200 mM NaCl, 2 mM EDTA, 10 μg/ml PMSF, 10 μg/ml leupeptin, by rotation for 2 h at 4°C. The samples were then centrifuged (280,000g, for 25 minutes) and the supernatant recovered as the solubilized membrane fraction. The membrane extract was incubated overnight at 4°C (rotation) with mixed monoclonal antibodies to PLC-β1 (5 μg of antibody to 350 μg membrane extract i.e., a ratio of 1:70 μg/ μg). The immunocomplex was captured by adding 100 μl of washed Protein G sepharose bead slurry (50 μl packed beads) at 4 °C by rotation for 2 h. The agarose beads were collected by pulse centrifugation (5 seconds) at 10,000 x g and assayed for PLC-β1 activity. The hydrolysis of

[^{3}H]PIP_2 was measured according to the method described by Wahl *et al.* with minor modification.[239] Briefly, the reaction was performed in the presence of 30 mM HEPES (pH 6.8), 100 mM NaCl, 70 mM KCl, 0.8 mM EGTA, 0.8 mM $CaCl_2$, and 20 μM [^{3}H]-PIP_2 dissolved in 14 mM Na-cholate overnight and an aliquot (10 μl) of immunoprecipitate suspension. The reaction was carried out at 37°C for 2.5 minutes after which the reaction was stopped by transfer to ice bath with the addition of 1% bovine serum albumin and 10% trichloroacetic acid (TCA). Precipitates were removed by centrifugation at 11,000g for 5 minutes and the supernatant collected for quantification of inositol phosphates by liquid scintillation counting.

3.14. Measurement of Cardiac IP_3 Accumulation

Cardiac tissues from sham, viable and scar + border regions were used for the measurement of IP_3 using the Biotrak radioimmunoassay kit (Amersham Life Science Inc. Canada). Briefly, cytosolic fraction from different regions of post-MI heart was prepared as was detailed in our Western blot analytical preparations.[238] All other procedures followed the manufacturer's instruction which was modified according to the method of Chilver *et al.*[240] Unlabelled IP_3 in the samples competes with fixed amount of [^{3}H]-labeled IP_3 for a limited number of bovine adrenal IP_3 binding proteins. Bound IP_3 is then separated from the free IP_3 by centrifugation. D-myo-Inositol 1,4,5-trisphosphate was used as standard. Results were expressed as pM/mg protein.

3.15. PKC Activity Assay

Cardiac PKC activity was determined with the use of a commercial PKC assay kit (Upstate Biotechnology Incorporated, Lake Placid, NY, USA). Myocardium was homogenized in a 50 mM Tris-HCl buffer (pH 7.5) containing 4 mM EDTA, 10 mM EGTA,

0.25 M sucrose, 10 μg/ml leupeptin, 10 μg/ml aprotinin, 5 mM DTT, and 0.1 mM PMSF for 3 x10 seconds. The homogenates were sonicated for 3 x 5 seconds. Cytosolic and membrane fractions were separated as described above. The membrane fraction was then solublized with homogenization buffer containing 1% Triton X-100 for 1 h on ice. After centrifugation, the resulting supernatant was used for detection of PKC activity in the membrane fraction. Total protein concentration of both cytosolic and membrane fractions were determined with the BCA assay. The PKC activity is based on the measurement of the incorporation of ^{32}P from [γ-^{32}P]ATP into a specific synthesized substrate peptide (QKRPSQRSKYL).[241,242] The reaction is initiated by the addition of [γ-^{32}P]ATP and allowed to proceed at 30°C for exactly 10 minutes. The reaction mixture (25 μl) was removed and transferred onto the P81 phosphocellulose paper. After 30 seconds, the phosphocellulose paper was washed 2 x 5 minutes with 0.75% phosphoric acid and 5 minutes with acetone. The filter was then put into scintillation vials for measuring the radioactive phosphopeptide bound to the filter, using a standard by scintillation counter. Resultant PKC activity was expressed as μM Pi/mg protein/minute.

3.16. ELISA Assay for Cardiac TGF-β1

TGF-β1 concentration was determined using a "sandwich" ELISA by the method as described by Danielpour with minor modifications.[243] After excision, the heart was perfused with 5 ml cold PBS to flush out the remaining blood in the myocardial vascular lumen in order to eliminate contamination by TGF-β1 from blood sources. Approximately 0.5 g heart tissue was homogenized in 4 ml cold acid-ethanol (93% ethanol, 2% HCl, 85 μg/ml PMSF and 5 μg/ml pepstatin A). Three samples were pooled in the case of border and scar tissues. After overnight extraction at 4°C by gentle rocking, extracts were subjected to centrifugation

at 10,000 x g for 10 minutes. The resulting supernatants were dialyzed extensively (3 x 100 volume) against 4 mM HCl at 4°C, using a 3,500 MW-cutoff Spectrapore dialysis membrane. Plate wells were coated with either soluble TβRII or PBS (control). Recombinant human TGF-β1 was used to generate a standard curve (triplicate). Standards and samples were incubated for 1 h at room temperature on a rotating platform, washed, and incubated with chicken anti-TGF-β1 antibody (<5% cross-reactivity with TGF-β2 and -β3). Wells were washed again before incubation with phosphatase-linked, goat, anti-chicken antibody for 1 h. After washing, the plates were incubated overnight at 4°C with phosphatase substrate in diethanolamine buffer (Kirkegaard & Perry Laboratories Inc., Gaithersburg, MD). The difference in optical density between 405 and 450 nm was measured on a V_{max} microplate ELISA reader (Molecular Devices, Menlo Park, CA). TGF-β1 concentrations in the samples were calculated by a four-parameter regression equation (after correction for the background from control wells) with Molecular Device's Sofmax program. TGF-β1 concentration was expressed as ng/g of tissue. This assay measured total cardiac TGF-β_1 since latent TGF-β_1 was activated during the acid-ethanol extraction step.

3.17. Statistical Analysis

All values are expressed as mean ± SEM. The difference between control and experimental groups were calculated using the student's *t*-test. One way analysis of variance (ANOVA) followed by Student-Newman-Keuls Test was used for comparing the differences among multiple groups at each time point (SigmaStat). Significant differences among groups were defined by a probability of less than 0.05. The Northern blot data in multiple time point study was expressed as a percentage of control according to the method of Fisher and Periasamy.[244]

Chapter 4. Cardiac Collagen Remodeling After Myocardial Infarction

4.1. Summary

Although increased deposition of collagen proteins has been described after MI, little is known of time-dependent transcriptional alteration of specific cardiac collagen sub-types as well as the degradative mechanisms for cardiac collagen in LV and RV tissues remote to the infarct. We sought to study collagen mRNA abundance and the deposition of specific collagen subtypes in noninfarcted LV and RV muscles at different times after MI. We also assessed the activity of different myocardial MMPs using zymography to gain some information regarding collagen degradation. Furthermore, we assessed passive compliance properties of the RV in experimental hearts. We observed that the mRNA abundance of types I and III collagen were increased 3 days after MI in both viable LV and RV tissues, that they peaked at 1 to 2 weeks, and were maintained at relatively high levels in the 4 and 8 weeks experimental groups. Stiffness of the RV was significantly increased in the 8 weeks experimental group when compared to that of control values. These findings correlated with increased immunofluorescent staining patterns of different collagen species in the surviving cardiac interstitium of 2, 4, and 8 weeks experimental groups. MMP-2 activity was increased in viable LV at 2, 4, and 8 weeks and at 2 weeks in the RV in experimental animals when compared to controls. These results indicated that i) activation of transcription of collagen types I and III gene occurs in acute and chronic MI, and that fibrillar collagen proteins are deposited in the noninfarcted cardiac interstitium after a lag period relative to increased corresponding mRNA abundance; ii) an increase in MMP activity in chronic experimental hearts indicates that increased collagen deposition may be due to an increment in collagen synthesis rather than by reduced degradation of collagen, and that MMP activation may be

important in remodeling for the noninfarcted cardiac stroma; and iii) an increase of RV stiffness was associated with increased deposition of collagen.

4.2. Introduction

MI induces morphological and molecular alterations in the infarcted and noninfarcted regions of the heart and these changes are collectively referred to as ventricular remodeling.[3] Only recently has the role of cardiac fibroblasts and ECM in the process of remodeling of viable myocardium after MI gained attention.[7,36,58] Fibroblasts account for ~70% of the total cell population, and they are known to synthesize fibrillar collagen types I and III in the heart; unlike terminally differentiated cardiac myocytes, they can be recruited back into the cell cycle to proliferate under certain pathological conditions.[36] Previous findings support the hypothesis that fibroblasts and/or myofibroblasts are mitotically active in heart failure, and that active DNA-synthesizing cells in the surviving myocardium of infarcted rat hearts have been identified as nonmyocytes.[179] Results of either clinical or experimental studies from our laboratory[8] and others[64,180] provide evidence for the increase in total collagen protein in LV remote to the infarct site. One limitation common to the studies listed above resides in the estimation of total collagen protein by either sirius red dye staining or 4-hydroxyproline measurement, as either provide no information on the relative contribution of specific collagen sub-types in cardiac fibrosis. Although it has been shown that fibrillar collagen and fibronectin expression within the infarcted regions was enhanced in acute changes,[245] there is only limited information about the alteration of cardiac collagen mRNA abundance and characterization of the collagen subtypes in the hypertrophied noninfarcted tissues in this model of heart failure. Therefore we have undertaken studies to resolve the expression of collagen mRNA in both ventricles remote to the infarction. We have also carried out

immunofluorescent studies to determine the pattern of deposition for specific collagen types I and III after MI. As the concentration of collagen in the interstitial space depends on a balance between synthetic pathways and degradation for collagen mediated mainly by myocardial MMPs, we carried out experiments to assess the specific activity of some specific MMPs in noninfarcted and scar tissues. Furthermore, none of the aforementioned studies address diastolic function of the RV in this model of MI. As altered diastolic behavior of the RV has important clinical implications, characterization of passive compliance in lieu of enhanced presence of collagen in this chamber was required.

4.3. Results

4.3.1. Infarction size and cardiac hypertrophy

We observed that the transmural infarct size was 42 ± 3 % of the total LV circumference. Experimental animals in this study were characterized by the presence of large MI which was comparable to values reported earlier and the development of time-dependent LV and RV hypertrophy in experimental rats (Table 2).[224,246,247] We found that in experimental animals at 3 days post-MI, neither RV wet weight (RVW) nor LV wet weight (LVW) were significantly different from control. In the 1, 2, 4, and 8 weeks experimental groups, a significant increase in the viable LVW, RVW, the ratio of LVW and RVW to body weight (BW) were noted when compared to values from sham-operated control hearts. Thus the incidence of hypertrophy for LV and RV chambers noted in this study were comparable to our previous findings.[224]

4.3.2. Cardiac collagen mRNA abundance

We addressed mRNA abundance changes in the myocardium at several points very early after the induction of infarction (3 days, 1, and 2 weeks), prior to the development of overt heart failure. For comparative purposes, we also assayed collagen mRNA expression at

later stages of heart failure (4 and 8 weeks). Verification of the integrity of total fractionated RNA samples are provided by visualization of the 28S and 18S rRNA bands in a representative photograph of an agarose gel stained with ethidium bromide (Figure 1, upper panel). Specific hybridization of cDNA probes revealed characteristic mRNA bands, and these are shown in autoradiographs of representative blots probed with cDNAs of collagen types I and III, GAPDH and an oligonucleotide specific for 18S rRNA (Figure 1, bottom panel). In the viable LV, collagen type I mRNA abundance was increased significantly when compared with sham-operated animal at 3 days after MI. Furthermore, collagen type I mRNA expression was increased ~ 9-fold in the experimental samples 1 week after induction of MI. The mRNA abundance for this collagen sub-type remained significantly elevated over control levels at all time points within the current experimental design (2, 4 and 8 weeks) (Figure 2A). Similarly, in the RV, collagen type I gene mRNA abundance was found to be significantly elevated when compared to samples of sham-operated RV total RNA at 3 days. RV collagen type I mRNA expression peaked in the experimental animals (~ 2.3-fold vs. control level) at 2 weeks after MI. The RV collagen type I/GAPDH ratio remained elevated in the 4 and 8 weeks experimental groups, and this was comparable to the pattern of collagen type I expression in LV after MI (Figure 2C). Ventricular collagen type III expression was elevated in both LV and RV at all times after the induction of infarction, however, the relative increases in expression of collagen type III mRNA were less dramatic when compared to the increases in collagen type I mRNA abundance (Figure 2B and D).

4.3.3. Total collagen protein and Immunofluorescent staining of collagen types I and III

Immunofluorescent staining of collagen types I and III in viable LV and RV from 1, 2, 4 and 8 weeks after MI and age-matched sham-operated animals were visualized by

epifluorescence microscopy. Relatively low levels of collagen (bright, wavy appearance) are present in the interstitial space in those sections of sham-operated rats in both viable LV and RV (Figure 3). The immunofluorescent results showed that the interstitium of viable LV and RV is marked by progressive accumulation of collagen type I at day 2, 4 and 8 weeks after MI (Figure 3). Collagen type III was found to be present throughout the entire ECM and was arranged in a true network in the extracellular space (Figure 4). Collagen type III in the viable LV and RV is present in greater amounts than in sham-operated animals (Figure 4).

4.3.4. Cardiac matrix metalloproteinase activity

Cardiac MMP activity was detected by the appearance of a lytic band in the gelatin-containing SDS-PAGE-gelatin gel. We included serine proteinase inhibitors, PMSF and leupeptin, to indicate that the lytic bands are not due to serine proteinase. The specificity of this method was verified by using MMPs inhibitor 1,10 phenanthroline, which abolished the gelatinolytic activity. Using zymography, a major lytic band from viable tissue was observed to correspond to MMP-2 (72 kDa) which is gelatinase A. On the other hand, two lytic bands MMP-1 (54 kDa) and MMP-2 were observed in the scar tissues (Figure 5).[51] MMP-1 activity was found to be significantly increased in border and scar tissues when compared to values from viable tissue. There was a modest but significant increase in MMP-2 activity in viable LV at day 1, 2, 4 and 8 weeks after MI. In contrast, MMP-2 activity was significantly increased at 2 weeks after the induction of MI and back to normal at 4 and 8 weeks in the RV (Figure 6).

4.3.5. Right ventricular passive pressure-volume relation

To test whether the presence of increased collagen concentration in the interstitium of the RV after infarction is indeed accompanied by decreased RV tissue compliance, we obtained data to construct passive pressure-volume curves obtained from RV of 8 weeks

sham-operated and age-matched experimental animals (Figure 7). Our results indicate that the RV pressure-volume curve from 8 weeks experimental animals were characterized by a significant leftward shift indicating the increment of RV chamber stiffness.

Table 2. Cardiac hypertrophy and transmural scar weight in experimental rats at 3 days, 1, 2, 4 and 8 weeks after induction of myocardial infarction.

Parameters	3-days		1-week		2-week		4-week		8-week	
	Sham	MI	Sham	MI	Sham	MI	Sham	MI	Sham	MI
BW, g	246 ± 8.4	219 ± 11*	280 ± 7.0	269 ± 9.6	354 ± 5.7	340 ± 5.5	409 ± 13	415 ± 13	507 ± 9.4	509 ± 12
LVW, g	0.57 ± 0.01	0.56 ± 0.03	0.64 ± 0.02	0.66 ± 0.03	0.79 ± 0.01	0.86 ± 0.02*	0.78 ± 0.02	0.87 ± 0.02*	0.89 ± 0.03	0.99 ± 0.03*
Scar, g	...	0.21 ± 0.03	...	0.21 ± 0.01	...	0.25 ± 0.03	...	0.28 ± 0.03	...	0.29 ± 0.03
RVW, g	0.18 ± 0.01	0.19 ± 0.01	0.19 ± 0.01	0.22 ± 0.02*	0.25 ± 0.01	0.30 ± 0.02*	0.23 ± 0.01	0.31 ± 0.03*	0.23 ± 0.01	0.48 ± 0.05*
LV/BW, mg/g	2.02 ± 0.30	2.57 ± 0.09	2.27 ± 0.04	2.45 ± 0.04*	2.22 ± 0.06	2.53 ± 0.05*	1.92 ± 0.04	2.09 ± 0.04*	1.75 ± 0.06	1.95 ± 0.04*
RV/BW, mg/g	0.74 ± 0.04	0.89 ± 0.08	0.68 ± 0.04	0.82 ± 0.03*	0.71 ± 0.04	0.88 ± 0.03*	0.57 ± 0.02	0.76 ± 0.08*	0.45 ± 0.03	0.94 ± 0.11*

MI indicates experimental animals with large left ventricular myocardial infarction; sham, noninfarcted age-matched control animals; BW, body weight; LVW, left ventricle wet weight; RVW, right ventricle wet weight. Results are mean ± SEM of 8-10 experiments. *P<0.05 *vs* sham-operated control at each time point.

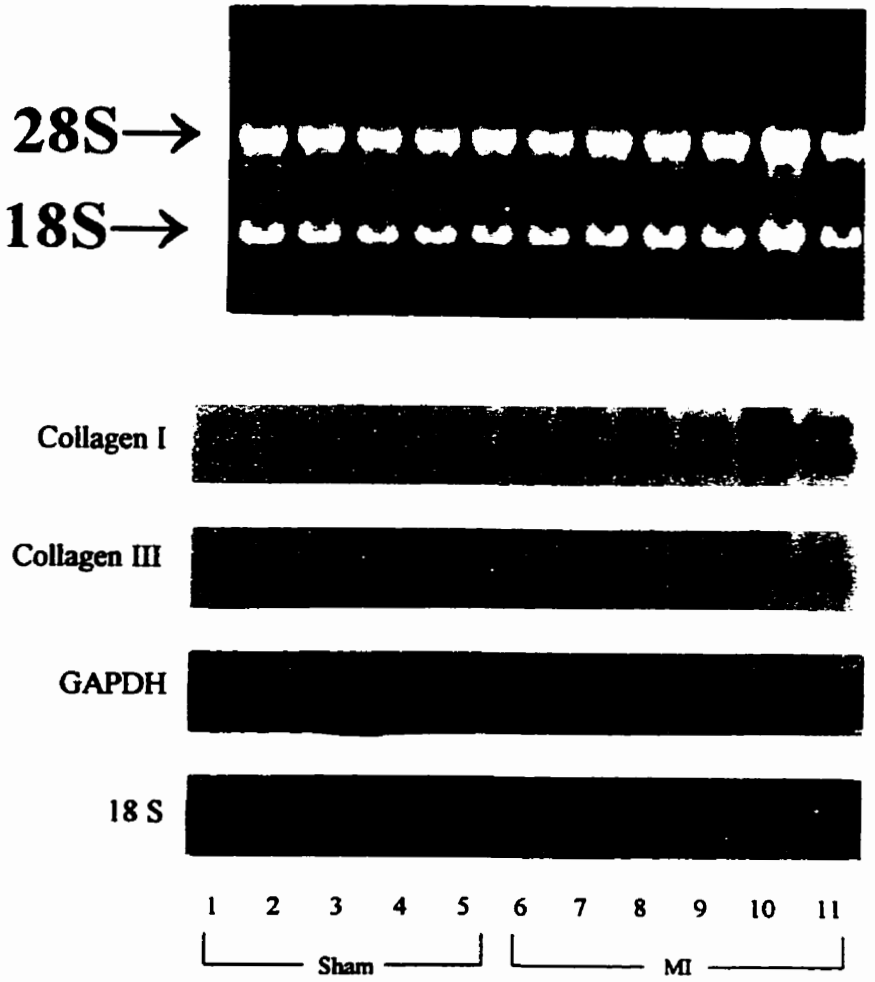

Figure 1. Upper panel: representative agarose gel stained with ethidium bromide to visualize the 28 S and 18 S rRNA bands in total RNA samples extracted from cardiac ventricular tissues. **Lower panel**: Autoradiograph from Northern blot analysis wherein each lane was loaded with 20 μg left ventricular total RNA extracted from noninfarcted control animals (sham, lanes 1-5) and animals 2 weeks after myocardial infarction (MI, lanes 6-11). The control group was age-matched. Hybridization of fractionated total RNA with cDNA probes for procollagen α1(I), procollagen α1(III) (i.e., collagen types I and III, respectively), glyceraldehyde 3-phosphate dehydrogenase (GAPDH) and 18 S rRNA indicate relative steady-state mRNA levels for each gene tested.

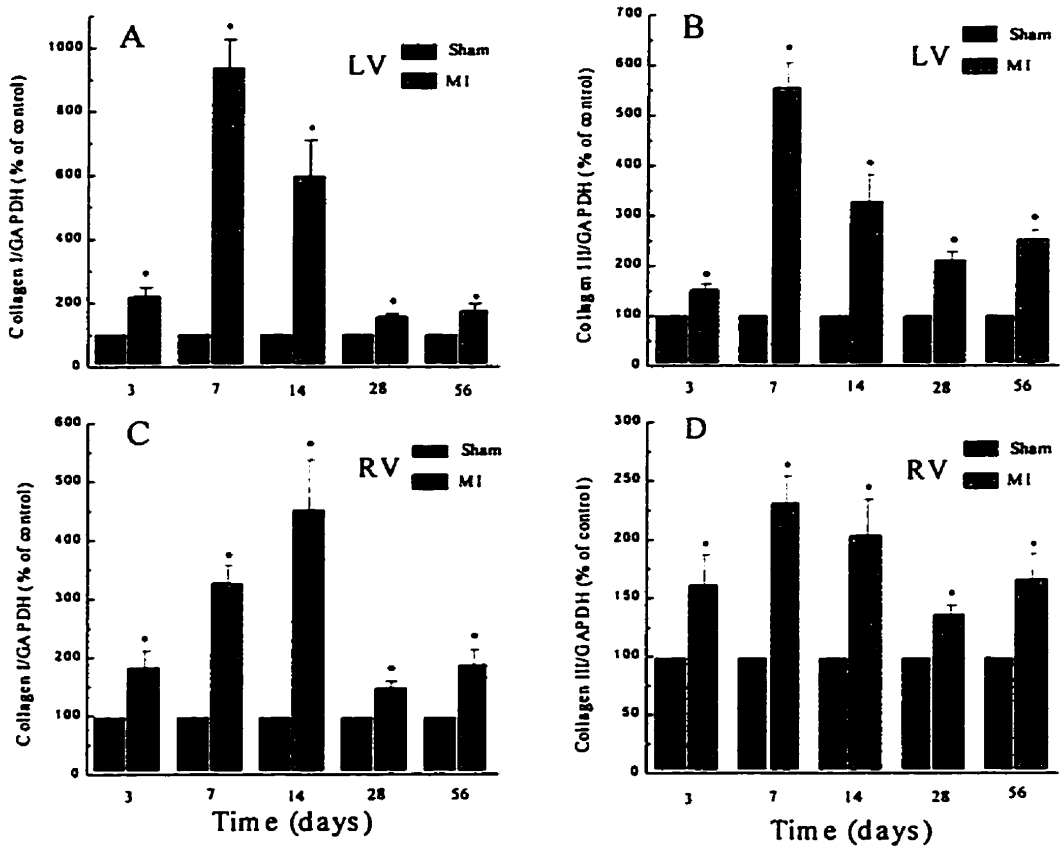

Figure 2. Estimation of the relative steady-state abundance of viable left (LV) and right ventricular (RV) collagen types I and III mRNAs at different times after myocardial infarction (MI = experimental animals) or in noninfarcted controls (sham). **Panel A**: Collagen type I/GAPDH signal ratio in LV; **Panel B**: Collagen type III/GAPDH signal ratio in LV; **Panel C**: Collagen type I/GAPDH signal ratio in RV; and **Panel D**: Collagen type III/GAPDH signal ratio in RV. The data were expressed in arbitrary densitometric units, normalized to glyceraldehyde-3-phosphate dehydrogenase (GAPDH) autoradiographic band intensity and noted as a *percent* value of control expression levels (%). The data depicted is the mean $\pm$ S.E.M. of 4-8 experiments. *$P < 0.05$ for each experimental group value *vs* age-matched sham operated values.

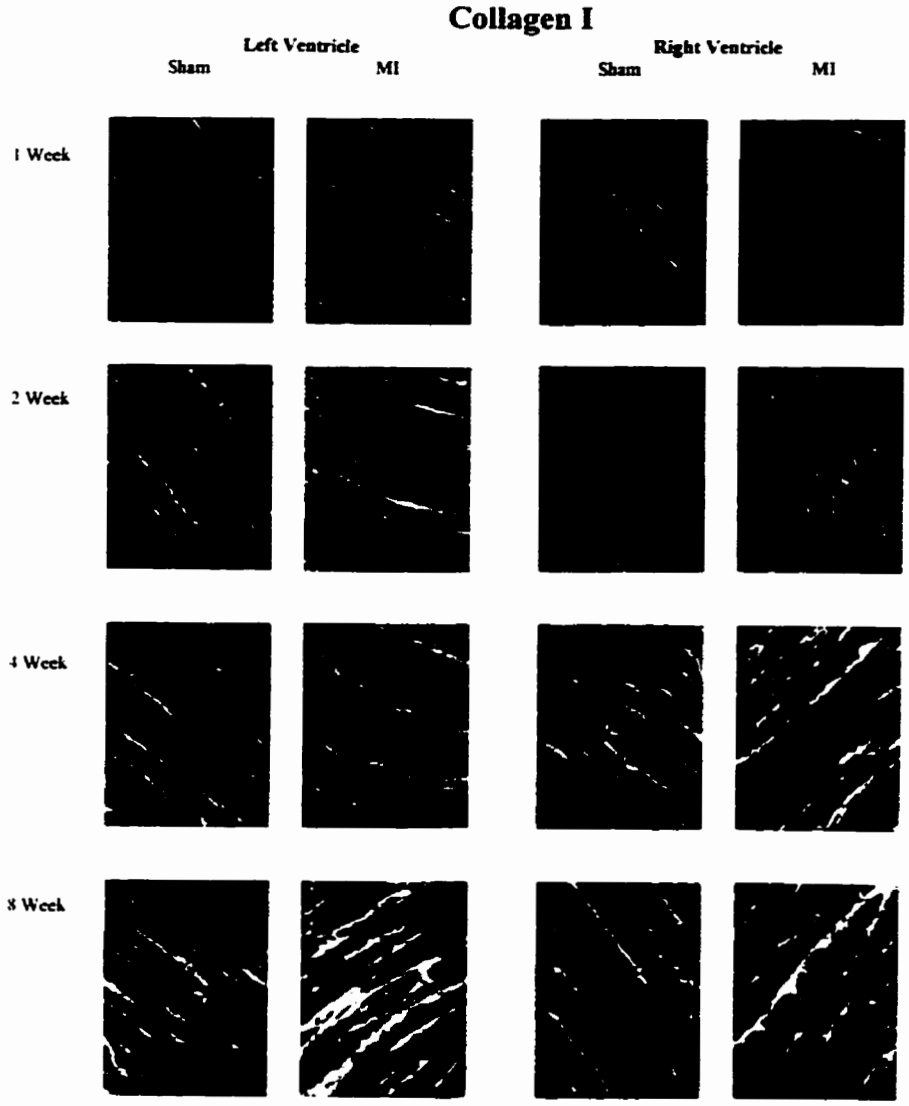

Figure 3. Immunofluorescent staining of collagen type I in sham-operated animals and in viable left and right ventricles at 1, 2, 4, and 8 weeks after myocardial infarction (MI). Left and right panels show the immunoreactive staining of left and right ventricles, respectively. Collagen type I appears as wavy fibers between myocytes. Magnification, x 400.

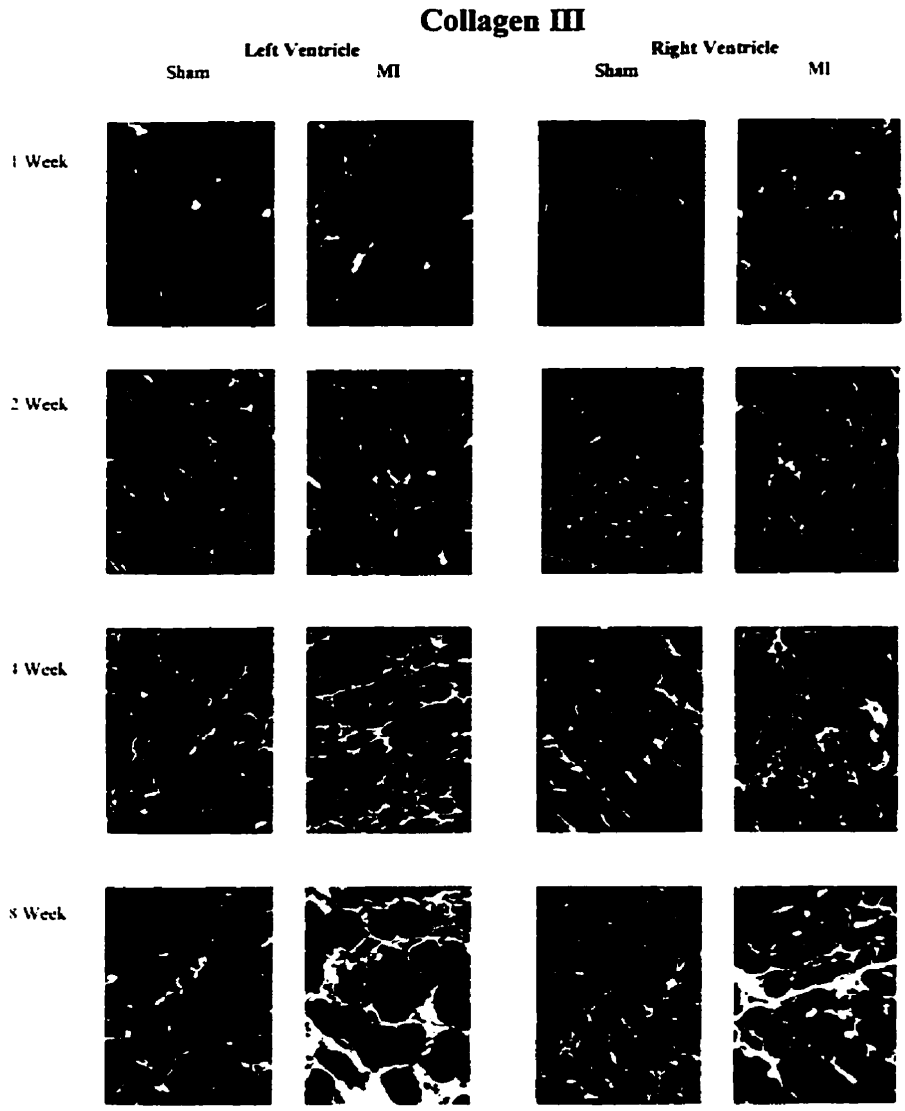

Figure 4. Immunofluorescent staining of collagen type III in sham-operated animals and in viable left and right ventricles at 1, 2, 4, and 8 weeks after myocardial infarction (MI). Left and right panels show the results of left and right ventricles respectively. Collagen type III appears as brightly stained material between myocytes. Magnification, x 400.

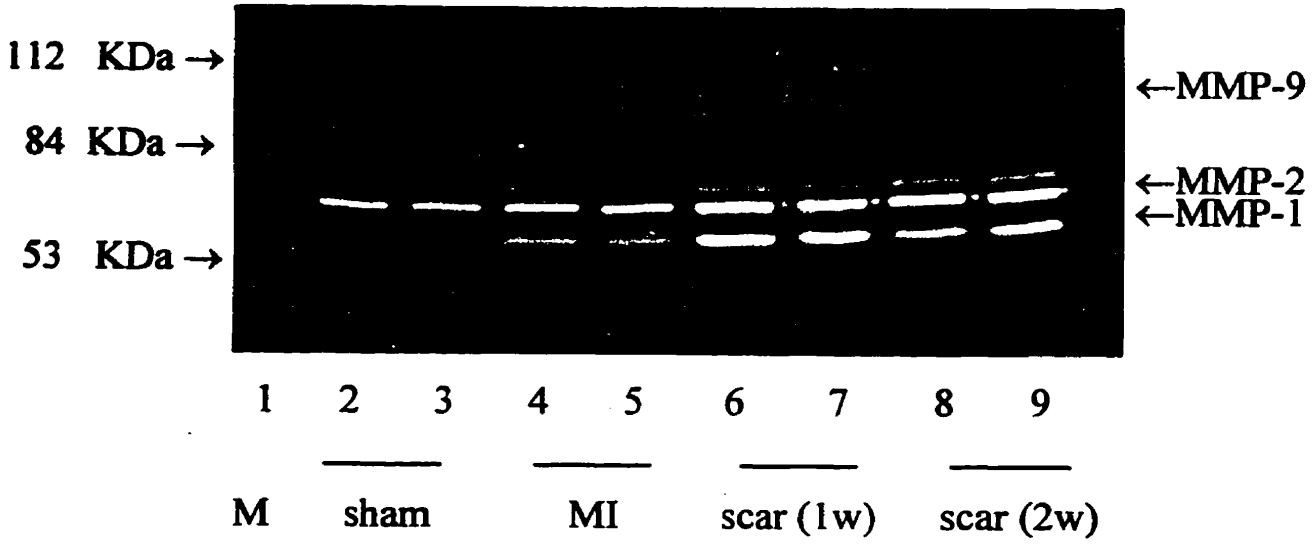

Figure 5. Representative zymography showing matrix metalloproteinase (MMP) activity in viable left ventricle (1 week post MI) and scar tissues (1 and 2 weeks post MI). Lane 1 is low molecular weight marker, lanes 2-3 are sham-operated animal, lanes 4-5 are viable left ventricle, lanes 6-7 are 1 week scar, and lanes 8-9 are 2 weeks scar. MMP-1(54 kDa), MMP-2 (72 kDa) and MMP-9 (92 kDa) are indicated and were increased in viable left ventricle and scar tissues.

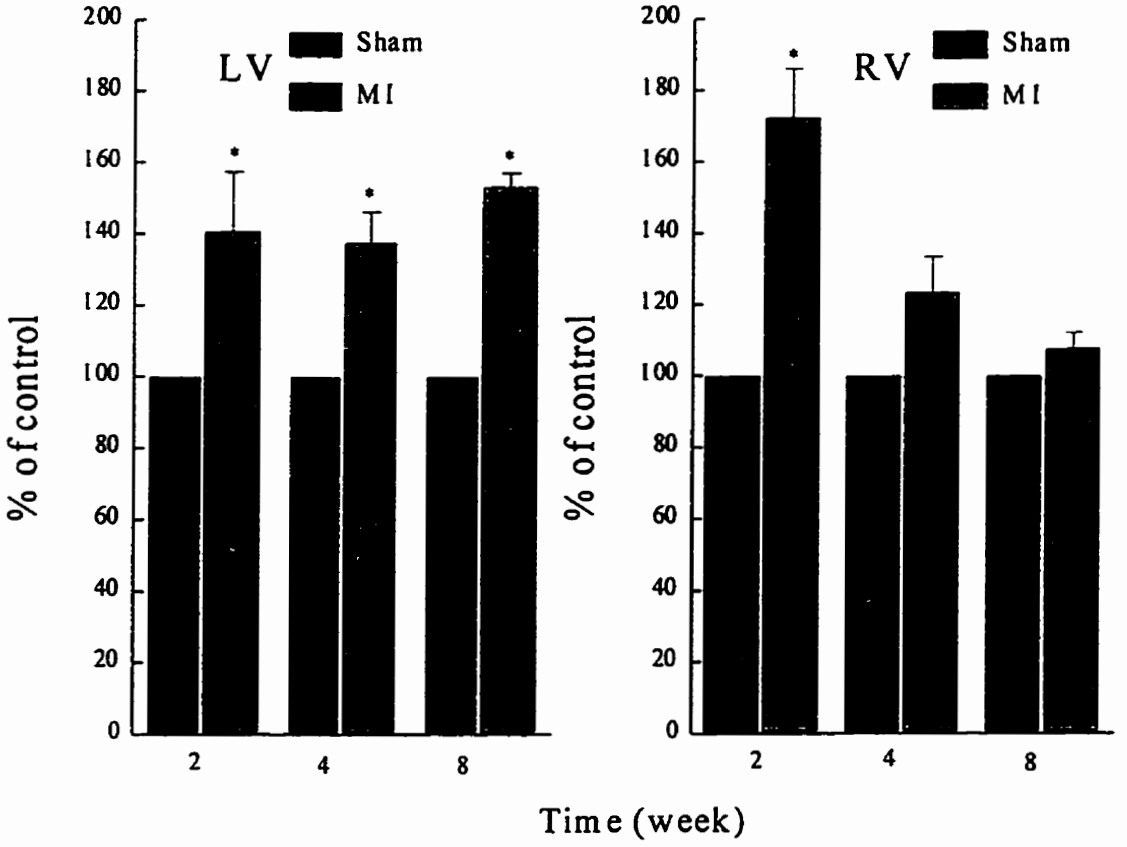

Figure 6. Estimation of the relative activity of viable left and right ventricular matrix metalloproteinase 2 (MMP-2) at different time points after myocardial infarction (MI = experimental animals) or in noninfarcted controls (sham). The data were expressed in arbitrary densitometric units, and noted as a *percent* value of control levels (%). The data depicted is the mean $\pm$ S.E.M. of 4-9 experiments. *$P < 0.05$ for each experimental group value vs. age-matched sham operated values.

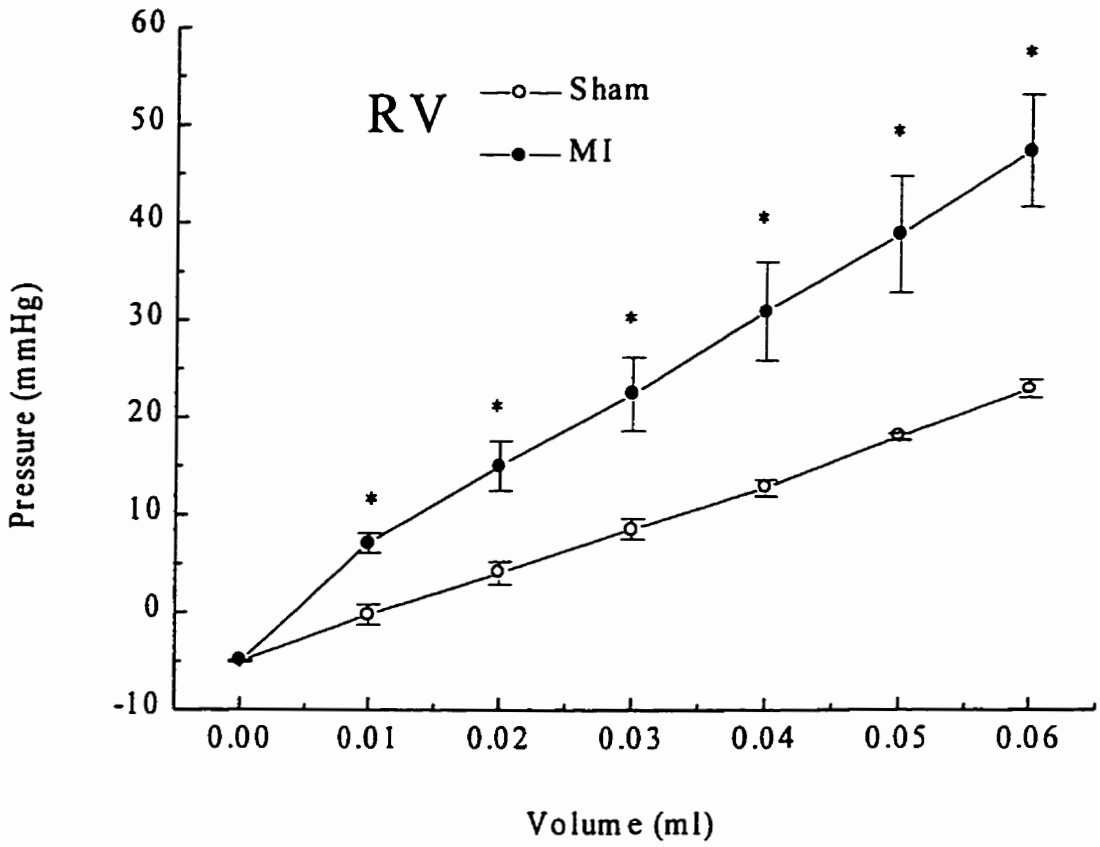

Figure 7. Right ventricular pressure-volume relation in control (o = sham) rats and in 8 weeks experimental (• = MI) animals. The data depicted is the mean ± S.E.M. of 5 experiments. *P < 0.05 at each time point as compared with control.

4.4. Discussion

Cardiac remodeling after MI is characterized by hypertrophy of cardiac myocytes and hyperplasia of non-myocytes.[179,248] Cardiac function depends on the remodeling of both the surviving and infarcted tissues.[3] We have previously characterized the development of heart failure with the attend of cardiac hypertrophy and fibrosis in experimental animals with large infarction ($\geq$ 40% of the LV free wall).[8,224,227] In the present study, we examined both synthetic and degradative aspects of collagen metabolism in hypertrophied and failing myocardium remote to the site of MI. Our immunofluorescent results have shown that both collagen types I and III progressively accumulated in the interstium of viable LV and most notably in RV from experimental hearts. The advantage of immunofluorescent staining over the commonly used Sirius staining method is that collagen types I and III can be distinguished by using specific antibodies. This data extends a report which addressed the immunofluorescent staining of collagen types I and III in the infarcted zone.[249] These findings agree with our previous results from 4-hydroxyproline assay which detected absolute levels of cardiac total collagen concentration.[8] Increased RV collagen was associated with significantly increased chamber stiffness in the 8 weeks experimental group.

It has been suggested that altered ECM may play a role in the development of heart failure.[6,58] Excessive deposition of collagen proteins may impair heart function due to morphological and functional separation of myocytes with subsequent increased oxygen distribution distance and decreased ventricular compliance.[12,13,17] Although it is well known that increased interstitial collagen concentration may result in decreased cardiac compliance, little information is available in the literature with respect to the appearance of collagen in the RV. Nevertheless, the clinical implications of RV fibrosis are considerable in view of the eventual contractile failure of this chamber and subsequent development of

pulmonary and systemic congestion in severe stages of heart failure.[2] We observed that total collagen concentration was found to be increased not only in viable LV but also in RV in 2, 4 and 8 weeks experimental animals. Studies using the rat model of chronic infarction have revealed that the apparent LV stiffness exhibited a pattern of biphasic time-dependent changes, increasing up to one day and then progressively decreasing until 22 days.[237] Infarct expansion or ventricular aneurysm is associated with increased LV volume, and thus the effects of volume predominate over changes in viable myocardial stiffness in the LV. To avoid this problem, Litwin and coworkers used noninfarcted LV papillary muscle to study compliance, and found that stiffness was increased 6 weeks after MI.[15] In the present study, RV stiffness was significantly increased in the 8 weeks experimental group. Thus increased cardiac collagen concentration in the RV was associated with altered passive compliance of this chamber in these animals. Recent studies have provided support for the hypothesis that marked myocardial fibrosis and increased passive stiffness are critical determinants for the transition from compensated hypertrophy to heart failure in spontaneously hypertensive rats.[250] Our results support the hypothesis that fibrosis is associated with the transition of viable muscle from the compensated stage (2 weeks) to heart failure (8 weeks post-MI) and that this change is associated with global changes in heart muscle stiffness.

The precise mechanism(s) for increased collagen mRNA abundance in LV and RV after induction of MI is unclear. As we observed similar patterns of collagen mRNA alteration in both LV and RV in the early phase post-MI, our results support the hypothesis that diffusible hormones are responsible for the increase of cardiac collagen deposition.[41,65] However, the role of mechanical load on heart in this process can not be ruled out because of mechanical stretching also play a role in the induction of collagen gene expression.[251] As both LV and RV chambers are subject to altered hemodynamic loading at 8 weeks after MI

in this experimental model, we cannot rule out the possibility that hemodynamic loading was involved in the regulation of collagen mRNA and proteins. Several hormones including Ang II and TGF-β1 may regulate collagen gene expression and therefore mediate collagen deposition in the interstitium of heart muscle.[208,252] A distinct lag period among gene and protein activation was observed in noninfarcted tissue taken from the 3 days and 1 weeks (acute phase study) experimental animals. These data highlight the temporal differences between the onset of increased collagen mRNA abundance and collagen types I and III protein deposition in noninfarcted heart. A discrepancy between collagen gene activation and collagen protein deposition has been reported in aging rats,[47] and it is suggested that this may be due to the involvement of complex posttranslational modification i.e., hydroxylation, cleavage and secretion steps in collagen metabolism. The sustained elevation of mRNA abundance of type I and type III collagen seen in the present study suggests that biventricular reactive fibrosis continues into chronic heart failure (8 weeks), and that a progressive rise in collagen concentration occurs. The immunofluorescent staining pattern of cardiac collagen types I and III in 2, 4, and 8 weeks experimental animals support this suggestion. Nonetheless, this is the first comprehensive study to provide information comparing immunofluorescent localization of collagen subtypes and quantification of collagen mRNA level, and indicates that the entire heart is involved in the wound healing response following MI.

Relative cardiac collagen concentration is the product of a dynamic balance among collagen synthesis and degradation. Collagen types I and III can be cleaved by a 54 kDa interstitial collagenase (MMP-1) and a 75 kDa neutrophil collagenase (MMP-8).[51] In the present study we did not observe any increase of MMP-1 activity in the viable tissues, but a significant increase of MMP-1 in scar tissue was apparent at 1 to 2 weeks. We demonstrate

that there is a modest but significant increase of MMP-2 in the non-infarcted LV at 2 weeks and maintained at 8 weeks after MI. Others have used this experimental model to address collagen degradation, and have shown that MMP-1 activity was increased at day 2, peaked at 1 week and declined thereafter in the infarct site in the LV experimental animals.[55] As MMP-2 can degrade type IV collagen, increased MMP-2 activity may be responsible for degradation of collagen present in the basement membrane. Furthermore MMP-2 will degrade gelatin (a breakdown product of fibrillar collagen) to constitutive amino acids. This process may facilitate remodeling of ECM in the viable ventricle after infarction.

In summary, the results of this study indicate that prefailure and moderate CHF stages after induction of large MI are associated with i) a similar, significant elevation of mRNA levels of cardiac collagen species in LV and RV in acute and chronic MI, and that collagen protein were deposited in the noninfarcted myocardium after lag period relative to increased corresponding mRNA abundance; ii) marked RV fibrosis in experimental animals and increased chamber stiffness was present in the 8 weeks experimental group; and iii) an significant increase in MMP-2 activity in noninfarcted LV and RV and scar tissue in experimental animals, whereas MM-1 was found increased only in scar tissue. Thus net degradation of collagen may be increased in experimental hearts and this finding supports the hypothesis that increased deposition of collagen protein is a result of elevated synthesis of collagen. These results illustrate the respective time courses for activation of collagen mRNA expression and collagen protein deposition in the cardiac interstitium remote to the site of infarction. It is clear that not only the infarcted region, but the whole heart including RV becomes involved in the cardiac wound healing response. Cardiac interstitial collagen remodeling is sustained in the chronic phase of MI. The possible growth factors involved in

cardiac collagen remodeling especially in collagen synthesis in post-MI hearts need further study.

Chapter 5. Effect of AT_1 receptor Blockade on Cardiac Collagen Remodeling after Myocardial Infarction

5.1. Summary

Previous work has shown that cardiac fibrosis occurs after MI in noninfarcted ventricular tissue and that this event is associated with abnormal cardiac function. Our aim was to now investigate the effect of AT_1 receptor blockade on cardiac collagen remodeling in post-MI rat heart remote to the infarct site by addressing collagen mRNA abundance, posttranslational hydroxylation of collagen monomers, and the deposition of mature collagens. Prolyl 4-hydroxylase mediates hydroxylation of procollagen α-chains in the endoplasmic reticulum of cardiac fibroblasts and thus regulates the downstream formation and secretion of helical collagen molecules. The effects of losartan (15 mg/kg/day) on collagen deposition and mRNA abundance were monitored in viable LV and RV in sham-operated (control) and experimental groups in the presence or absence of losartan. Immunoreactive prolyl 4-hydroxylase protein concentration in control and experimental groups was determined by ELISA. Immunofluorescent staining and 4-hydroxyproline assays confirmed that losartan treatment attenuate fibrosis in experimental hearts. Northern analysis revealed that losartan treatment of 1, 2, or 4 week experimental groups had no effect on collagen mRNA abundance compared to untreated post-MI rats. On the other hand, immunoreactive prolyl 4-hydroxlase concentration was significantly decreased in the post-MI group treated with losartan. Determination of cardiac mass and cardiac function revealed that losartan treatment was associated with attenuated cardiac hypertrophy and improved LV function in experimental animals. AT_1 blockade was associated with a significant decrease in cardiac fibrosis in treated post-MI rats, and this trend was positively correlated to a significant decrease in immunoreactive prolyl 4-hydroxylase compared to untreated

experimental animals. The level of cardiac prolyl 4-hydroxylase may be regulated by angiotensin via AT_1 receptor activation, and the suppression of prolyl 4-hydroxylase with losartan treatment may be an important mechanism for modulation of collagen deposition in the post-MI rat heart.

5.2. Introduction

MI is associated with cardiac fibrosis not only in the scar but also in the viable tissue remote to the infarct. Results of either experimental studies from this laboratory[8] and others,[65] or those from clinical investigation,[64] have provided evidence for increased deposition of total collagen proteins in LV remote to the infarct. It has been suggested that cardiac fibrosis plays a role in the development of CHF in post-MI hearts.[7,58] In addition to regulation of collagen gene transcription, posttranslational regulation is an important step for control collagen synthesis. One important posttranslational regulatory point for fibrillar collagen secretion is mediated by prolyl 4-hydroxylase which is responsible for the hydroxylation of selected proline residues on the α-monomers of procollagen α-chains. This hydroxylation will facilitate the formation of the triple stranded helical procollagen molecules and their subsequent secretion to the extracellular space.[34,253]

Some recent evidence supports the hypothesis that Ang II is involved in the stimulation of cardiac fibrosis in post-MI hearts. Several studies indicate that administration of both captopril (an ACE inhibitor) and losartan (an AT_1 receptor antagonist) were associated with the inhibition of cardiac fibrosis in post-MI hearts.[171,179,180,254] However, little information is available to address the effect of losartan on steady-state collagen mRNA abundance or posttranslational regulation of collagen synthesis in the post-MI heart. Furthermore, no information is available regarding the mechanism of these reagents for attenuating cardiac fibrosis, and this is especially true with regard to the effects of these drugs on the regulation of collagen synthesis (mRNA and posttranslational regulation) in

cardiac remodeling after MI. As AT_1 receptors represent the predominant Ang II receptor subtype in cardiac fibroblasts, which are known to be responsive to hormonal signals mediated by Ang II.[255] We investigated the effect of losartan on cardiac collagen profile, collagen mRNA abundance, and immunoreactive cardiac prolyl 4-hydroxylase concentration in both LV and RV at sites remote to the infarct. To provide some information about the relationship between cardiac collagen deposition and LV function in these post-MI hearts, we assessed the effect of losartan on several hemodynamic parameters in experimental animals.

5.3. Results

5.3.1. Effect of AT1 receptor blockade on infarct size and cardiac hypertrophy

There was no significant increase in LVW or RVW in 1-week post-MI hearts. Thus, the increased ratios of LVW and RVW to BW observed in experimental animals 1 week after MI was due to decreased BW. The 2 and 4 week experimental groups exhibited a significant increase in the mass of RV and noninfarcted LV tissue when compared to values from sham-operated hearts noted by the indices of LVW, RVW, the ratio of RVW/BW and LVW/BW (Table 3). Losartan treatment of experimental animals for 4 weeks was associated with the complete prevention of both LV and RV hypertrophy. It should be pointed out that the administration of losartan to infarcted experimental groups had no effect on infarct size.

5.3.2. Effect of AT1 receptor blockade on cardiac function

Loss of normal LV function was apparent at 2 weeks post-MI, as indicated by a decrease in ±dP/dt and an increase of LVEDP in the MI group when compared with sham-operated animals. Treatment with losartan had no effect on heart rate (HR) or on LVSP in either 2 or 4 weeks experimental groups (Table 4). On the other hand, 2 weeks treated post-

MI animals were characterized by significantly decreased MAP and LVEDP compared to values from the untreated group. Administration of losartan for 4 weeks was also associated with decreased MAP and LVEDP, as well as significantly increased ± dP/dt *vs* untreated post-MI animals (Table 4).

5.3.3. Effect of AT_1 receptor blockade on total collagen and Immunofluorescent staining of collagen types I and III

Total cardiac collagen concentration in surviving LV at 2 and 4 weeks was increased by 91.3% ($P<0.05$) and 150.4% ($P<0.05$), respectively. Similarly, total collagen concentration in RV samples from 2 and 4 week experimental groups were increased by 66.4% ($P<0.05$) and 77.6%, ($P<0.05$) respectively. Losartan treatment was associated with significantly decreased total collagen concentrations in both viable LV and RV (32.7% and 26.8%, respectively) at 4 weeks after the induction of MI (Figure 8). Immunofluorescent staining of collagen types I and III and these proteins were visualized by epifluorescent microscopy. We used longitudinal sections to view collagen type I and cross-sectional views to show collagen type III according to the method of Schaper *et al.*[16] Relatively low levels of collagen (bright, wavy appearance) are present in the interstitial space in those sections of sham-operated rats in both viable LV and RV. In 2 and 4 week experimental groups, the interstitium of viable LV remote to the infarct were characterized by markedly increased deposition of collagen type I (Figure 9A and B, Figure 10A and B). The 4 week losartan-treated group was associated with a ~47% inhibition of collagen type I accumulation (Figure 10C) but was associated with no effect after only 2 weeks treatment (Figure 9C). Similarly, collagen type III was found to be present throughout the entire ECM and was arranged in a true network in the extracellular space (Figure 9 and Figure 10). Collagen type III was increased in viable LV when compared to control at 2 and 4 weeks post-MI (Figures 9 and

10 D E). Collagen type III in the viable LV was reduced by ~33% with the administration of losartan for 4 weeks *vs* untreated experimental animals (Figure 10F).

5.3.4. Effect of AT_1 receptor blockade on mRNA abundance of collagen genes

Verification of the integrity of total fractionated RNA samples are provided by visualization of the 28S and 18S rRNA bands in a representative photograph of an agarose gel stained with ethidium bromide (Figure 11, upper panel). Specific hybridization of cDNA probes revealed characteristic mRNA bands, and these are shown in autoradiographs of representative blots probed with cDNAs of collagen types I, III, GAPDH and 18S rRNA (Figure 11, bottom panel). The calculated ratios for collagen/GAPDH and collagen/18S were performed with similar results. For example, the absolute ratios of collagen type I to GAPDH were 0.188 ± 0.01 for control, 1.633 ± 0.17 for MI, and 1.67 ± 0.24 for MI treated with losartan for 1 week in LV. All subsequent calculated ratios of collagen type I/GAPDH and collagen type III/GAPDH were shown as percentage of control (control = 100%) in Figure 12. In the viable LV, losartan treatment was not associated with any difference in either collagen type I and III mRNA abundance compared to untreated post-MI values at 1, 2, and 4 weeks (Figure 12A and B). Similarly, normalized values of RV fibrillar collagen mRNA abundance in experimental animals treated with losartan were not different from untreated experimental animals (Figure 12C and D). While collagen type III expression was elevated in both LV and RV at all times after the induction of infarction, the relative increases in expression of collagen type III mRNAs were less marked when compared to increases in collagen type I mRNAs.

5.3.5. Effect of AT_1 receptor blockade on cardiac prolyl 4-hydroxylase concentration

We observed an increase in immunoreactive cardiac prolyl 4-hydroxylase concentration in viable LV from 2 and 4 week experimental groups of 68.4% and 68.1%, respectively, compared to control animals. Two week (short term) losartan treatment of

experimental animals was observed to have no effect on prolyl 4-hydroxylase concentration *vs* values from the untreated 2-week post-MI group. On the other hand, 4 week AT_1 blockade was associated with a significant decrease in prolyl 4-hydroxylase concentration ($P<0.05$) in the viable LV (Figure 13).

Table 3. Effect of losartan on cardiac hypertrophy and infarct size in experimental rats after 1, 2 and 4 weeks treatment.

Parameters	1-week			2-week			4-week		
	Sham	MI	MI+losartan	Sham	MI	MI+losartan	Sham	MI	MI+losartan
BW, g	274 ± 7.7	250 ± 6.4*	252 ± 4.9 *	315 ± 3.3	284 ± 10*	282 ± 5.9*	395 ± 6.6	392 ± 11	388 ± 6.4
LVW, g	0.58 ± 0.02	0.61 ± 0.01	0.55 ± 0.01	0.69 ± 0.01	0.69 ± 0.03	0.64 ± 0.01	0.78 ± 0.03	0.90 ± 0.04*	0.79 ± 0.02#
LV/BW, mg/g	2.12 ± 0.30	2.44 ± 0.07 *	2.21 ± 0.07	2.19 ± 0.04	2.43 ± 0.08*	2.27 ± 0.05	1.97 ± 0.04	2.29 ± 0.05*	2.04 ± 0.05#
RVW, g	0.17 ± 0.01	0.18 ± 0.02	0.19 ± 0.01	0.20 ± 0.00	0.29 ± 0.02*	0.25 ± 0.01*	0.24 ± 0.01	0.36 ± 0.01*	0.27 ± 0.01#
RV/BW, mg/g	0.63 ± 0.02	0.72 ± 0.08*	0.76 ± 0.05*	0.673 ± 0.01	1.02 ± 0.08*	0.88 ± 0.04*	0.60 ± 0.02	0.92 ± 0.05*	0.70 ± 0.02 #
Infarct size, %	...	41 ± 3	40 ± 1	...	42 ± 3	39 ± 2	...	42 ± 3	40 ± 2

MI, myocardial infarction; Sham, noninfarcted age-matched control animals; BW, body weight; LVW, left ventricular wet weight; RVW, right ventricular wet weight. All losartan treatment regimens were initiated one day following coronary occlusion. Results are mean ± SEM of 6- 10 experiments. *P<0.05 and #P<0.05 *vs* sham-operated control and MI respectively at each time point.

Table 4. Effect of losartan (15 mg/kg/day) on hemodynamic characteristics in experimental rats after 2 and 4 weeks treatment.

Parameters	2-week			4-week		
	Sham	MI	MI+losartan	Sham	MI	MI+losartan
HR (beat/min)	410 ± 7	408 ± 8	406 ± 6	396 ± 6	392 ± 8	396 ± 9
MAP (mmHg)	101 ± 10	102 ± 9	90 ± 8*	102 ± 11	101 ± 9	91 ± 8*
LVSP (mmHg)	120 ± 13	110 ± 8	112 ± 7	121 ± 12	109 ± 7	110 ± 7
LVEDP (mmHg)	4.2 ± 0.1	12 ± 0.2*	8.2 ± 0.1* #	4.7 ± 0.1	16 ± 0.2*	8.5 ± 0.2*#
$+dP/dt_{max}$ (mmHg/sec)	5656 ± 212	4209 ± 207*	4571 ± 218*	5583 ± 220	4109 ± 203*	5196 ± 214#
$-dP/dt_{max}$ (mmHg/sec)	4672 ± 207	3632 ± 198*	3868 ± 201*	4531 ± 199	3402 ± 189*	4286 ± 195#

MI, myocardial infarction; Sham, noninfarcted age-matched control animals; HR, heart rate; MAP, mean arterial pressure; LVSP, left ventricular systolic pressure; LVEDP, left ventricular end diastolic pressure; $+dP/dt_{max}$, the maximum rate of isovolumic pressure development; $-dP/dt_{max}$, the maximum rate of rate of isovolumic pressure decay. All losartan treatment regimens were initiated one day following coronary occlusion. Results are mean ± SEM of 6- 10 experiments. *P and #P <0.05 *vs* sham-operated control and MI respectively at each time point.

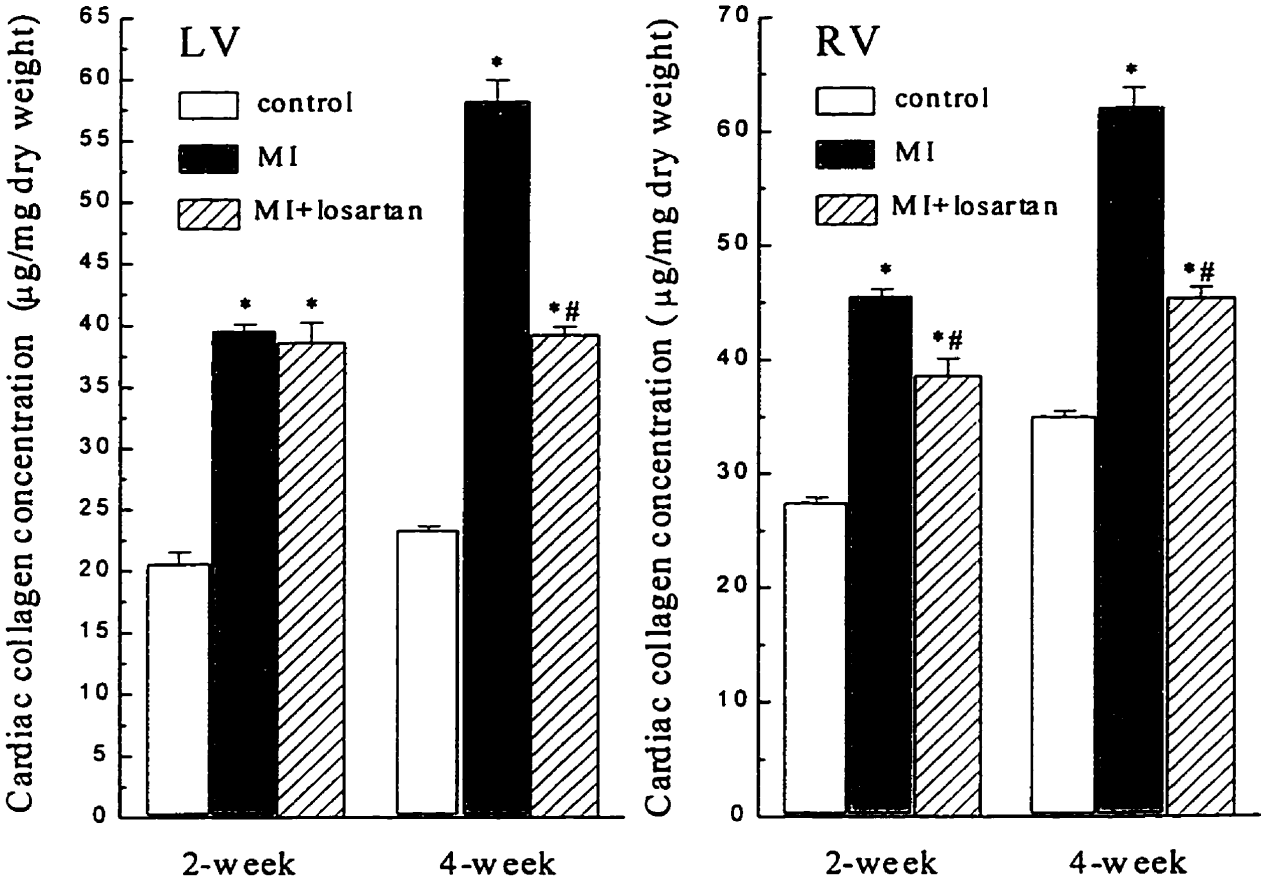

Figure 8. Effect of losartan (15 mg/kg/day) on total collagen concentration in viable left (LV) and right ventricles (RV) at different times after myocardial infarction (MI). All losartan treatment (2 and 4 weeks) regimens were initiated one day following coronary occlusion. The data depicted is the mean ± SEM of 8-10 experiments and were expressed as μg/mg dry weight. *P<0.05 and #P< 0.05 *vs* control and MI respectively.

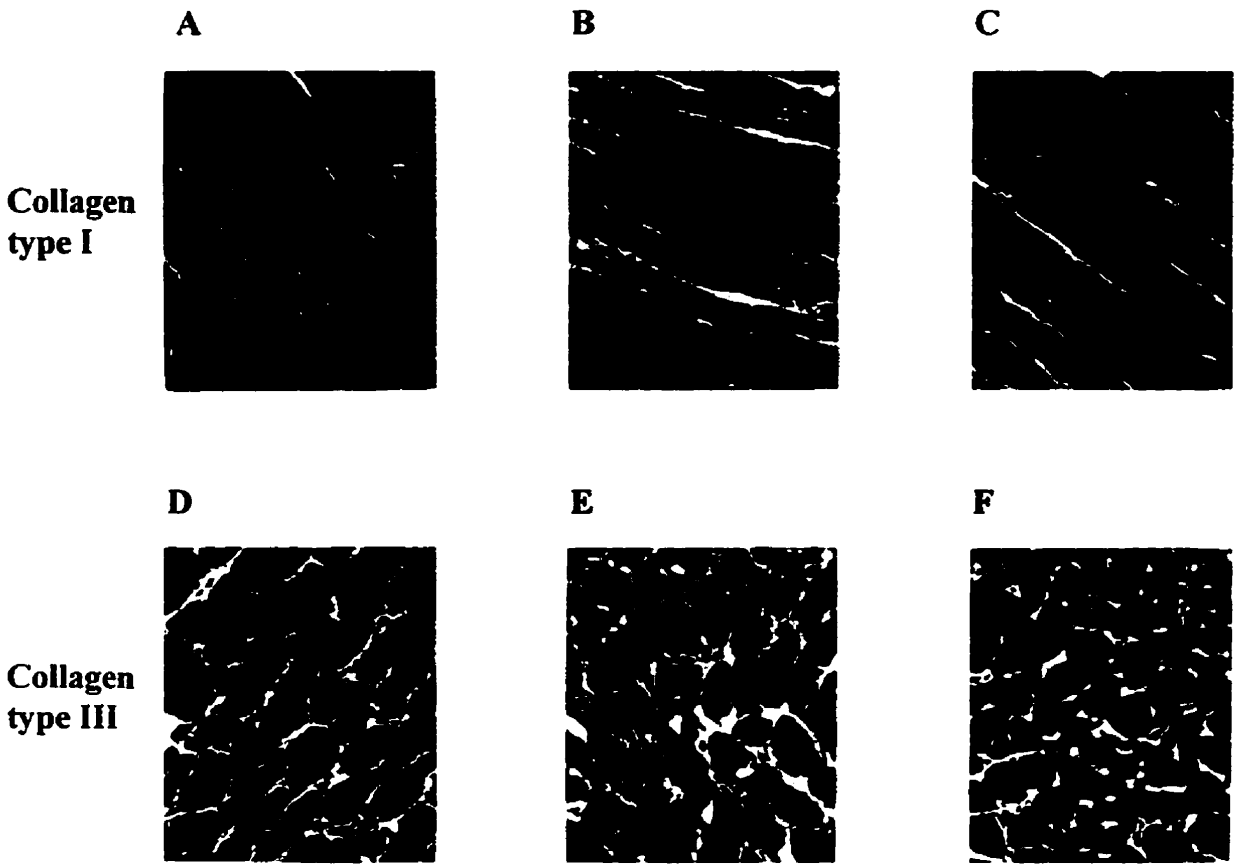

Figure 9. A representative immunofluorescent staining of collagen types I and III in viable left ventricular tissues 2 weeks post-MI. **A, B,** and **C** are collagen type I from sham-operated animals, myocardial infarction (MI) and MI treated with losartan for 2 weeks respectively. **D, E,** and **F** are collagen type III from sham-operated animals, myocardial infarction (MI) and MI treated with losartan for 2 weeks respectively. All losartan treatment regimens were initiated one day following coronary occlusion. Collagen type I appears as wavy fibers between myocytes and collagen type III appears as brightly stained material between myocytes. Magnification, x 400.

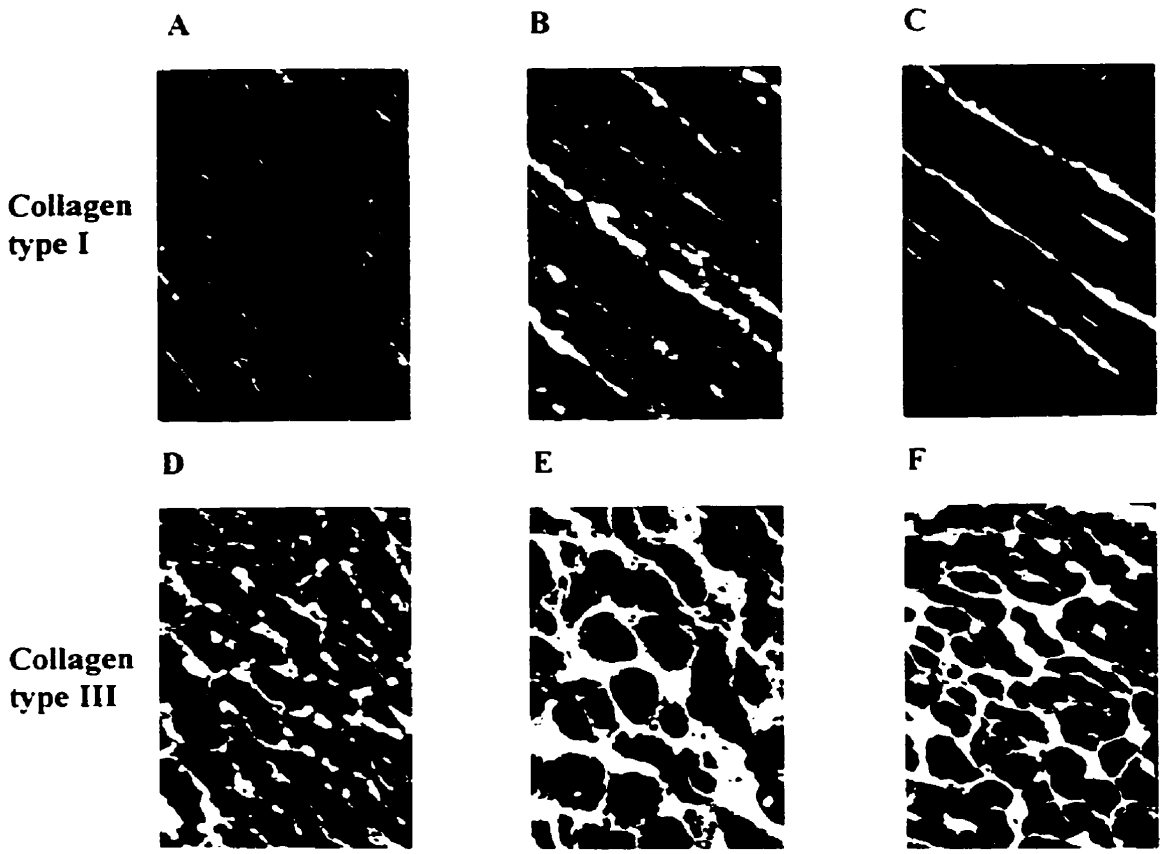

Figure 10. A representative immunofluorescent staining of collagen types I and III in viable left ventricular tissues 4 weeks post-MI. **A, B,** and **C** are collagen type I from sham-operated animals, myocardial infarction (MI) and MI treated with losartan for 4 weeks respectively. **D, E,** and **F** are collagen type III from sham-operated animals, myocardial infarction (MI) and MI treated with losartan for 4 weeks respectively. All losartan treatment regimens were initiated one day following coronary occlusion. Collagen type I appears as wavy fibers between myocytes and collagen type III appears as brightly stained material between myocytes. Magnification, x 400.

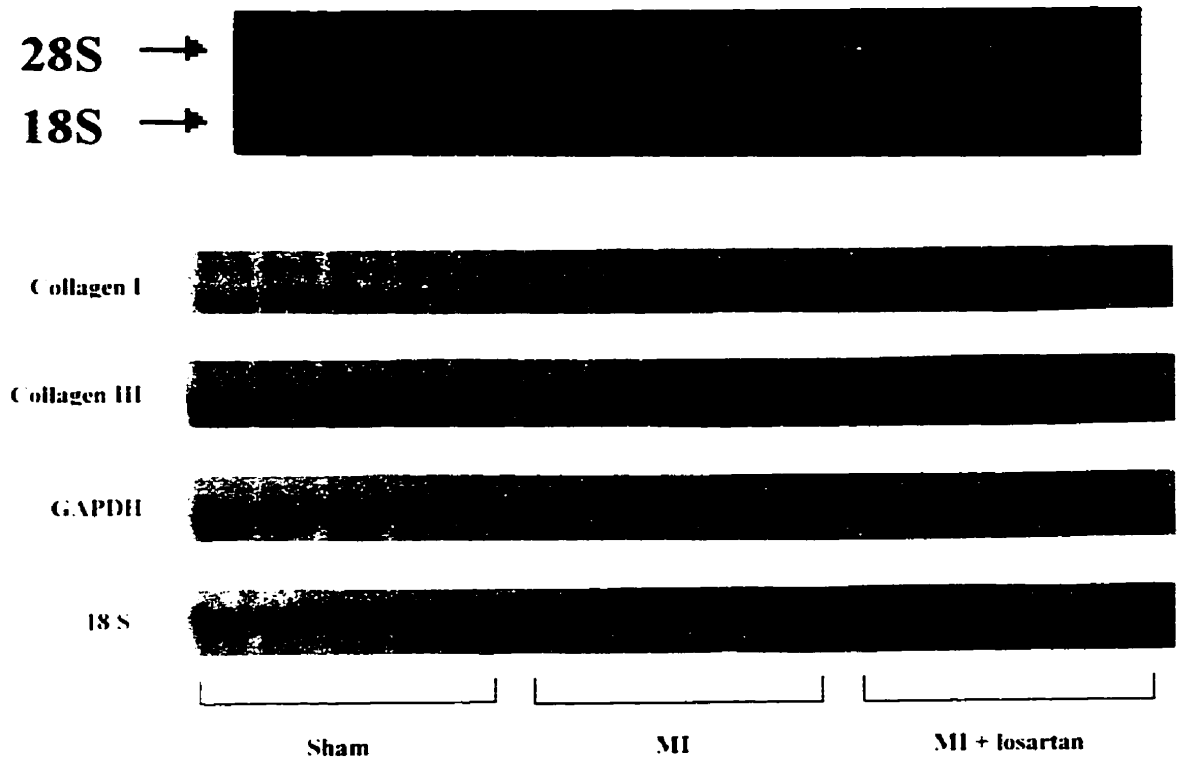

Figure 11. Upper panel: A representative agarose gel stained with ethidium bromide to visualize the 28 S and 18 S rRNA bands in total RNA samples extracted from viable left ventricular tissues at 4 weeks after MI. **Lower panel**: Autoradiograph from Northern blot analysis wherein each lane was loaded with 20 μg total RNA extracted from sham animals (lanes 1-5), myocardial infarction (MI, lanes 6-10) and MI treated with losartan (lanes 11-15) for 4 weeks after MI. All losartan treatment regimens were initiated one day following coronary occlusion. Hybridization of fractionated total RNA with cDNA probes for collagen types I and III, glyceraldehyde 3-phosphate dehydrogenase (GAPDH) and 18 S rRNA indicate relative steady-state mRNA levels for each gene tested.

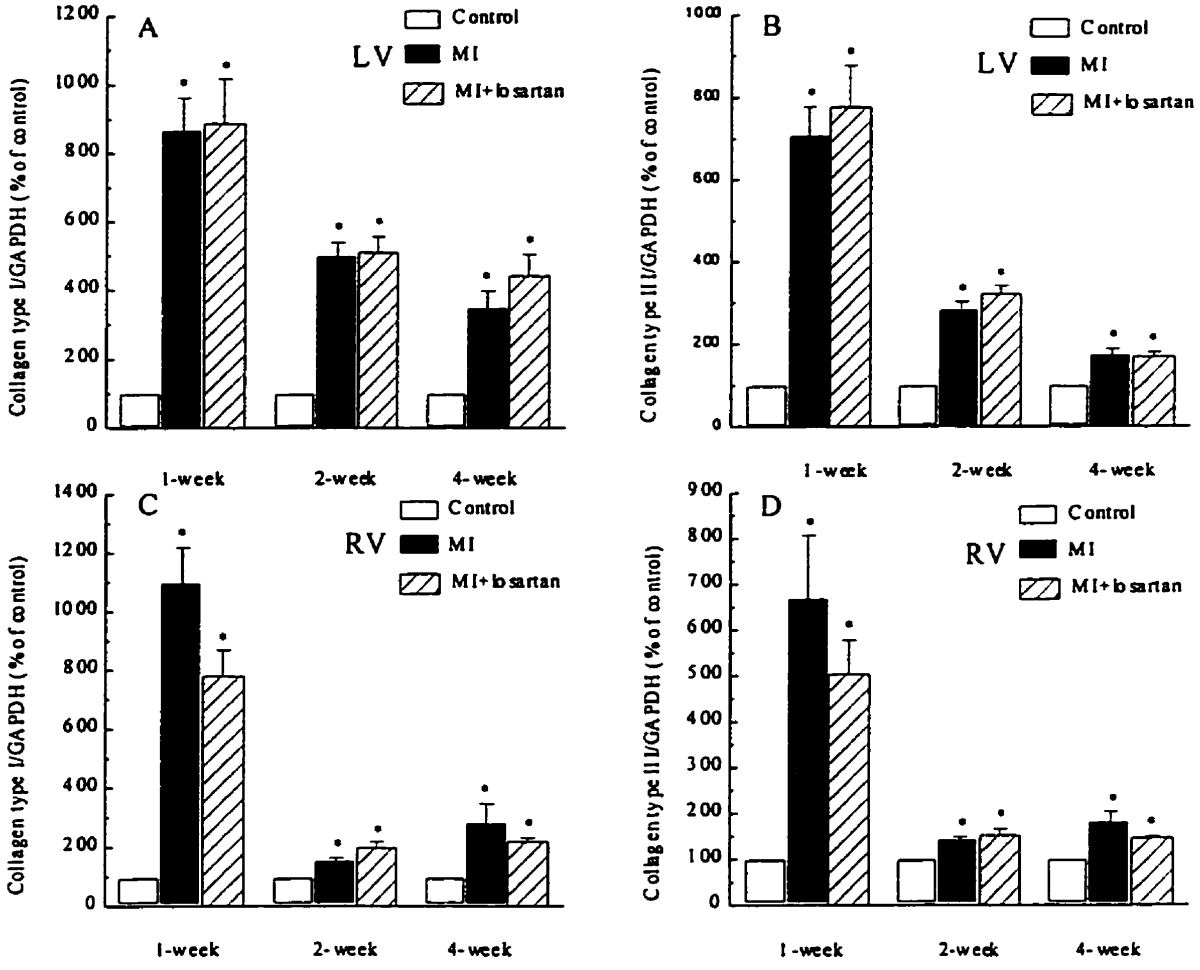

Figure 12. Effect of losartan (15 mg/kg/day) on collagen mRNA abundance in viable left (LV) and right ventricles (RV) at different times after myocardial infarction (MI). **Panel A**: Collagen type I/GAPDH signal ratio in LV; **Panel B**: Collagen type III/GAPDH signal ratio in LV; **Panel C**: Collagen type I/GAPDH signal ratio in RV; and **Panel D**: Collagen type III/GAPDH signal ratio in RV. All losartan treatment regimens were initiated one day following coronary occlusion. The data were expressed in densitometric units, normalized to glyceraldehyde-3-phosphate dehydrogenase (GAPDH) autoradiographic band intensity and noted as a *percent* value of control expression levels (%). The data depicted is the mean ± SEM of 5-6 experiments. *$P < 0.05$ for each MI value *vs* sham-operated values.

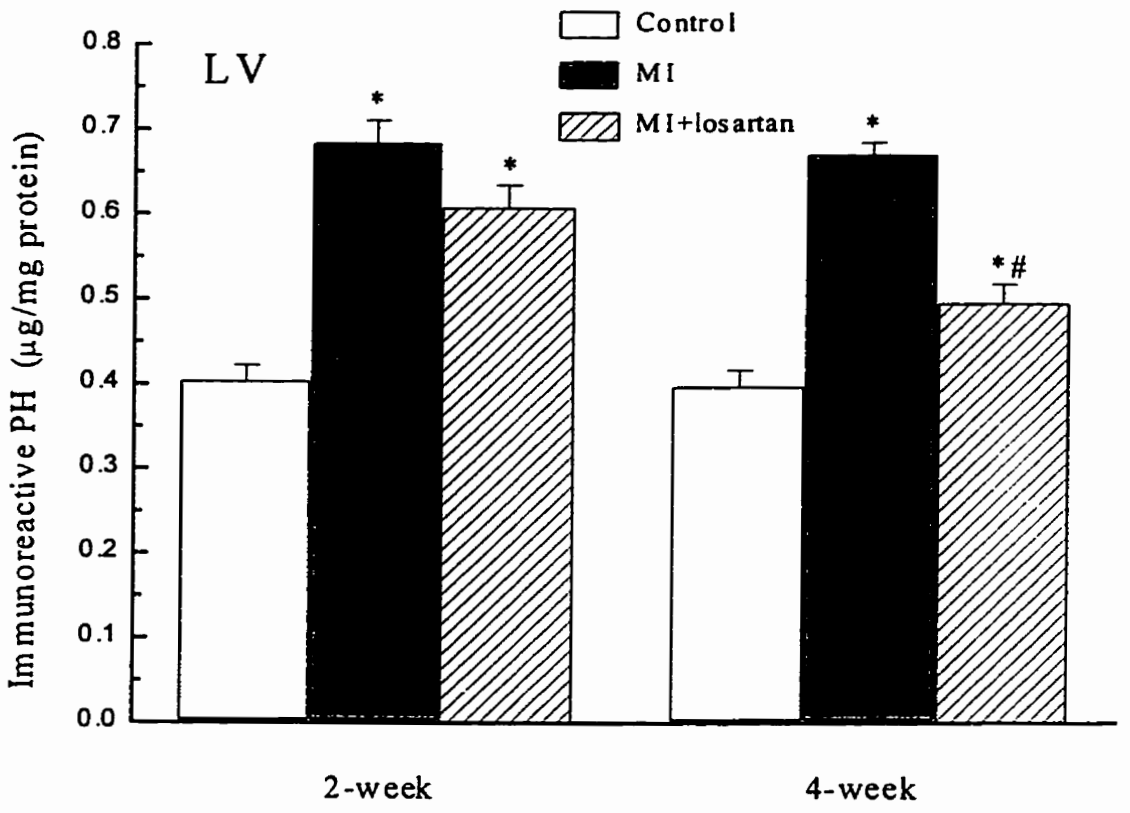

Figure 13. Effect of losartan (15 mg/kg/day) on prolyl 4-hydroxylase (PH) concentration in viable left ventricles in i) sham-operated animals, ii) myocardial infarction (MI) and iii) MI treated with losartan for 2 and 4 weeks. All losartan treatment regimens were initiated one day following coronary occlusion. The data depicted is the mean ± SEM of 6 experiments and were expressed as µg/mg protein. *P<0.05 and #P< 0.05 *vs* control and MI respectively.

5.4. Discussion

Ventricular remodeling in post-MI rat heart has been associated with increased concentration of Ang II in the infarct zone and with increased Ang II receptor density in the noninfarcted myocardium.[187,256] The classification system for the Ang II receptor population divides them into two major subtypes i.e., either AT_1 or AT_2, based on the binding affinities for the nonpeptide antagonists losartan and PD123177, respectively.[85-87] A great deal of work to date has shown that the cardiac AT_1 receptors mediate the majority of known physiological effects of Ang II in heart.[73] The rationale for conducting the current study using AT_1 receptor antagonism is based on findings to support the hypothesis that the AT_1 receptor subtype is the primary Ang II receptor in cardiac fibroblasts,[255] and that this receptor specifically mediates simulation of collagen synthesis by Ang II in these cells.[21,22] Furthermore, a recent study has shown that the AT_2 antagonist PD123319 had no effect on cardiac function or on interstitial fibrosis in post-MI rats with heart failure.[184] The prevention of cardiac hypertrophy in experimental animals from the current study after 4 weeks losartan treatment is in agreement with previous findings.[180] This result provides further support for the involvement of Ang II in the hypertrophic process via activation of the AT_1 receptor. Inhibition of cardiac hypertrophy may be related to i) attenuation of cardiac myocyte growth and/or ii) the inhibition of the cardiac fibroblast replication,[180] as well as the reduction of ECM protein accumulation. We have also shown that 4 week losartan treatment of post-MI rats was associated with prevention of the development of LV dysfunction, in agreement with previous studies.[174,257] Specifically, losartan treatment of post-MI animals was associated with prevention of abnormally elevated LVEDP, possibly due to the preservation of normal cardiac contraction and relaxation.

Administration of losartan for 2 weeks to experimental animals was associated with modest differences in the deposition of total collagens in RV, while this regimen had no

apparent effect on collagen concentration in noninfarcted LV samples *vs* untreated animals. Although others have reported significant inhibition of total collagen deposition in viable LV post-MI with the same dosage and duration of losartan treatment,[180] it is possible that this discrepancy at very early points may be due to methodological differences employed for cardiac collagen detection. In contrast to 2 week therapy of experimental animals, 4 week losartan treatment was associated with partial prevention of fibrosis in experimental animals compared to the untreated animals in both LV and RV samples. Our findings with respect to immunofluorescent studies of fibrillar collagens in noninfarcted muscle yielded similar results. Thus, the incidence of fibrosis in this experimental model may be mediated by activation of the AT_1 receptor localized on adult cardiac fibroblasts. The precise mechanism for the antifibrotic action of losartan in RV and LV after induction of MI is unclear. In this regard, inhibition of cardiac fibroblast proliferation and/or inhibition the synthesis of collagen may be considered as possible mechanisms. Although Ang II may directly stimulate DNA, RNA, and protein synthesis in cultured adult cardiac fibroblasts via AT_1 receptor activation,[22] previous work has shown that increased cardiac fibroblast proliferation in noninfarcted post-MI heart is a transient event (peak proliferation at 1 week after MI).[179] Furthermore, losartan treatment of post-MI rats was shown to lead to only slight attenuation of nonmyocyte proliferation (including endothelial cells and fibroblasts) 2 weeks after induction of MI.[180] Thus it is unlikely that cardiac fibroblast proliferation plays an major role in the attenuation of cardiac fibrosis losartan in the rat model of chronic MI. As the mRNA abundance of cardiac fibrillar collagens does not appear to be influenced by losartan treatment of any duration in this experimental model, our findings suggest that the partial prevention of collagen accumulation by AT_1 blockade may be mediated at other point(s) within cardiac collagen synthesis. It is pointed out that the current data does not rule out possible involvement of collagen transcriptional events with losartan treatment.

Nevertheless, our current results are in agreement with a recent report which demonstrated that treatment of rats with a novel AT_1 receptor antagonist (TCV-116) was not associated with any normalization of elevated collagen mRNA abundance after the induction of MI.[258] In contrast, others have shown that TCV-116 may significantly inhibit cardiac collagen type I and III mRNA abundance in stroke-prone spontaneously hypertensive rats (SPSHR).[259] Although the precise mechanism(s) for the differential responses of steady-state mRNA levels in rats with MI and those with spontaneous hypertension to AT_1 blockade remain unclear, they may be linked to the type and stage of disease. Presumably, Ang II is not the sole stimulus for the induction of cardiac fibrosis. Thus SPSHR and post-MI rat heart may be subject to unique hormonal and mechanical stimuli i.e., the presence or absence of hypertension, resulting in a disease-specific response to any given therapy. As the doses of TCV-116 associated with inhibition of collagen mRNA abundance is attended by significant reduction of systolic blood pressure,[259] the effect of TCV-116 in SPSHR may be related to normalization of blood pressure.

As we have shown a partial prevention of collagen deposition with AT_1 blockade, other factors such as transforming growth factor β1 (TGF-β1) may be involved in the regulation of collagen expression in post-MI heart,[208] although the role of this factor is not well understood in relation to the pathogenesis of heart failure and increased Ang II generation. Second, as both LV and RV chambers are subject to altered preloading and afterloading of post-MI hearts, it was hypothesized that hemodynamic loading is involved in the regulation of collagen mRNA expression.[175] Nevertheless, as losartan treatment has been associated with preservation of normal cardiac preload and afterload without corresponding normalization of collagen mRNA abundance in noninfarcted post-MI hearts, it is possible that other factor(s) may regulate fibrillar collagen expression.

A discrepancy between collagen gene activation and collagen deposition has been reported in aging rats.[47] It has been known that a significant proportion (36-96%) of newly synthesized procollagen monomers are routinely degraded upon their translation in both normal and hypertrophic hearts.[46,260] Thus, it is possible that the rate of intracellular procollagen degradation is controlled by posttranslational processing and that any alteration in protein modification may affect collagen deposition *in vivo*. The increase of immunoreactive prolyl 4-hydroxylase in viable heart muscle may be a major mechanism for increased deposition of collagen in post-MI heart. We found that losartan treatment prevented the elevation of prolyl 4-hydroxylase protein concentration in LV from experimental animals which correlated with the inhibition of total collagen protein in treated hearts. This finding supports the hypothesis that the antifibrotic effect of losartan is mediated via the inhibition of prolyl 4-hydroxylase. This study also provided evidence that Ang II may be involved in modulation of post-translational regulation of cardiac collagen in post-MI myocardium. The signaling pathway mediated by Ang II in post-MI remodeling need further investigation.

In summary, our results indicated that Ang II is involved in the development of cardiac hypertrophy and cardiac fibrosis in post-MI rat heart. Secondly, losartan treatment was not associated with any effect on increased steady-state collagen mRNA abundance in ventricular tissues after MI. We provide evidence that the partial prevention of fibrosis mediated by losartan in post-MI rat heart may be effected at the posttranslational level of collagen synthesis, and may be due to normalization of increased prolyl 4-hydroxylase protein concentration in tissues remote to the site of infarction.

Chapter 6. Expression of $G_{q\alpha}$ and PLC-β in Scar and Border Tissue in Heart Failure Due to Myocardial Infarction

6.1. Summary

Large transmural MI leads to the maladaptive cardiac remodeling, and places patients at increased risk of CHF. Ang II, endothelin (ET), and α_1 adrenergic receptor agonists are implicated in the development of cardiac hypertrophy, interstitial fibrosis and heart failure after MI. As these agonists are coupled to and activate $G_{q\alpha}$ protein in the heart, the aim of the current study was to investigate $G_{q\alpha}$ expression and function in cardiac remodeling and heart failure after MI. MI was produced in rats by ligation of the left coronary artery, and $G_{q\alpha}$ protein concentration, localization and mRNA abundance were noted in surviving LV remote to the infarct, in border and in scar tissues from 8 week post-MI hearts with moderate heart failure. Immunofluorescent staining localized elevated $G_{q\alpha}$ expression in the scar and border tissues. Western analysis confirmed significant upregulation of $G_{q\alpha}$ proteins in these regions *vs* controls. Furthermore, Northern analysis revealed that the ratios of $G_{q\alpha}$/GAPDH mRNA abundance in both scar and viable tissues from experimental hearts were significantly increased *vs* controls. Increased expression of PLC-β1and PLC-β3 proteins was apparent in the scar and viable tissues after MI *vs* controls, and is associated with increased PLC-β1 activity in experimental hearts. Furthermore, cardiac IP_3 concentration and total PKC activity were significantly increased in the border and scar tissues when compared to control values. Upregulation of the $G_{q\alpha}$/PLC-β pathway was observed in the viable, border and scar tissues in post-MI hearts. $G_{q\alpha}$ and PLC-β may play important roles in scar remodeling as well as cardiac hypertrophy and fibrosis of the surviving tissue in post-MI rat heart. It is suggested that the $G_{q\alpha}$/PLC-β pathway may provide a possible novel target for altering post infarct remodeling.

6.2. Introduction

MI is characterized by early infarct expansion in which the infarct region thins and elongates, and is followed by discrete scar formation via the wound healing response.[3,6] The effect of scar formation after MI is contingent upon the size of the MI insofar as decreased net contractile force associated with relatively small MI is sufficiently compensated by the viable myocardium and thereby ventricular performance and geometry are maintained. After large MI, ventricular chamber dilatation and sphericalization is attended by cardiac hypertrophy and interstitial fibrosis, leading to the loss of normal cardiac function.[2] An understanding of the molecular mechanisms that underlie processes at the site of infarct healing as well as those during the development of interstitial cardiac fibrosis and hypertrophy is warranted.[5,6]

Although the signaling properties of $G_{i\alpha 2}$ and $G_{s\alpha}$ in heart failure secondary to MI and hypertension have been investigated,[261,262] specific information addressing the status of $G_{q\alpha}$ expression and function in heart failure is lacking. The $G_{q\alpha}$ protein is necessary and sufficient for the induction of cardiac myocyte hypertrophy mediated by phenylephrine in cultured cardiac myocytes.[263] Ang II, ET and α_1 adrenergic receptor agonists have been implicated in the development of maladaptive cardiac hypertrophy and fibrosis.[41,185,264] Stimulation of AT_1,[23,24] ET,[265,266] or α_1 adrenergic receptors[263] has been demonstrated to induce myocyte hypertrophy, which is mediated by $G_{q\alpha}$. Activated $G_{q\alpha}$ protein is known to stimulate PLC-β,[25] which hydrolyzes phosphatidylinositol 4, 5-bisphosphate to release IP_3 and DAG. Both IP_3 and DAG are involved in proliferation of cardiac fibroblasts and myocyte hypertrophy mediated by further downstream signaling mechanisms.[24] It should be noted that Ang II concentration is increased at the site of infarct healing (scar) after induction of MI.[187] Furthermore, increased expression of AT_1 receptors in both viable and

scar tissues of post-MI rat hearts have been reported[183,189,267] suggesting that Ang II may be involved in wound healing of scar tissues as well as in myocyte hypertrophy. Similarly, increased ET and ET receptor density has been demonstrated in post-MI rat heart.[264] Furthermore, increased cardiac α_1 adrenergic receptor density is present in rat with chronic heart failure.[268]

It is conceivable that $G_{q\alpha}$ is upregulated in post-MI hearts and is involved in the ongoing alteration of scar tissue as well as in the development of myocyte hypertrophy and fibrosis of surviving myocardium. The present study was conducted to examine myocardial $G_{q\alpha}$ protein quantity and localization in the ventricular myocardium remote to the site of infarction as well as in border and scar regions of failing hearts subsequent to MI; in addition, cardiac $G_{q\alpha}$ mRNA abundance was investigated. To examine the functional significance of $G_{q\alpha}$ in post-MI hearts, we addressed the protein levels of PLC-β1 and PLC-β3 (downstream effector), PLC-β1 as well as PKC activities and IP_3 accumulation in experimental hearts.

6.3. Results

6.3.1. General observations: Left ventricular cardiac hypertrophy, fibrosis and heart failure

Experimental animals in this study were characterized by the presence of large MI which was comparable to values reported earlier. Hearts of experimental animals underwent significant cardiac hypertrophy which was reflected by increase in the mass of viable LV weight and also by the increased ratio of LVW to BW in 8 weeks experimental animals compared to control values (Table 5). The incidence and magnitude of LV hypertrophy noted in this study was comparable to our previous findings.[224] Animals were assessed for LV function at 8 weeks post-MI, and these data revealed an increase in LVEDP and a

decrease in $\pm$ dP/dt_{max} relative to their controls. Lung congestion was noted by the wet weight/dry weight ratio (Table 5). Collagen concentration in myocardium remote to the site of infarct (47.0 ± 3.2 μg/mg dry wt) and border + scar tissues (110.4 ± 12.4 μg/mg dry wt) were both significantly higher than that of the sham control value (22.4 ± 2.4 μg/mg dry wt).

6.3.2. Localization of cardiac $G_{q\alpha}$

$G_{q\alpha}$ protein distribution in 8-week experimental and age-matched control tissues was localized using immunofluorescent techniques. In the representative photograph (Figure 14), the staining pattern of immunoreactive $G_{q\alpha}$ is marked by bright clusters along the myocyte cell membranes. The results demonstrate that relatively strong staining of $G_{q\alpha}$ was localized in scar tissue proper and in hypertrophied cardiac myocytes that bordered on scar tissue; comparatively less immunoreactive protein was visualized in surviving (viable) tissues and in control myocardium (Figure 14).

6.3.3. Changes in cardiac $G_{q\alpha}$ protein abundance in hearts with MI

Quantitative assessment of cardiac membrane $G_{q\alpha}$-protein level in control and LV tissues of 8-week post-MI rats was carried out using Western blot techniques. Figure 15A provides a representative autoradiograph illustrating the presence of a characteristic 42 kDa band for $G_{q\alpha}$ protein. These data indicated that $G_{q\alpha}$ was increased by approximately 2.0 - and 2.5-fold in border and scar tissue, respectively, compared to band intensity from control animals. There was no significant alteration of the $G_{q\alpha}$ band intensity in samples from viable LV *vs* controls (Figure 15 B).

6.3.4. Alteration of steady-state mRNA abundance of cardiac $G_{q\alpha}$

We addressed mRNA abundance of the cardiac $G_{q\alpha}$ gene in tissues taken from various LV regions of rats 8 weeks post-MI. Figure 16A shows a representative Northern

blot with autoradiographic bands for $G_{q\alpha}$ and GAPDH mRNAs from LV samples of sham, viable, as well as border + scar tissues. The transcription of the $G_{q\alpha}$ gene is variably processed, as reported by other;[269] we found the presence of three different $G_{q\alpha}$ transcripts of 7.5 kb, 6 kb and 5 kb in our blots (Figure 16A). Estimation of $G_{q\alpha}$ mRNA abundance was calculated by the ratio of $G_{q\alpha}$ to GAPDH signal; this ratio was significantly increased in both the viable (1.4-fold) and border + scar tissue (3-fold) regions of the LV vs controls (Figure 16B). Furthermore, mRNA signals ratios from border and scar tissue samples were significantly increased (2.2-fold) in $G_{q\alpha}$/GAPDH mRNA values *vs* those obtained from surviving viable LV.

6.3.5. Alteration of cardiac PLC-β protein and activity

Western analysis was used to determine immunoreactive PLC-β protein bands. Figure 17A and 17B depicts a representative blot with bands corresponding to PLC-β1 (150 and 140 kDa) and PLC-β3 (152 kDa) proteins respectively. Densitometric analysis of band intensity revealed a significant increase in both PLC-β1 (Figure 17C) and PLC-β3 (Figure 17D) protein abundance in viable, border and scar tissues compared to scanned samples from control hearts. In order to determine whether actual PLC-β1 activity was altered in the surviving (viable) and scar tissue from experimental hearts, PLC-β1 proteins were immunoprecipitated from solubilized membrane extracts of the aforementioned tissues. These experiments revealed that PIP_2 hydrolysis by PLC-β1 was significantly increased in surviving myocardium from experimental hearts *vs* age-matched controls (Figure 18). Furthermore, PLC-β1-mediated PIP_2 hydrolysis activity from scar lysates was significantly elevated compared to values from both control and viable groups (Figure 18).

6.3.6. Alteration of cardiac IP_3

IP_3 is a downstream signal molecule generated by PLC activity and its concentration was detected in various tissues from post-MI and control hearts. IP_3 concentration was markedly increased in border + scar tissue when compared to values derived from assays of viable and sham control samples (Figure 19).

6.3.7. Alteration of cardiac PKC activity

Cardiac total PKC activities were detected in different region of LV tissues from sham-operated and MI rats. The results revealed that PKC activities of both cytosolic and membrane fractions in border and scar tissues were significantly elevated when compared with values from sham and viable tissues (Figure 20, $P<0.05$).

Table 5. General and hemodynamic characteristics of sham and experimental rats 8 weeks after induction of myocardial infarction (MI).

Parameters	Sham	MI
BW, g	514 ± 8.5	482 ± 11
LVW, g	0.91 ± 0.03	0.99 ± 0.02*
LV/BW, mg/g	1.77 ± 0.04	2.01 ± 0.04*
Lung wet/dry wt. Ratio	3.55 ± 0.26	4.83 ± 0.29*
LVEDP, mmHg	3.38 ± 0.70	13.35 ± 1.50*
LVSP, mmHg	136 ± 10	117 ± 12
$+dP/dt_{max}$, mmHg/s	5667 ± 286	4464 ± 220*
$-dP/dt_{max}$, mmHg/s	5404 ± 230	3915 ± 252*

MI indicates experimental animals with large left ventricular myocardial infarction; sham, noninfarcted age-matched control animals; Bw, body weight; LVW, left ventricular weight; LVEDP, LV end-diastolic pressure; LVSP, LV systolic pressure; $+dP/dt_{max}$, the maximum rate of isovolumic pressure development; $-dP/dt_{max}$, the maximum rate of isovolumic pressure decay. The data depicted is the mean ± SEM of 8-10 experiments. *$P < 0.05$ *vs* sham-operated animals.

Figure 14. Immunofluorescent stained sections showing $G_{q\alpha}$ in sham hearts, as well as viable, border and scar tissues from post-myocardial infarction (MI, 8 weeks). Immunoactive $G_{q\alpha}$ protein appear as brightly stained material as indicated by arrows. Magnification, x 400.

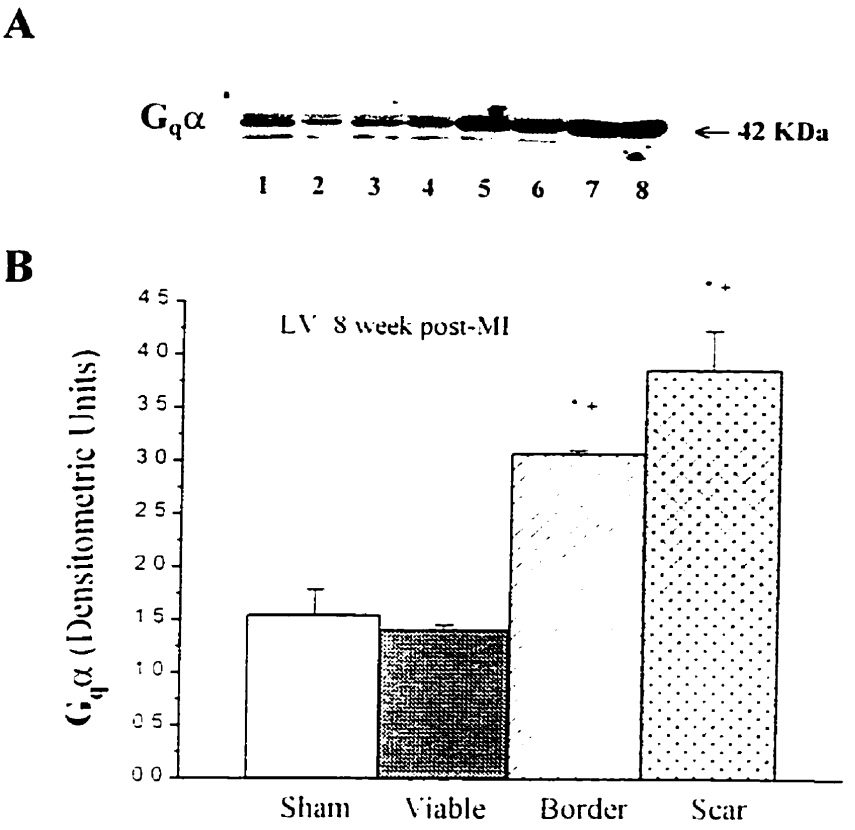

Figure 15. Western blot for $G_{q\alpha}$ in sham, viable, border and scar tissues from 8 weeks experimental animals. **A.** Representative Western blot showing specific band for 42 KDa $G_{q\alpha}$. Lanes 1 and 2 are sham, lanes 3 and 4 are viable LV, lanes 5 and 6 represent border tissue, and lanes 7 and 8 are scar. **B.** Quantified data of $G_{q\alpha}$ protein concentration in sham, viable, border and scar tissue. The control group is sham-operated rats, age matched to the 8-week post-MI experimental group. The data depicted is the mean ± SEM of 6 experiments. $^{*}P < 0.05$ and $^{+}P < 0.05$ *vs* sham and viable sample values, respectively.

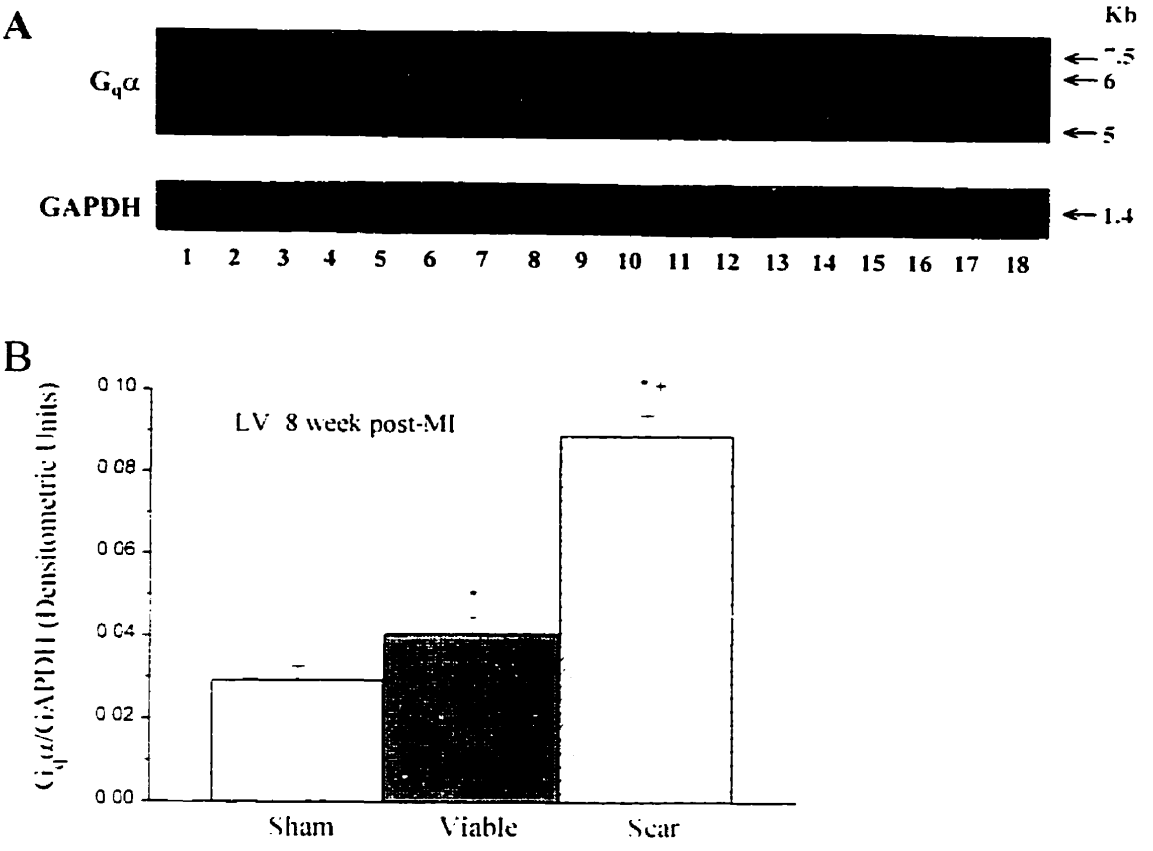

Figure 16. A. A representative autoradiograph from Northern blot analysis showing $G_{q\alpha}$ bands of 7.5 kb, 6 kb and 5 kb in sham (lanes 1-6), viable (lanes 7-12) as well as border and scar tissues (lanes 13-18) from hearts of 8 week post-myocardial infarction (MI) rats. Hybridization of fractionated total RNA with cDNA probes for $G_{q\alpha}$ and glyceraldehyde 3-phosphate dehydrogenase (GAPDH) indicates relative steady-state mRNA levels for each gene tested. **B.** Quantified data of $G_{q\alpha}$/GAPDH in sham, viable, as well as border and scar tissue. The data depicted is the mean $\pm$ SEM of 6 experiments. $^{*}P < 0.05$ and $^{+}P < 0.05$ vs sham and viable sample value, respectively.

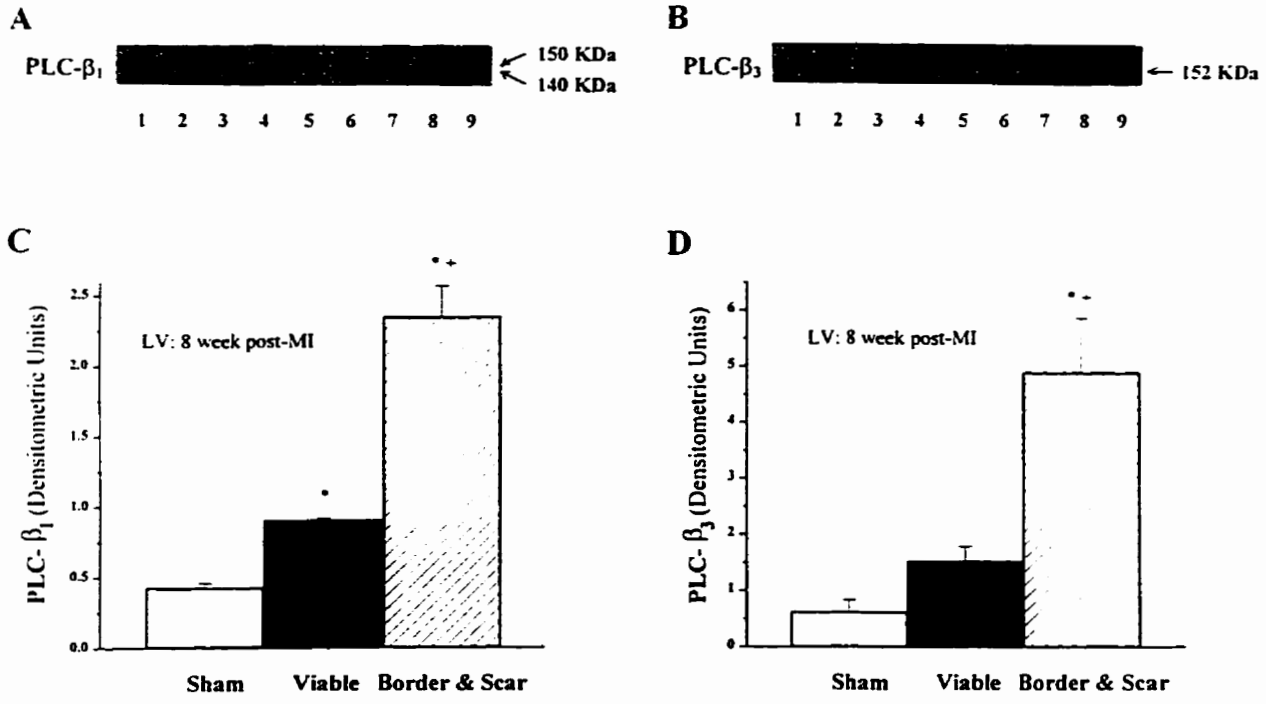

Figure 17. Western blot for phospholipase C-β (PLC-β) in sham, viable, border and scar tissue in post-MI (8 weeks) cardiac tissues. **A.** Representative Western blot showing 150 and 140 KDa PLC-β1. Lanes 1-3 are sham, lanes 4-6 are viable LV, lanes 7-9 represent border tissue and scar. **B.** Representative Western blot showing 152 KDa PLC-β3. Lanes 1-3 are sham, lanes 4-6 are viable LV, lanes 7-9 represent border tissue and scar. **C.** Quantified data of PLC-β1 protein concentration in sham, viable, border and scar tissues. **D.** Quantified data of PLC-β3 protein concentration in sham, viable, border and scar tissues. The data depicted is the mean ± SEM of 6 experiments. $^{*}P < 0.05$ and $^{+}P < 0.05$ *vs* sham and viable sample values, respectively.

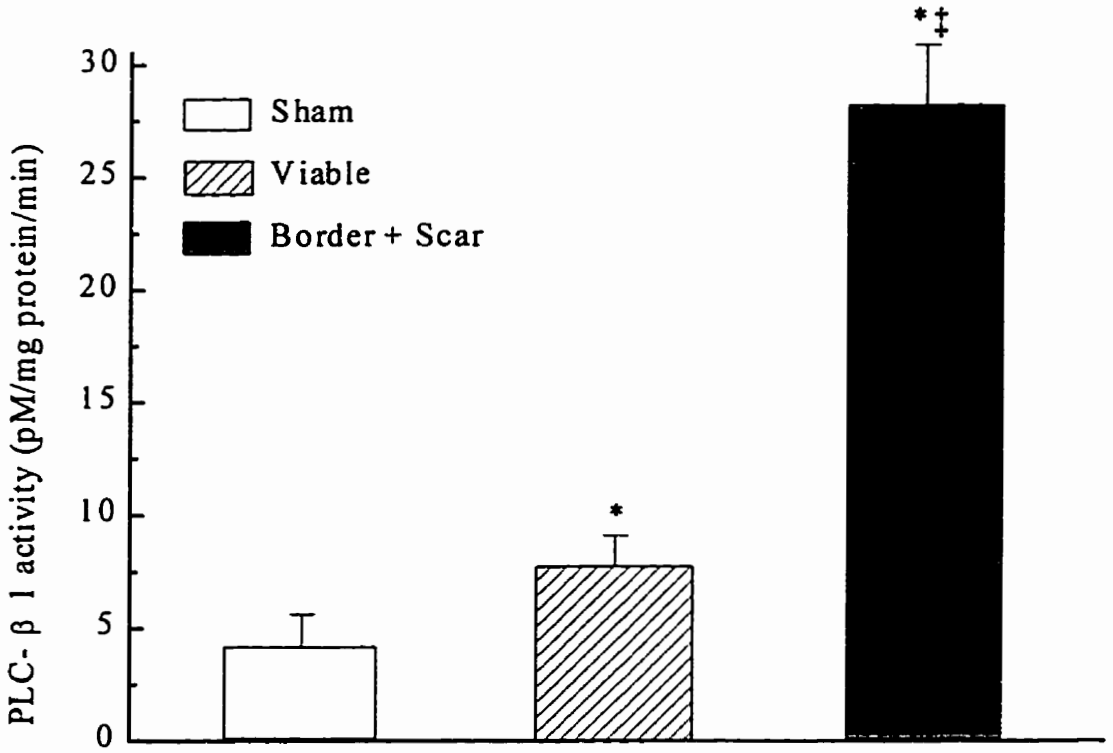

Figure 18. Cardiac phospholipase C-β1 (PLC-β1) activity in membrane fraction isolated from sham, viable, border and scar tissues in post-MI (8 weeks). PLC-β1 activity is expressed as pM/mg protein/minute. The data depicted is the mean ± SEM of 6 experiments. *P<0.05 and $^{+}$P<0.05 *vs* sham and viable sample values, respectively.

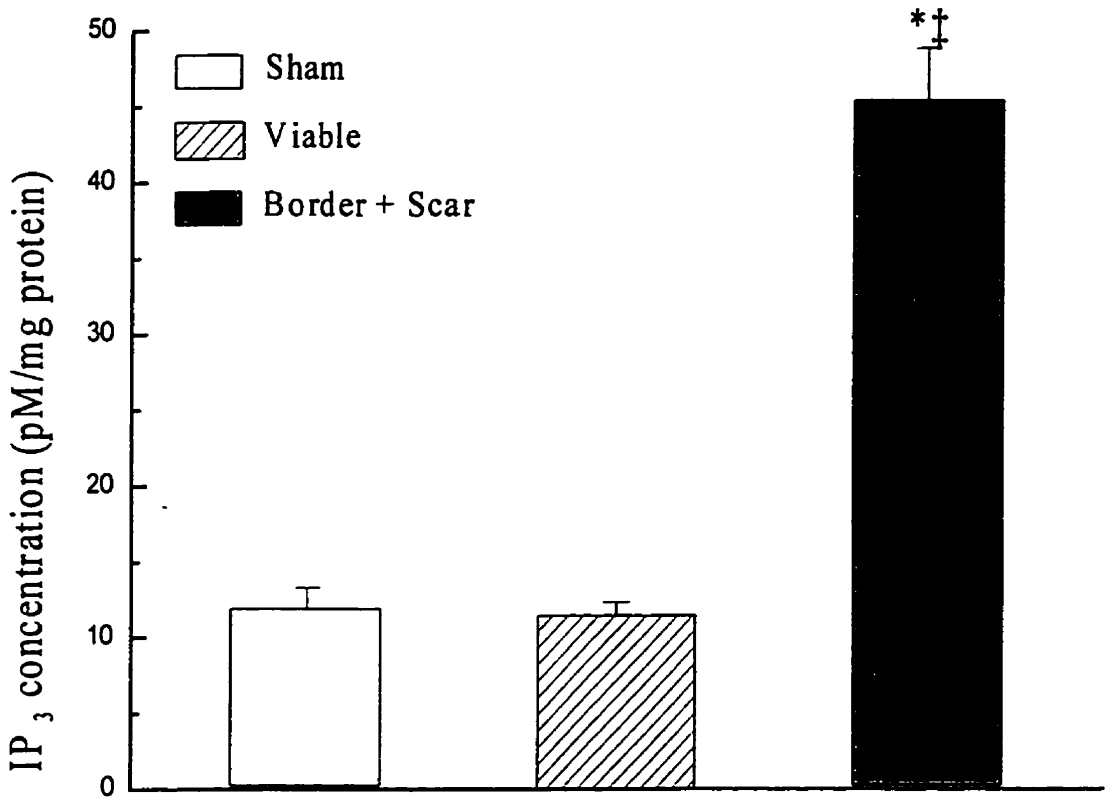

Figure 19. Cardiac inositol 1,4,5-trisphosphate (IP_3) concentration in cytosolic fraction isolated from sham, viable, border and scar tissues in post-MI (8 weeks). IP_3 concentration is expressed as pM/mg protein. The data depicted is the mean ± SEM of 4-6 experiments. *P<0.05 *vs* sham and viable sample values, respectively.

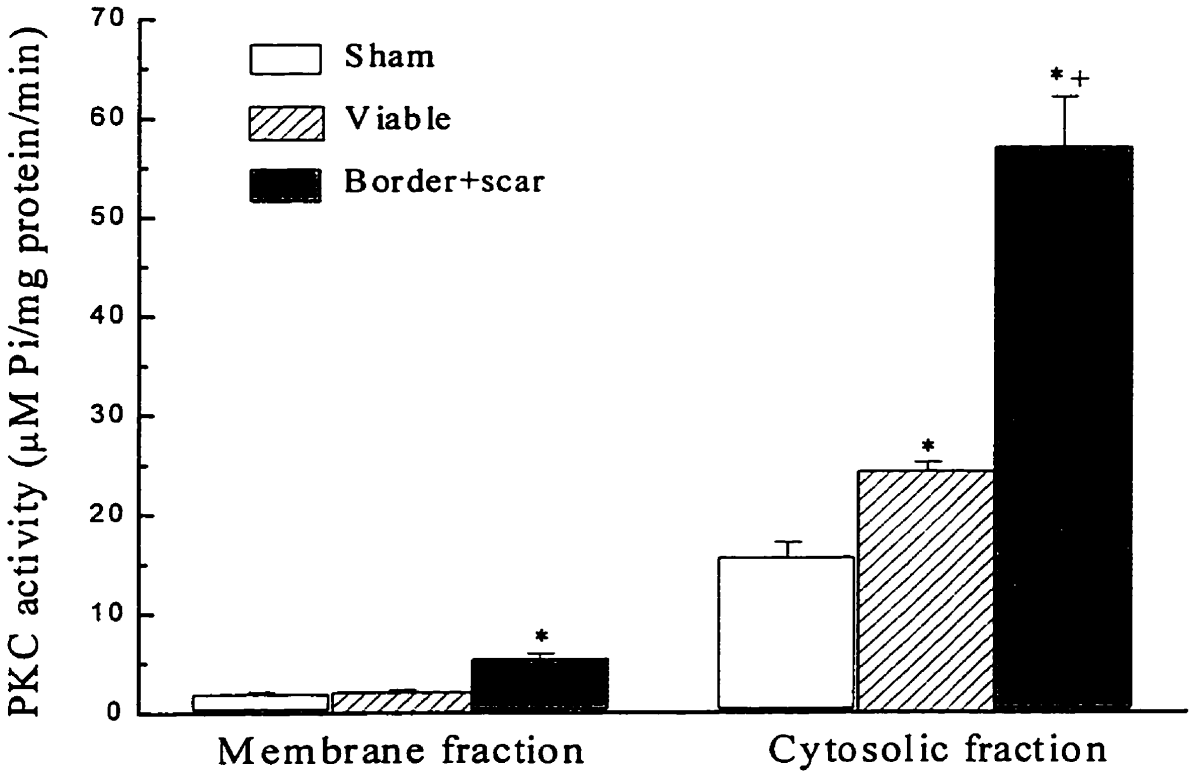

Figure 20. Cardiac total protein kinase C (PKC) activities in cytosolic and membrane fractions isolated from sham, viable, border and scar tissues in post-MI (8 weeks). PKC activity is expressed as μM Pi/mg protein/minute. The data depicted is the mean ± SEM of 4-6 experiments. *P<0.05 *vs* sham and viable sample values, respectively.

6.4. Discussion

6.4.1. Myocardial infarction and heart failure

Loss of normal LVSP and elevated LVEDP, decreased $\pm dP/dt_{max}$ as well as the presence of pulmonary congestion were noted in the 8-week experimental animals, it is thus the current experimental group was considered to be in a stage of "moderate heart failure". This classification matched our previous observation that the development of post-MI heart failure in rats with relatively large MI ($\geq$ 40% LV free wall) is time-dependent, and was in agreement with our previous arbitrary classification system established to facilitate the comparison of differently timed experimental groups.[224] The incidence of heart failure with clinical signs was established in the current study to provide a basis for objective comparison of cardiac dysfunction with changes in ventricular expression and function of target genes and gene products, respectively. In the current study, cardiac hypertrophy in the experimental group, as indicated by the LV weight and the ratio of LV to body weight was noted. Cardiac fibrosis in the viable remnant and scar tissues in post-MI hearts was confirmed in this investigation and was similar to the pattern of fibrosis observed in our previous studies.[8]

6.4.2. Role of $G_{q\alpha}$ expression and function in failing hearts: Experimental and clinical studies

The neurohormonal activation of the sympathetic and renin-angiotensin axes as well as the stimulation of various growth factors is important for the development of failure.[185,270] Among these factors, Ang II, norepinephrine and ET are major players in the regulation of cardiac fibrosis and myocyte hypertrophy, and $G_{q\alpha}$ is known to serve as the common signal coupler for these factors.[262] In a variety of clinical and experimental studies, altered $G_{i\alpha}$ and $G_{s\alpha}$ expression and function has been suggested as a mechanism mediating

the development of heart failure.[262] Heart failure subsequent to MI has been reported to be associated with altered bioactivity and/or expression of $G_{s\alpha}$ and $G_{i\alpha}$.[261,271] Although it has been reported that both $G_{q\alpha}$ and PLC-β are expressed in the heart,[272] the alteration of this signaling pathway in heart disease is unknown. The present study demonstrates for the first time that $G_{q\alpha}$ expression (both mRNAs and protein) is increased at the site of infarct healing and in myocardium bordering the scar. Upregulated expression of the $G_{q\alpha}$ and PLC-β pathway was evidenced in scar itself, and in myocardium bordering the scar, as well as viable tissue from post-MI heart. $G_{q\alpha}$ expression in tissues from post-MI hearts positively correlated with increased expression of its downstream effectors (PLC-β1 and PLC-β3) as well as increased PLC-β1 activity. The latter findings together with increased IP_3 accumulation and elevated total cardiac PKC activities suggest that the signal amplification function of $G_{q\alpha}$ is activated in scar tissue and border myocardium in experimental hearts. Translocation of cardiac PKC is known to occur in association with $G_{q\alpha}$ activation, this parameter remains to be demonstrated in our experimental hearts. The high level of $G_{q\alpha}$ and PLC-β activity and expression in the relatively hypocellular scar may be explained by the presence of myofibroblasts at this site which are distinguished from other fibroblasts by their expression of α-actin.[65,273] These cells have been localized in the scar 90 days after MI in rat heart[65] and are known to express Ang II, ACE, and Ang II receptors.[267,274] We have observed the presence of a substantial number of these cells in the scar from 8 week experimental animals. Furthermore, scar from post-MI patients are known to be populated by myofibroblasts and persist in these hearts for years.[275] The high level of $G_{q\alpha}$ and PLC-β expression may reflect the hyperfunctionality of these myofibroblasts in ongoing scar remodeling. Our data provides strong evidence of a correlation between the enhanced

expression and function of the $G_{q\alpha}$/PLC-β pathway at the site of infarct healing as well as in the development of post-MI cardiac hypertrophy and heart failure. This hypothesis is supported by a recent study demonstrating that overexpression of $G_{q\alpha}$ induces cardiac hypertrophy and heart failure.[276]

6.4.3. Increased $G_{q\alpha}$ expression: molecular mechanisms

The precise molecular mechanisms for increased $G_{q\alpha}$ expression in scar and border regions in infarcted heart are unknown. Upstream receptors (Ang II, ET, etc) for $G_{q\alpha}$ activation are characteristically upregulated in surviving LV myocardium in experimental animals, and these alterations occur in relatively early stages of healing after MI.[183,264] Administration of losartan, an AT_1 receptor antagonist, has been associated with the attenuation of cardiac hypertrophy and fibrosis in post-MI hearts.[171] Recently the application of an ET receptor blocker (BQ-123) was associated with improved heart function and reduced mortality after MI.[264] We suggest that changes in the receptor density of multiple neurohormonal factors may lead to increased downstream $G_{q\alpha}$ expression, and further experiments are required to test this hypothesis. Our data provide new evidence that expression/function of the common molecular pathway for these receptors are augmented in scar and surviving post-MI myocardium.

It is well known that $G_{q\alpha}$ selectively activates PLC-β1, but not PLC-γ1 or PLC-δ isoforms[25,277], and that the activation of PLC-β isoforms may occur in the following order; PLC-β1 ≥ PLC-β3 ≥ PLC-β2.[278] Thus, increased PLC-β activity in experimental hearts may be mediated mainly through the activation of $G_{q\alpha}$. The significance of the elevated PLC-β1 activity is as yet unclear. We suggest that activation of PLC-β is associated with incidence of wound healing at the site of infarction as well as in cardiac hypertrophy and fibrosis in

viable tissue, based on its regulatory role in cell growth and differentiation. As multiple hormonal systems have been implicated in the pathogenesis of heart failure, abrogation of a single system may be insufficient to prevent the development of subsequent hypertrophy and fibrosis in heart failure. However, the specific modulation of the $G_{q\alpha}$/PLC-β pathway may provide a new therapeutic approach for prevention and treatment of heart failure.

6.4.4. Ongoing remodeling of scar tissue: a case for chronic wound healing

Heart failure due to MI is characterized not only by cardiac hypertrophy but also by fibrosis of scar and myocardium remote to infarcted tissue both in patients and in the rat experimental model.[185] While interstitial fibrosis and attendant decreased compliance of the surviving myocardium is believed to contribute to the occurrence of cardiac dysfunction,[36] it has become clear that the size of the scar is a reliable marker for the development of heart failure post-MI.[279] Recently, examination of collagen architecture from scars of post-MI rats has revealed that scars develop as highly anisotropic tissues, allowing the scar to resist circumferential stretching while maintaining longitudinal deformation compatibility with adjacent noninfarcted myocardium.[280] This finding supports a specific role for the healing scar in preservation of function of the infarcted ventricle. In this regard, it has been suggested that progressive regional cardiac remodeling of the infarcted ventricle may depend upon scar size, transmurality, scar wall thickness, and collagen content of the healed scar.[281] Although gross morphological examination of experimental hearts has indicated that scar formation is complete 3 weeks after MI,[9] our findings suggest that the scar is not quiescent even after 8 weeks post-MI, as indicated by the activation of $G_{q\alpha}$/PLC-β in scars. Our finding agrees with recent work which has shown that Ang II receptors are highly expressed in scar during the chronic phase of post-MI wound healing.[182,196,267] We suggest that altered $G_{q\alpha}$/PLC-β expression/function occurs beyond the classically defined period of infarct

healing. It is possible that enhanced $G_{q\alpha}$/PLC-β expression is involved in the ongoing remodeling of scar morphology. Therefore, the mechanisms that are activated during the wound healing of the infarct *per se* may not be terminated within a brief defined period.

In conclusion, the present study has demonstrated that the cardiac $G_{q\alpha}$/PLC-β pathway was activated in heart failure subsequent to MI. Therefore it is suggested that $G_{q\alpha}$ and PLC-β may play an important role in the evolution of scar remodeling, cardiac hypertrophy and fibrosis of the surviving tissue in post-MI rat heart, and that these events may be linked to the development of heart failure. Thus, pharmacological modulation of the $G_{q\alpha}$/PLC-β pathway may provide a possible novel target for altering post infarct remodeling.

Chapter 7. Expression and Localization of TGF-β1, TGF-β Receptors and Smad Proteins in Heart Failure Due to Myocardial Infarction in Rat

7.1. Summary

Previous studies indicate that TGF-β1 may be involved in cardiac fibrosis and myocyte hypertrophy. However, the significance of the altered TGF-β signaling in heart failure after MI remains unexplored. Cardiac TGF-β1, TβRI and TβRII, and Smad protein levels were investigated in the chronic phase (8 weeks) after MI. Both TGF-β1 mRNA abundance and protein levels were significantly increased in scar and border tissues when compared to viable tissue and sham-operated rats. Increased active TGF-β1 was noted in viable and border tissues. TβRI (53 kDa) protein was significantly reduced in the scar, while the 75 kDa and 110 kDa isoforms of TβRII was unchanged and significantly increased in scar samples respectively. Cardiac Smad2 and 4 proteins were significantly increased in border and scar tissues *vs* sham-operated rats. Immunofluorescent studies localized Smad protein accumulation in the nuclei of myofibroblasts in scar tissue. Protein concentrations of TGF-β1-inducible cyclin-dependent kinase (CDK) inhibitors (p15 and p21) were increased in scar compared to control. These results indicated that TGF-β1 may be involved in the ongoing remodeling of scar and remnant heart after MI, and that TGF-β1 mediated inhibition of proliferation of myofibroblasts via increased CDK inhibitor may occur in the scar after MI.

7.2. Introduction

TGF-β has been implicated in many fibrotic disorders including glomerulonephritis, cirrhosis, lung fibrosis and vascular restenosis.[26] As yet there is only limited information regarding the role of TGF-β in cardiac fibrosis and hypertrophy.[28,29] Increased expression of

TGF-β1 mRNA and protein have been shown in myocardium bordering the infarct region 2 days after MI suggesting a role in the cardiac wound healing response.[27] Recently, a major advance in TGF-β signaling has been achieved with the identification of Smad proteins as downstream effectors of TGF-β. These proteins translocate to nuclei and initiate gene transcription in response to TGF-β binding to its receptors, designated as TβRI and TβRII.[31,32] The significance and expression of cardiac TβRI, TβRII, and Smad proteins in heart failure post-MI is unknown.

TGF-β1 is known to be expressed in the heart,[138] it has been shown that both cardiac myocytes and fibroblasts may release TGF-β1.[139,141,143,144] Similarly, TGF-β receptors are localized in both cardiac myocytes and nonmyocytes,[148] and TGF-β1 is known to alter myocardial genes expression in cultured neonatal cardiac myocytes including the induction of MHC, skeletal α-actin, smooth muscle α-actin and ANP as well as downregulation of α-MHC and SERCA2 mRNA.[28] TGF-β1 is a powerful initiator for the production of collagens and other major ECM components in a variety of cell types.[136] In cultured cardiac fibroblasts, TGF-β1 has been shown to stimulate collagen deposition, and augment the synthesis of fibronectin and proteoglycans.[20,207,208,282] These effects of TGF-β1 mimic changes that characteristically transpire during the development of cardiac fibrosis, hypertrophy and failure.

It is conceivable that TGF-β is involved in the development of cardiac hypertrophy and fibrosis of surviving myocardium and in the continued remodeling of scar tissue in post-MI hearts. The present study was conducted to investigate cardiac TGF-β1, TβRI (ALK-5), and TβRII protein level and localization in noninfarcted LV tissues from sham animals, viable LV remote to infarct, border and scar tissues of failing hearts subsequent to MI. In order to

examine the functional significance of altered TGF-β1 expression in post-MI hearts, we also addressed the expression patterns of the downstream effectors of TGF-β receptors, including Smad proteins and CDK inhibitors p15 and p21, in scar and border, and noninfarcted tissues.

7.3. Results

7.3.1. General observations: cardiac hypertrophy, fibrosis and heart failure

Hearts of experimental animals were characterized by significant cardiac hypertrophy as reflected by an increase in the weight of the viable LV and also by the increased ratio of LV to BW in experimental animals compared to control values. The incidence and magnitude of LV hypertrophy noted in this study was comparable to our previous findings.[224] Cardiac collagen in surviving myocardium remote to infarct (48.6 ± 4.3 μg/mg dry wt) and border + scar tissues (128.5 ± 12.1 μg/mg dry wt) were both significantly higher than that of control value (21.9 ± 2.7 μg/mg dry wt). Heart failure reflected by an increase in LVEDP and a decrease in the $\pm dP/dt_{max}$ relative to their controls, along with congested lung, has been characterized in this model from our previous studies.[224]

7.3.2. Localization and alteration of cardiac TGF-β1

Quantitative assessment of cardiac TGF-β1 protein concentration in control and viable LV tissues as well as border + scar tissues of 8-week post-MI rats was carried out using ELISA. The results indicated that TGF-β1 was increased by approximately 2.4-fold in border and scar tissues compared to that from control animals (Figure 21). There was no significant alteration of TGF-β1 in samples from viable LV *vs* controls. Active TGF-β1 was localized using immunofluoresent staining. The active TGF-β_1 proteins were localized

mainly in the interstitial space. There was intense staining of active TGF-β1 in the viable and border + scar tissues in post-MI hearts as compared with that of sham hearts (Figure 22).

7.3.3. Alteration of cardiac TGF-β1, collagen type I and decorin mRNA abundance

We addressed steady-state mRNA abundance of cardiac TGF-β1, collagen type I and decorin in tissues taken from various LV regions of rats 8 weeks post-MI. Figure 23 (upper panel) shows a representative Northern blot with autoradiographic bands specific for TGF-β1, collagen type I and decorin and GAPDH mRNAs from LV samples of sham, viable, as well as border + scar tissues. Estimation of the target gene mRNA abundance was calculated by the ratio of target gene to GAPDH signal. The ratios for TGF-β1, decorin, and collagen type I were significantly increased in the border and scar regions *vs* values from viable tissue and controls (Figure 23, bottom panel).

7.3.4. Localization and quantification of TβRI and TRβII

TGF-β1 receptors and their distribution in 8-week experimental and age-matched control tissues were localized using immunofluorescent techniques. In a representative photomicrograph (Figure 24), the staining pattern of immunoreactive TβRI and TβRII appears as bright clusters along the myocyte cell membranes. The results demonstrated relatively weak staining of TβRI in scar tissue and in cardiac myocytes bordering scar tissue; comparatively more immunoreactive protein was visualized in surviving tissue and in control myocardium. In contrast to the results addressing TβRI, a stronger staining of TβRII was present in the scar and border region compared with sham and viable tissues. Western blot analysis revealed that both TβRI and TβRII are detectable in the membrane fraction but not in the cytosolic fraction. Figure 25A (upper panel) provides a representative blot

illustrating the presence of a characteristic 53 kDa band for TβRI. It shows that there is a dramatic decrease of TβRI in the border and scar tissues. Figure 25A (bottom panel) illustrates the bands specific for TβRII at 75 and 110 kDa.[283] In contrast to TβRI, the major isoform of TβRII (75 kDa) was modestly deceased, but the 110 kDa isoform was markedly increased in the border + scar region. Figure 25B indicates even loading of samples by amido black 10B staining of the same Western blot membrane.

7.3.5. Localization and quantification of cardiac Smad2, and Smad4

Immunofluoresent staining results indicated that cardiac Smad proteins are localized mainly in small arteries and veins as shown in Figure 26A. We observed enhanced accumulation of Smad2 and Smad3 proteins in the nuclei of cells from scar tissue (Figure 26B). Western analysis was used to determine cardiac Smad protein concentration from different regions. Total cardiac Smad2 (55 kDa) (Figure 27) and 4 (62 kDa) (Figure 28) protein concentrations were significantly increased in border and scar tissues when compared to control values. There was a decrease of Smad2 protein in cytosolic fraction isolated from border + scar tissue from post-MI heart compared with sham and viable tissues.

7.3.6. Alteration of p15 and p21

Cardiac p15 and p21 protein concentration was determined by Western blot analysis. Both p15 (26 kDa) (Figure 29) and p21 (28 kDa) (Figure 30) were found to be significantly increased in border and scar tissues when compared to sham-operated rats. The representative blots showing the specific bands for p15 and p21 were included in the inset of Figure 29 and Figure 30 respectively.

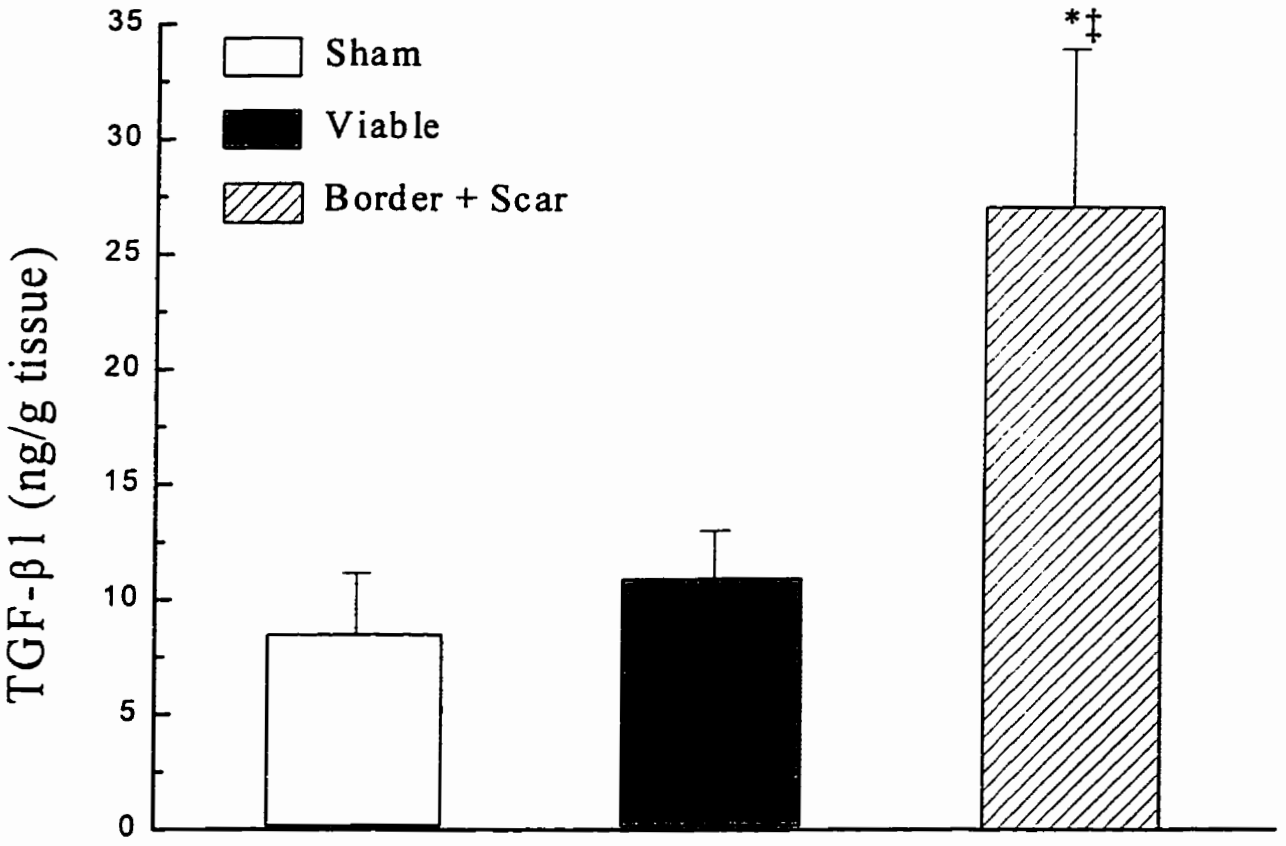

Figure 21. Cardiac transforming growth factor-β1 (TGF-β1) protein concentration in sham hearts, as well as viable, border and scar tissues from 8 week post-myocardial infarction (MI) as detected by enzyme-linked immunosorbent assay (ELISA). The data depicted is the mean ± SEM of 5 experiments. $^{*}P < 0.05$ and $^{\ddagger}P < 0.05$ *vs* sham and viable sample values, respectively.

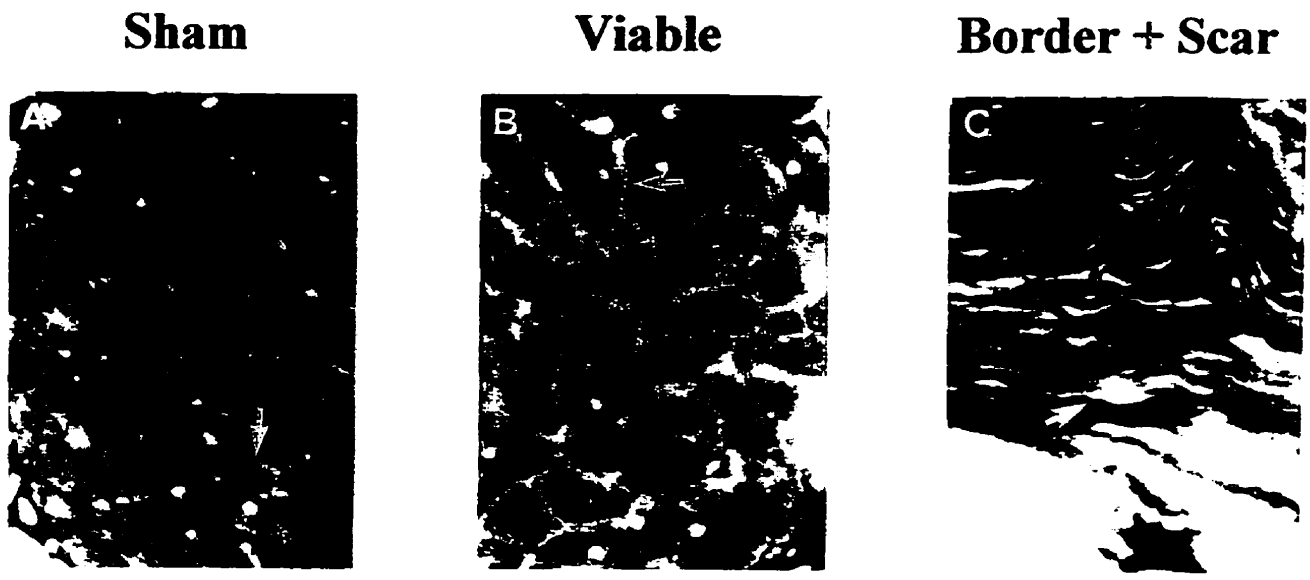

Figure 22. Immunofluorescent staining showing active transforming growth factor-β1 (TGF-β1) in sham, as well as viable, border and scar tissues from rat hearts 8 week post-MI. Active TGF-β1 protein appears as brightly stained material that is mainly localized in the interstitium as indicated by arrow. Magnification, x 400.

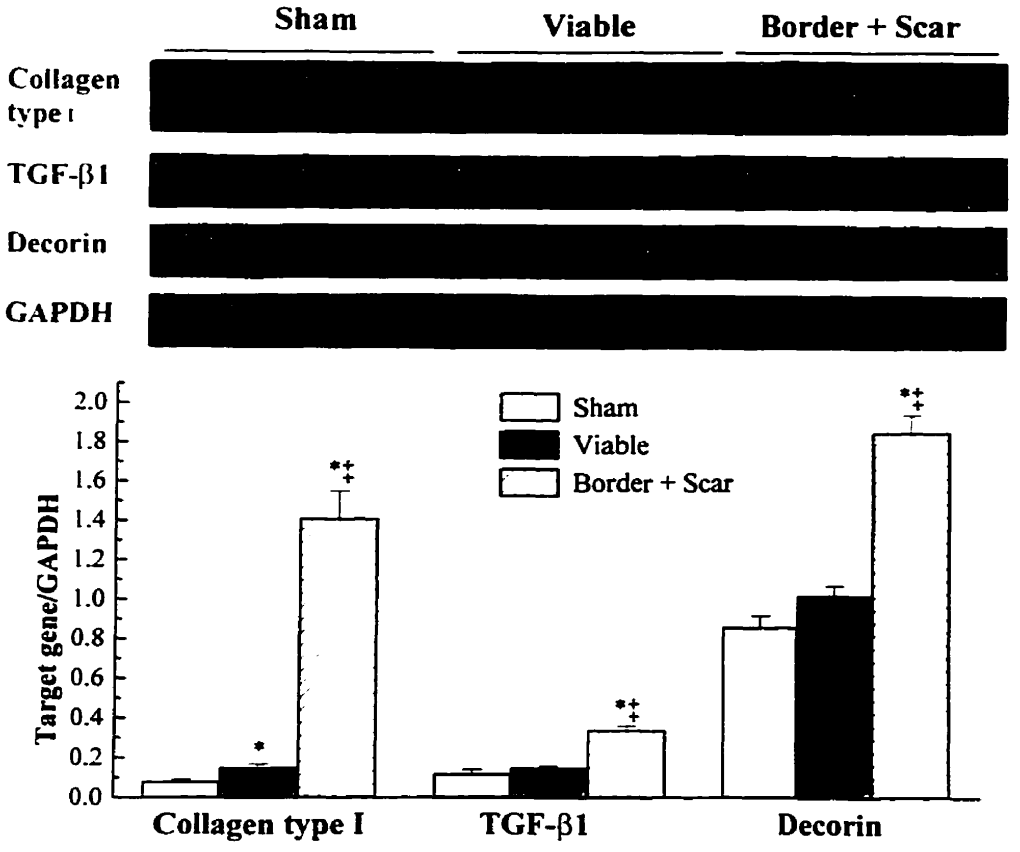

Figure 23. Upper panel. A representative autoradiograph from Northern blot analysis showing transforming growth factor-β1 (TGF-β1), collagen type I, decorin and glyceraldehyde-3-phosphate dehydrogenase (GAPDH) bands in sham, viable as well as border and scar tissues from rat hearts 8 week post-MI. **Bottom panel.** Quantified data of target gene/GAPDH in sham, viable, as well as border and scar tissues. The data depicted is the mean ± SEM of 6 experiments. $^{*}P < 0.05$ and $^{\ddagger}P < 0.05$ *vs* sham and viable sample values, respectively.

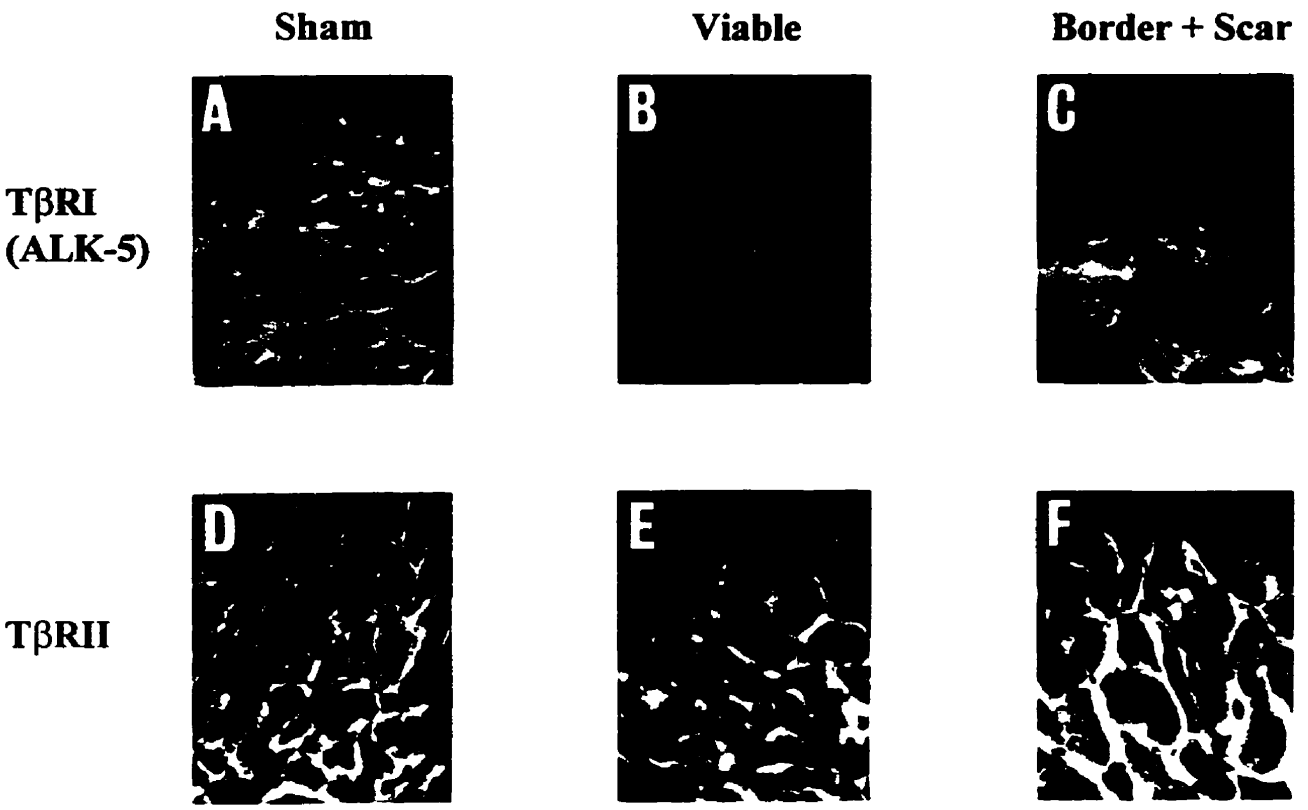

Figure 24. Immunofluoresent staining showing transforming growth factor-β receptor type I (TβRI, ALK-5) and transforming growth factor-β receptor type II (TβRII) in sham hearts (A and D), as well as viable (B and E), border and scar (C and F) tissues from rat hearts 8 week post-MI. Immunoactive TβRI and TβRII proteins appear as brightly stained material. Magnification, x 400.

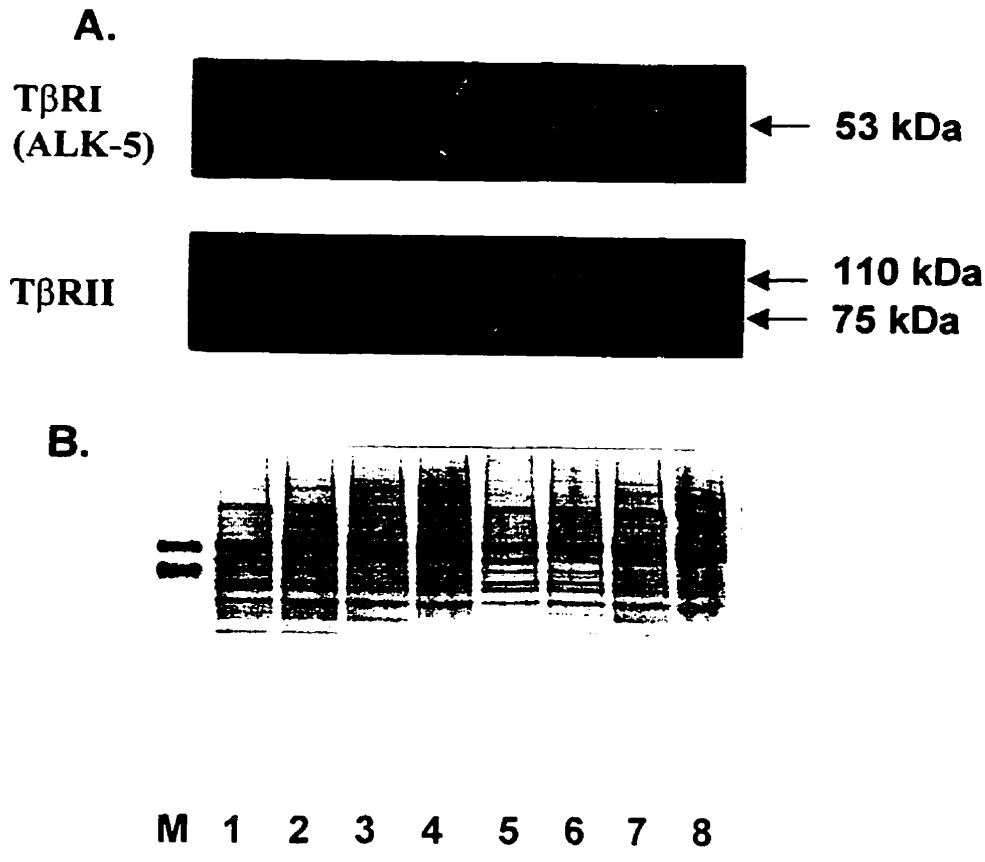

Figure 25. Western blot analysis of transforming growth factor-β receptor type I (TβRI, ALK-5) and transforming growth factor-β receptor type II (TβRII) protein concentration in sham, viable, as well as border and scar tissues from 8 week experimental animals. **A.** Representative Western blot showing specific bands of TβRI (ALK-5, 53 kDa) and TβRII (75 kDa and 110 kDa). Lanes 1 and 5 are sham, lanes 2 and 6 are viable LV, lanes 3 and 7 are border tissue, and lanes 4 and 8 represent scar. **B.** Amido black staining of the PVDF membrane showing the loading of protein.

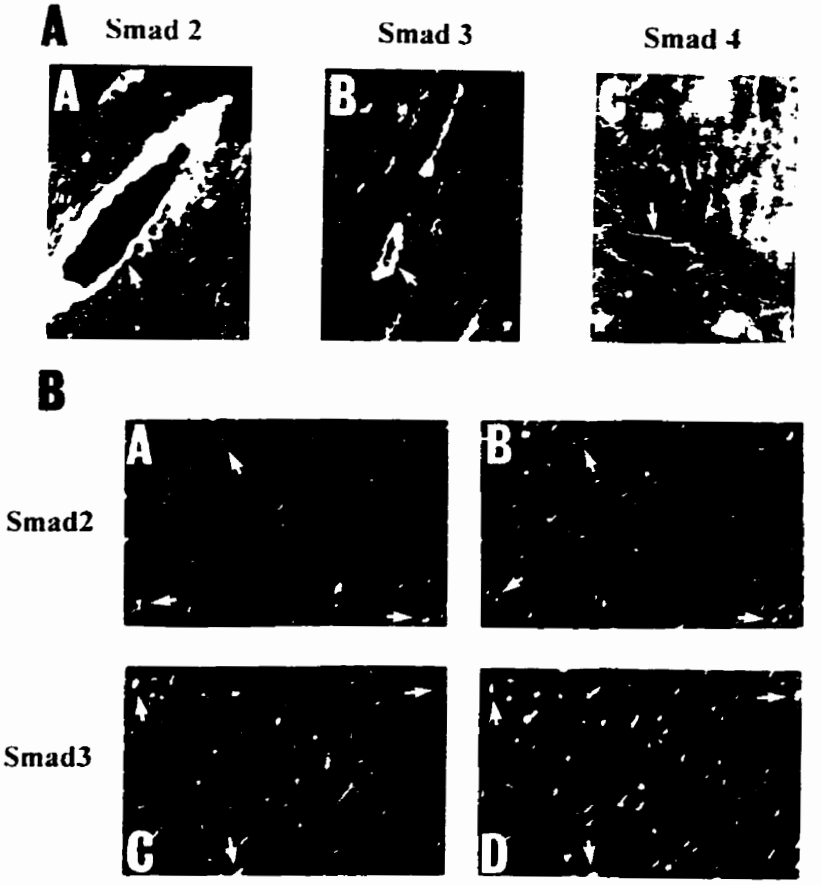

Figure 26. Immunofluoresent staining showing Smad proteins in sham, as well as viable, border and scar tissues from rat hearts 8 week post-MI. **Panel A**: Smad 2 (A), Smad3 (B), and Smad4 (C) were localized mainly in vasculature as indicated by the arrow. **Panel B**: A: immunofluoresent staining for Smad2; B: the same field as shown in A stained by Hoechst showing nuclei indicated by the arrow. C: immunofluoresent staining of Smad3; and D: the same field as shown in B stained by Hoechst showing nuclei indicated by the arrow. Magnification, x 400.

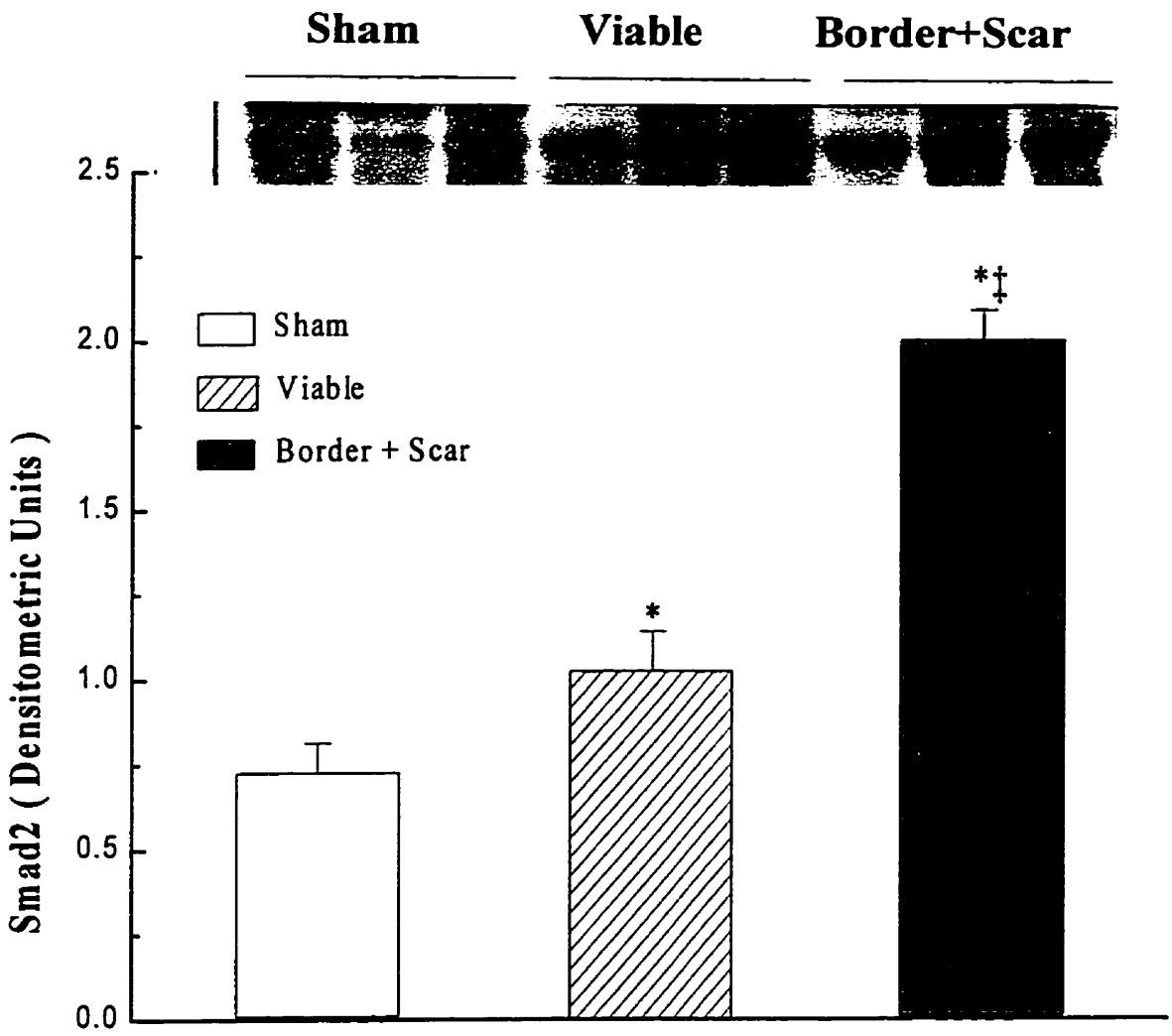

Figure 27. Western blot analysis for Smad2 in sham, viable, border and scar tissue in experimental rat hearts, 8 weeks after MI. The quantified data depicted is the mean ± SEM of 3 different experiments. $^{*}P < 0.05$ and $^{‡}P < 0.05$ *vs* sham and viable sample values, respectively. Inset: The Western blot autoradiograph showing the 55 kDa bands specific for Smad2. Similar results were obtained in 3 experiments.

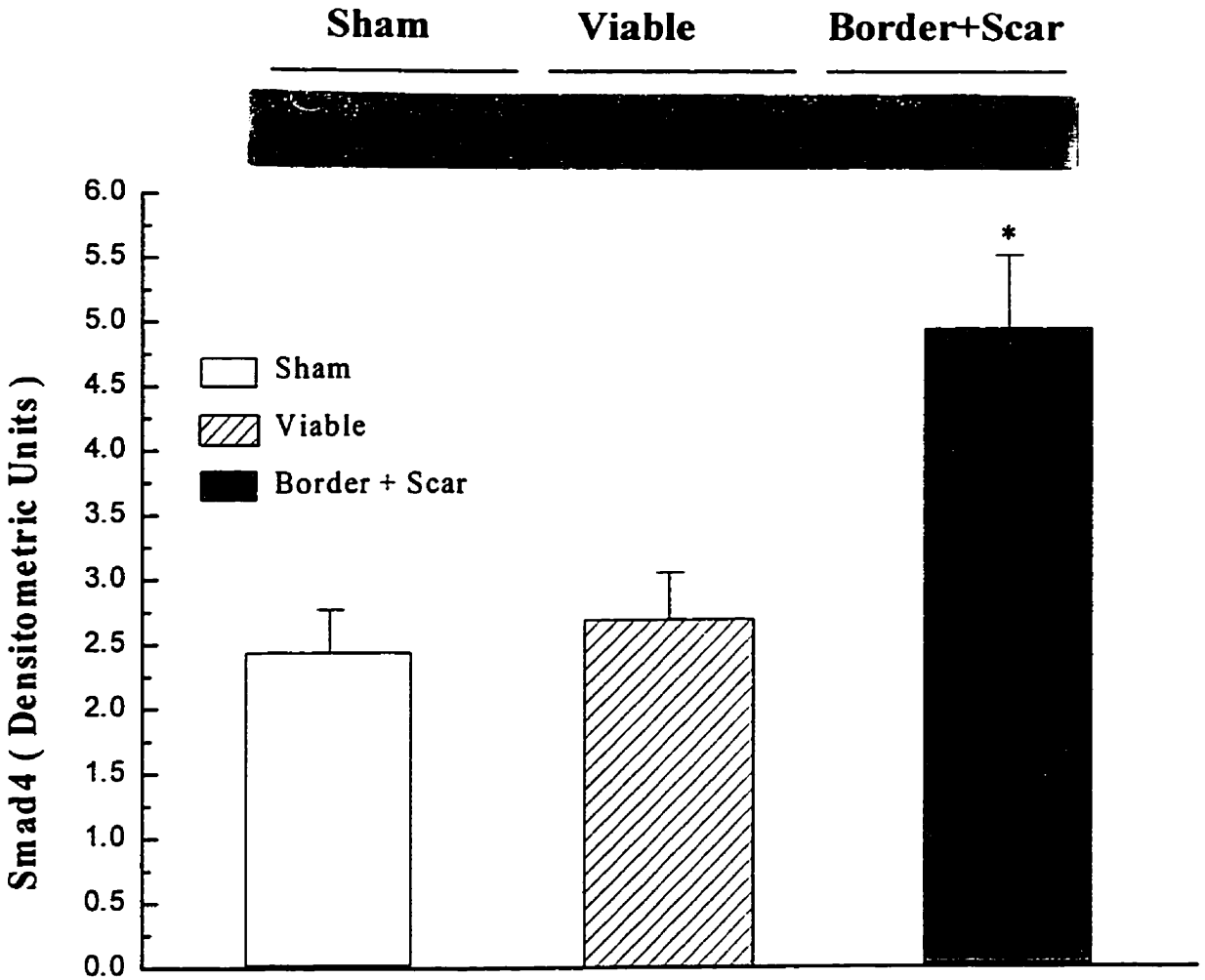

Figure 28. Western blot analysis for Smad4 in sham, viable, border and scar tissue in experimental rat hearts, 8 weeks after MI. The quantified data depicted is the mean ± SEM of 3 different experiments. $^{*}P < 0.05$ and $^{\ddagger}P < 0.05$ *vs* sham and viable sample values, respectively. Inset: Western blot autoradiograph showing the 62 kDa bands specific for Smad4. Similar results were obtained in 3 experiments.

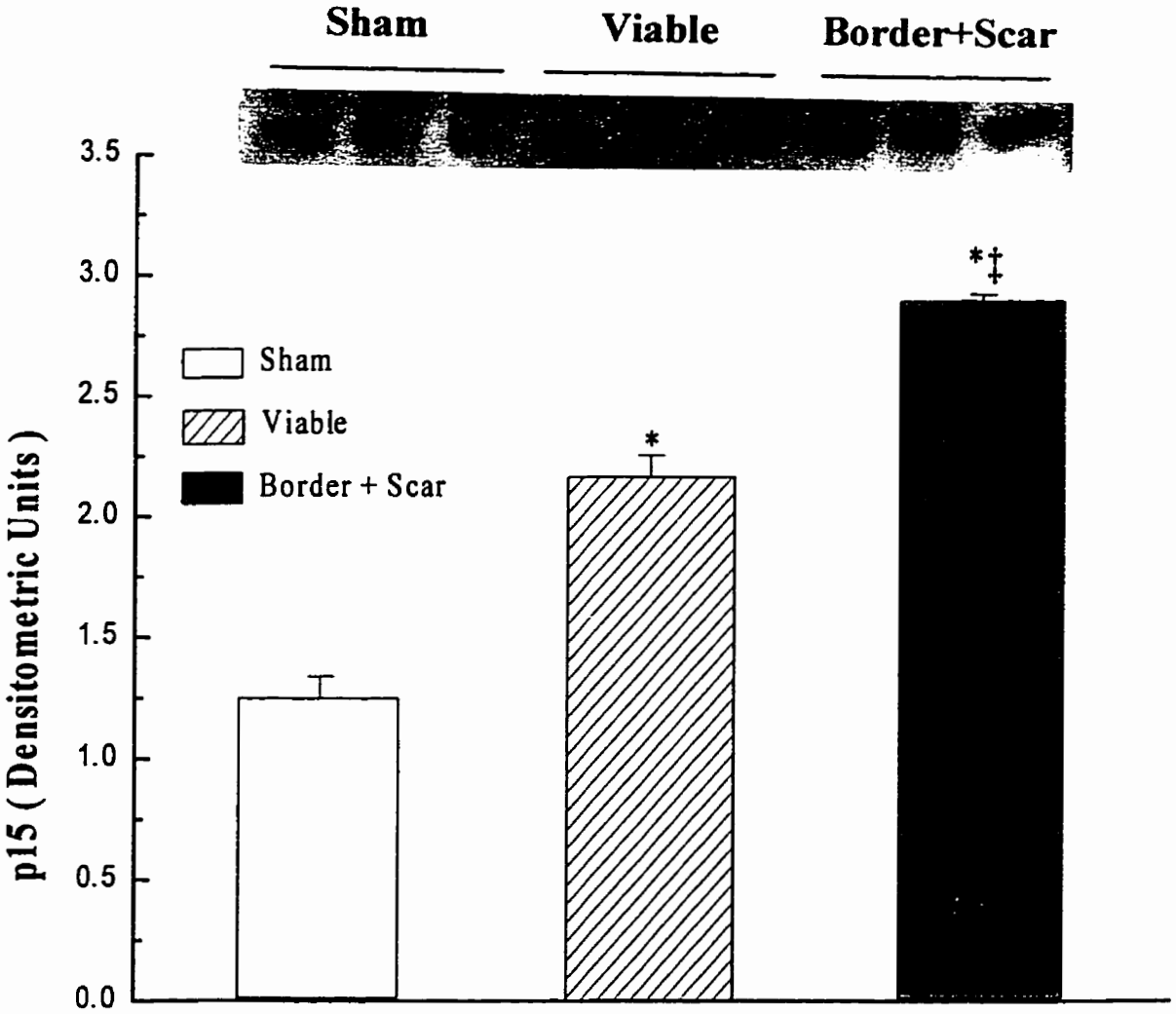

Figure 29. Western blot analysis for p15 in sham, viable, border and scar tissue in experimental rat hearts, 8 weeks after MI. The quantified data depicted is the mean ± SEM of 3 different experiments. $^{*}P < 0.05$ and $^{\ddagger}P < 0.05$ *vs* sham and viable sample values, respectively. Inset: Western blot autoradiograph showing the 26 kDa bands specific for p15. Similar results were obtained in 3 experiments.

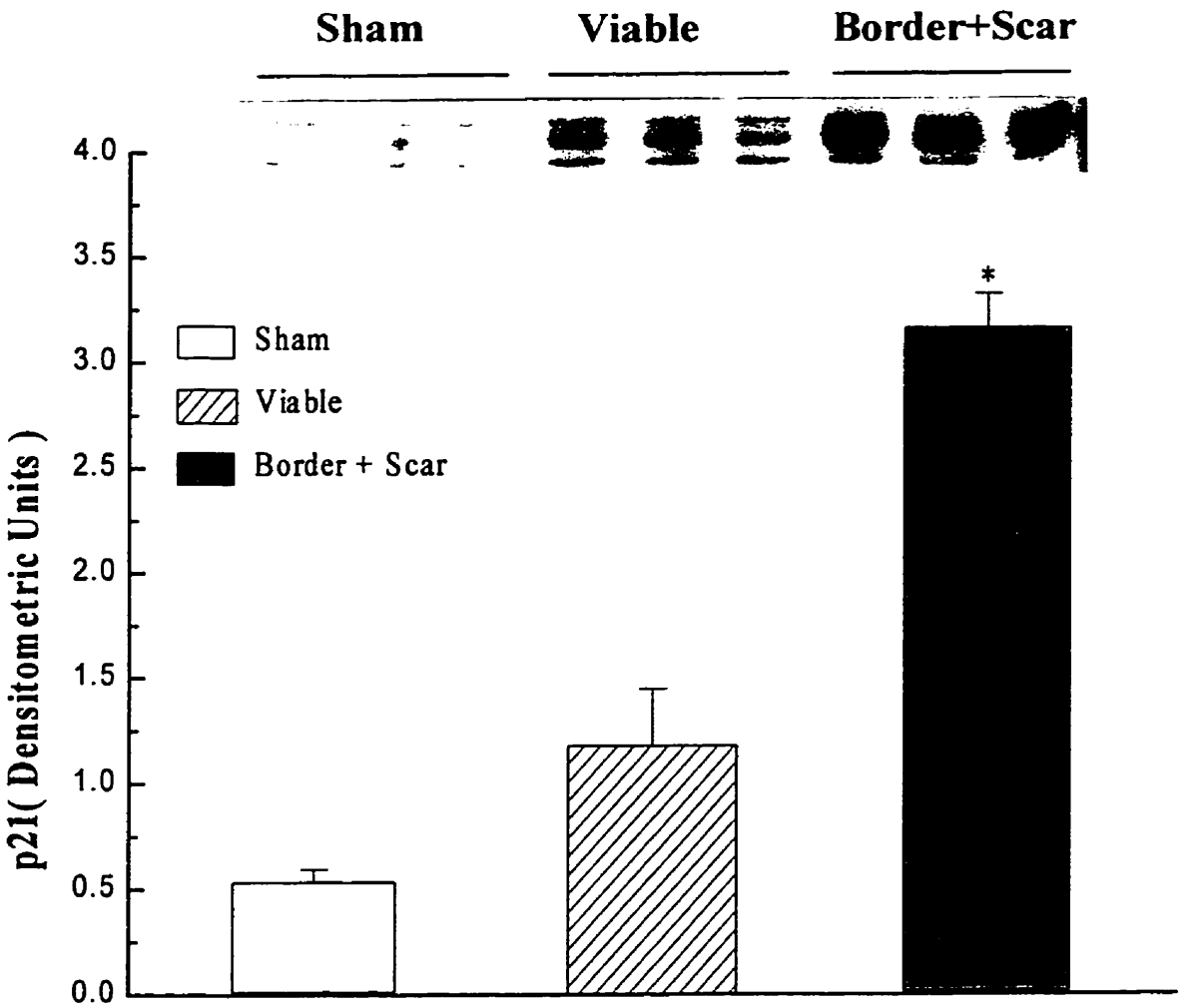

Figure 30. Western blot analysis for p21 in sham, viable, border and scar tissue in experimental rat hearts, 8 weeks after MI. The quantified data depicted is the mean ± SEM of 3 experiments. $^{*}P < 0.05$ and $^{\ddagger}P < 0.05$ *vs* sham and viable sample values, respectively. Inset: Western blot autoradiograph showing the 28 kDa bands specific for p21. Similar results were obtained in 3 experiments.

7.4. Discussion

7.4.1. Alteration of TGF-β signaling, cardiac fibrosis and ongoing remodeling of scar tissue

TGF-β contributes to an array of biological functions including regulation of ECM production, wound repair, and growth inhibition.[136,137] These phenomena are mediated through transmembrane TGF-β receptors (TβRI and TβRII) that display serine/threonine kinase activity.[32] TGF-β receptor activation occurs upon the binding of TGF-β to TβRII, which then recruits and phosphorylates TβRI.[151] The phosphorylated TβRI is activated and phosphorylates the downstream target Smad2 (or Smad3) protein.[31,32] Phosphorylated Smad2 (and/or Smad3) then form(s) a heteromeric complex with Smad4 and this complex accumulates in the nucleus leading to the activation of target gene expression.[32,155,156]

Although TGF-β is involved in ECM production which may contribute to the development of heart failure,[29] the alteration of TGF-β signaling in heart disease, especially during heart failure after MI, is unknown. The present study demonstrated that the expression (both mRNA and protein) of TGF-β1 was increased in the healing infarct and myocardium bordering the scar in the chronic phase after MI. Furthermore, enhanced active TGF-β1 was localized mainly in scar tissue and in the interstitium of the viable myocardium. This increased TGF-β1 in post-MI heart tissue may contribute to the development of cardiac fibrosis in the myocardium remote to the infarct and scar remodeling. The precise cell type expressing TGF-β_1 in scar and remnant heart is unclear, myofibroblasts (distinguished by their expression of α-actin) have been shown to be the predominant cell type in post-MI scar tissue, and are likely candidate cells in this regard.[65,275] Interstitial fibrosis and attendant decreases in compliance of the surviving myocardium are believed to contribute to the occurrence of cardiac dysfunction,[36] and it has

become clear that the size of the scar is a reliable marker for the development of heart failure post-MI.[279] This finding supports a putative role for the healing scar in preservation of function of the infarcted ventricle. In addition, the decrease in cytosolic Smad protein concentration in combination with an increase in total Smad protein levels in border and scar tissues suggests net nuclear translocation of these Smad proteins. Smad translocation was further supported by marked nuclear accumulation of immunoreactive Smad 2 and 3 in cells localized in the scar. On the other hand, both total and cytosolic Smad4 protein was increased in border and scar tissues when compared with sham-operated animals. These findings are again in keeping with activation of TGF-β1 signaling in post-MI hearts. Elevation of TGF-β1 signaling pathways may play an important role in the stimulation of ECM production by myofibroblasts in the remodeling scar and the current data lay further support to the argument that scar remodeling occurs beyond the classically defined period of infarct healing. Thus, it would appear that these mechanisms that are activated early on during wound healing of the infarct may not be terminated within a brief defined period and hence may be amenable to therapeutic intervention even in the late stage of heart failure.

7.4.2. Alteration of TGF-β signaling and proliferation of cardiac fibroblasts and myocytes

TGF-β1 affects growth inhibition in a variety of cell types by arresting the cell-cycle at the G1 phase.[210,211] This effect is known to be mediated by the induction of CDK inhibitors p15 and p21 by TGF-β.[212,213] It has been demonstrated that the administration of TGF-β1 to rats is associated with inhibition of cardiac DNA synthesis.[215] The finding of increased p15 and p21 expression in border and scar tissues indicates that TGF-β1 may inhibit myofibroblast proliferation during the chronic phase of wound healing in post-MI hearts. The upregulation of p15 and p21 together with increased Smad protein levels

provide strong evidence for enhanced TGF-β signaling in the border and scar tissues. As Smad2 and Smad3 may mediate growth inhibition and stimulation of collagen production by TGF-β1,[155,284,285] increased Smad protein levels may play a crucial role in the regulation of cardiac fibroblast proliferation and collagen remodeling in post-MI hearts. It has been reported that ANG II concentration and AT_1 receptor density in myofibroblasts are significantly increased in the scar tissue post-MI.[187,196,267] As Ang II has been implicated in the stimulation of cardiac fibroblast proliferation,[21,22,117] we propose that the net proliferation of myofibroblasts may depend upon a balance between TGF-β signaling and by other growth factors, i.e., Ang II during post-MI wound healing.

Although our results from ELISA assay revealed that there is no significant increase of TGF-β1 in the viable tissue, it is should be noted that this assay reflected the total amount of cardiac TGF-β1 including active and latent TGF-β1. Apparent enhanced immunostaining of active TGF-β1 in remnant heart, although not quantitative, is in keeping with the hypothesis specifying activation of TGF-β1 in this region. Although current knowledge supports the hypothesis that TGF-β1 may be involved in stimulation of cardiac myocyte growth,[214] the precise significance of altered active TGF-β1in hypertrophied hearts after MI is as yet unclear. It has been demonstrated that increased protein synthesis in adult myocytes induced by isoproterenol is abolished by co-incubation with neutralizing antibody against TGF-β1, while exposure to TGF-β1is associated with restoration of low serum induced hypertrophic response in these cells.[218] Previous studies demonstrate that increased expression of TGF-β1is associated with the development of cardiac hypertrophy.[144,220] Nonetheless, the *in vivo* effects of TGF-β1 on cardiac myocytes are less clear. We have noted a marked increase of active TGF-β1in the viable tissue from post-MI hearts,

suggesting that TGF-β1 may be involved in myocyte hypertrophy. This finding is consistent with recent studies which have demonstrated increased expression of TGF-β1 in pressure overload-induced hypertrophic and idiopathic hypertrophic cardiomyopathic hearts.[222,223]

7.4.3. Alteration of TGF-β receptors and Smad proteins: molecular mechanisms

The downregulation of TβRI in scar and border tissues in post-MI heart is in agreement with a previous study which provides data addressing TβRI and TβRII expression during liver regeneration after partial hepatectomy.[286] A possible explanation for the downregulation of TβRI and TβRII may be due to the reciprocal regulation or "desensitization" caused by stimulation of high concentration of TGF-β1in the scar and border tissues. This hypothesis is supported by the demonstration that pre-exposure of osteoblasts to TGF-β1is associated with decreased receptor density.[287] Thus it is possible that the downregulation of TβRI may reflect the rapid turnover of this receptor in the remodeling scar tissue. As it has been reported that collagen proteins may induce the downregulation of TβRI and TβRII,[288] excessive deposition of collagens in the scar during wound healing may contribute to altered TβRI expression in the post-MI rat heart.

In conclusion, increased active TGF-β1with attendant alteration in TβRI, TβRII and Smad proteins in post-MI hearts suggests that this cytokine is involved in ongoing remodeling of scar and viable regions and is likely associated with the development of heart failure. Increased Smad proteins with concomitant induction of p15 and p21 indicated that activation of the TGF-β pathway may lead to the inhibition of the proliferation of cardiac fibroblasts (or myofibroblasts) in the chronic phase of scar remodeling.

Chapter 8. General Summary and Conclusion

Post-MI cardiac remodeling was characterized by the appearance of cardiac hypertrophy, progressive fibrosis and the development of heart failure. Our results indicate that prefailure and moderate CHF stages after the induction of large MI were associated with i) a significant elevation of mRNA levels of cardiac collagen in LV and RV myocardium occurred in acute and chronic MI, ii) a progressive accumulation of cardiac collagen evidenced in viable LV and RV after a lag period to increased corresponding mRNA; iii) marked RV fibrosis occurred in experimental animals and was associated with increased chamber stiffness at 8 weeks post-MI; iv) an increased MMP-2 activity noted in noninfarcted LV and RV in experimental animals, whereas MMP1 activity was significantly increased only in border and scar tissues compared to control values. Thus net degradation of collagen may be increased in experimental hearts and this finding supports the hypothesis that increased deposition of collagen proteins is a specific result of *elevated synthesis* of collagen. The results illustrate the respective time courses for activation of collagen mRNA expression and collagen protein deposition in the cardiac interstitium remote to the site of infarction. It is clear that not only the infarcted region, but the whole heart becomes involved in collagen remodeling. Finally, it is likely that the global cardiac wound healing response (remote to the infarct) is not completed in conjunction with remodeling of the scar, but is sustained in the chronic phase of MI.

AT_1 receptor blockade is associated with significant attenuation of cardiac collagen and inhibition of cardiac hypertrophy suggesting that Ang II, via activation of AT_1 receptor, is involved in the development of cardiac fibrosis and hypertrophy in post-MI heart. However, This effect was not associated with any alteration of steady-state fibrillar collagen

mRNA abundance by AT_1 blockade in ventricular tissues after MI. We provide evidence that the attenuation of fibrosis mediated by losartan in post-MI heart may be effected at the posttranslational level of collagen synthesis, and may be due to normalization of increased prolyl 4-hydroxylase protein concentration in tissue remote to the site of infarction. In our study on $G_{q\alpha}$/PLC-β signaling, we demonstrated that the cardiac $G_{q\alpha}$/PLC-β pathway was activated in both myocytes of the remnant heart and fibroblasts in scar during the development of heart failure subsequent to MI. Therefore it is suggested that $G_{q\alpha}$ and PLC-β may play an important role in the evolution of scar remodeling, cardiac fibrosis and hypertrophy of the viable tissue in post-MI rat heart. We suggest that altered $G_{q\alpha}$/PLC-β expression/function occurs beyond the classically defined period of infarct healing. It is possible that enhanced $G_{q\alpha}$/PLC-β expression was involved in the ongoing remodeling of scar morphology. Therefore, the mechanisms that are activated during the wound healing of the infarct *per se* may not be terminated within a brief defined period.

Increased active TGF-β1with attendant elevation of downstream effectors (Smad proteins) in post-MI hearts suggests that this cytokine is involved in ongoing remodeling of scar and viable regions and is likely associated with the development of heart failure. Activation of TGF-β1signaling pathways may play an important role in the stimulation of ECM production by fibroblasts and/or myofibroblasts in the remodeling scar and the current data provide further support for the argument that scar remodeling occurs beyond the classically defined period of infarct healing. Thus, it would appear that these mechanisms that are activated early on during wound healing of the infarct may not be terminated within a brief defined period and hence may be amenable to therapeutic intervention (even in the stage of heart failure). Increased Smad protein levels with concomitant induction of p15 and p21 indicated that activation of the TGF-β pathway may lead to the inhibition of the

proliferation of cardiac fibroblasts (or myofibroblasts) in the chronic phase of scar remodeling. Nonetheless, the net proliferation of cardiac fibroblasts in post-MI heart depends upon the balance struck between the stimulatory effect mediated by Ang II signaling pathway and the inhibitory effects via TGF-β1signaling pathway. Thus, pharmacological modulation of the $G_{q\alpha}$/PLC-β and TGF-β pathways may provide a possible novel target for altering post-infarct remodeling.

Chapter 9. References

1. Antman EM, Braunwald E: Acute myocardial infarction, in Braunwald E (ed): *Heart Disease*. Philadelphia, W.B. Saunders Company, 1997, pp 1184-1288

2. Pfeffer JM, Fischer TA, Pfeffer MA: Angiotensin-converting enzyme inhibition and ventricular remodeling after myocardial infarction. *Annu Rev Physiol* 1995;57:805-826

3. Pfeffer MA, Braunwald E: Ventricular remodeling after myocardial infarction. Experimental observations and clinical implications. *Circulation* 1990;81:1161-1172

4. Cohn JN: Critical review of heart failure: the role of left ventricular remodeling in the therapeutic response. *Clin Cardiol* 1995;18(Suppl 4):IV4-IV12

5. Cohn JN, Bristow MR, Chien KR, Colucci WS, Frazier H, Leiwand LA, Moss AJ, Sonnenblick EH, Walsh RA, Mockrin SC, Reinlib L: Report of the National Heart, Lung, and Blood Institute special emphasis panel on heart failure research. *Circulation* 1997;95:766-770

6. Weber KT, Sun Y, Katwa LC: Wound healing following myocardial infarction. *Clin Cardiol* 1996;19:447-455

7. Swan HJ: Left ventricular dysfunction in ischemic heart disease: fundamental importance of the fibrous matrix. *Cardiovasc Drugs Ther* 1994;8(Suppl 2):305-312

8. Pelouch V, Dixon IM, Sethi R, Dhalla NS: Alteration of collagenous protein profile in congestive heart failure secondary to myocardial infarction. *Mol Cell Biochem* 1993;129:121-131

9. Fishbein MC, Maclean D, Maroko PR: Experimental myocardial infarction in the rat: qualitative and quantitative changes during pathologic evolution. *Am J Pathol* 1978;90:57-70

10. Jugdutt BI, Amy RW: Healing after myocardial infarction in the dog: changes in infarct hydroxyproline and topography. *J Am Coll Cardiol* 1986;7:91-102

11. Przyklenk K, Connelly CM, McLaughlin RJ, Kloner RA, Apstein CS: Effect of myocyte necrosis on strength, strain, and stiffness of isolated myocardial strips. *Am Heart J* 1987;114:1349-1359

12. Thiedemann KU, Holubarsch C, Medugorac I, Jacob R: Connective tissue content and myocardial stiffness in pressure overload hypertrophy. A combined study of morphologic, morphometric, biochemical, and mechanical parameters. *Basic Res Cardiol* 1983;78:140-155

13. Jalil JE, Doering CW, Janicki JS, Pick R, Shroff SG, Weber KT: Fibrillar collagen and myocardial stiffness in the intact hypertrophied rat left ventricle. *Circ Res* 1989;64:1041-1050

14. Granzier HL, Irving TC: Passive tension in cardiac muscle: contribution of collagen, titin, microtubules, and intermediate filaments. *Biophys J* 1995;68:1027-1044

15. Litwin SE, Litwin CM, Raya TE, Warner AL, Goldman S: Contractility and stiffness of noninfarcted myocardium after coronary ligation in rats. Effects of chronic angiotensin converting enzyme inhibition. *Circulation* 1991;83:1028-1037

16. Schaper J, Speiser B: The extracellular matrix in the failing human heart. *Basic Res Cardiol* 1992;87:303-309

17. Sabbah HN, Sharov VG, Lesch M, Goldstein S: Progression of heart failure: a role for interstitial fibrosis. *Mol Cell Biochem* 1995;147:29-34

18. Sharov VG, Sabbah HN, Shimoyama H, Goussev AV, Lesch M, Goldstein S: Evidence of cardiocyte apoptosis in myocardium of dogs with chronic heart failure. *Am J Pathol* 1996;148:141-149

19. Sigel AV, Centrella M, Eghbali Webb M: Regulation of proliferative response of cardiac fibroblasts by transforming growth factor-β1. *J Mol Cell Cardiol* 1996;28:1921-1929

20. Chua CC, Chua BH, Zhao ZY, Krebs C, Diglio C, Perrin E: Effect of growth factors on collagen metabolism in cultured human heart fibroblasts. *Connect Tissue Res* 1991;26:271-281

21. Brilla CG, Zhou G, Matsubara L, Weber KT: Collagen metabolism in cultured adult rat cardiac fibroblasts: response to angiotensin II and aldosterone. *J Mol Cell Cardiol* 1994;26:809-820

22. Crabos M, Roth M, Hahn AW, Erne P: Characterization of angiotensin II receptors in cultured adult rat cardiac fibroblasts. Coupling to signaling systems and gene expression. *J Clin Invest* 1994;93:2372-2378

23. Wang C, Jayadev S, Escobedo JA: Identification of a domain in the angiotensin II type 1 receptor determining Gq coupling by the use of receptor chimeras. *J Biol Chem* 1995;270:16677-16682

24. Sadoshima J, Qiu Z, Morgan JP, Izumo S: Angiotensin II and other hypertrophic stimuli mediated by G protein-coupled receptors activate tyrosine kinase, mitogen-activated protein kinase, and 90-kD S6 kinase in cardiac myocytes. The critical role of Ca^{2+}-dependent signaling. *Circ Res* 1995;76:1-15

25. Taylor SJ, Chae HZ, Rhee SG, Exton JH: Activation of the β1 isozyme of phospholipase C by α subunits of the Gq class of G proteins. *Nature* 1991;350:516-518

26. Border WA, Noble NA: Transforming growth factor β in tissue fibrosis. *N Engl J Med* 1994;331:1286-1292

27. Thompson NL, Bazoberry F, Speir EH, Casscells W, Ferrans VJ, Flanders KC, Kondaiah P, Geiser AG, Sporn MB: Transforming growth factor β-1 in acute myocardial infarction in rats. *Growth Factors* 1988;1:91-99

28. Brand T, Schneider MD: The TGFβ superfamily in myocardium: ligands, receptors, transduction, and function. *J Mol Cell Cardiol* 1995;27:5-18

29. Eghbali M, Sigel A: Role of transforming growth factor β-1 in the remodeling of collagen matrix in the heart, in Dhalla NS, Pierce GN, Panagia V, Beamish RE (eds): *Heart Hypertrophy and Failure*. Boston, Kluwer Academic Publishers, 1995, pp 287-297

30. Heldin CH, Miyazono K, ten Dijke P: TGF-β signalling from cell membrane to nucleus through SMAD proteins. *Nature* 1997;390:465-471

31. Macias Silva M, Abdollah S, Hoodless PA, Pirone R, Attisano L, Wrana JL: MADR2 is a substrate of the TGFβ receptor and its phosphorylation is required for nuclear accumulation and signaling. *Cell* 1996;87:1215-1224

32. Massague J, Hata A, Liu F: TGF-β signalling through the Smad pathway. *Trends Cell Biol* 1997;7:187-192

33. Lin CQ, Bissell MJ: Multi-faceted regulation of cell differentiation by extracellular matrix [see comments]. *FASEB J* 1993;7:737-743

34. Alberts S, Bray D, Lewis J, Raff M, Roberts K, Watson JD: Cell junction, cell adhesion, and the extracellular matrix, in Alberts B, Bray D, Lewis J, Raff M, Roberts K, Watson JD (eds): *Molecular Biology of the Cell*. New York, Gardland Publishing, Inc. 1994, pp 971-1000

35. Weber KT, Brilla CG: Pathological hypertrophy and cardiac interstitium. Fibrosis and renin- angiotensin-aldosterone system. *Circulation* 1991;83:1849-1865

36. Weber KT: Cardiac interstitium in health and disease: the fibrillar collagen network. *J Am Coll Cardiol* 1989;13:1637-1652

37. Bishop JE, Laurent GJ: Collagen turnover and its regulation in the normal and hypertrophying heart. *Eur Heart J* 1995;16(Suppl C):38-44

38. Bashey RI, Martinez Hernandez A, Jimenez SA: Isolation, characterization, and localization of cardiac collagen type VI. Associations with other extracellular matrix components. *Circ Res* 1992;70:1006-1017

39. Medugorac I, Jacob R: Characterisation of left ventricular collagen in the rat. *Cardiovasc Res* 1983;17:15-21

40. Pelouch V, Dixon IM, Golfman L, Beamish RE, Dhalla NS: Role of extracellular matrix proteins in heart function. *Mol Cell Biochem* 1993;129:101-120

41. Weber KT, Sun Y, Tyagi SC, Cleutjens JP: Collagen network of the myocardium: function, structural remodeling and regulatory mechanisms. *J Mol Cell Cardiol* 1994;26:279-292

42. Robinson TF, Factor SM, Sonnenblick EH: The heart as a suction pump. *Sci Am* 1986;254:84-91

43. Borg TK, Johnson LD, Lill PH: Specific attachment of collagen to cardiac myocytes: *in vivo* and *in vitro*. *Dev Biol* 1983;97:417-423

44. Eng C, Zhao M, Factor SM, Sonnenblick EH: Post-ischaemic cardiac dilatation and remodelling: reperfusion injury of the interstitium. *Eur Heart J* 1993;14(Suppl A):27-32

45. Bishop JE, Rhodes S, Laurent GJ, Low RB, Stirewalt WS: Increased collagen synthesis and decreased collagen degradation in right ventricular hypertrophy induced by pressure overload. *Cardiovasc Res* 1994;28:1581-1585

46. Eleftheriades EG, Durand JB, Ferguson AG, Engelmann GL, Jones SB, Samarel AM: Regulation of procollagen metabolism in the pressure-overloaded rat heart. *J Clin Invest* 1993;91:1113-1122

47. Besse S, Robert V, Assayag P, Delcayre C, Swynghedauw B: Nonsynchronous changes in myocardial collagen mRNA and protein during aging: effect of DOCA-salt hypertension. *Am J Physiol* 1994;267:H2237-H2244

48. Birkedal-Hansen H, Moore WG, Bodden MK, Windsor LJ, Birkedal-Hansen B, DeCarlo A, Engler JA: Matrix metalloproteinases: a review. *Crit Rev Oral Biol Med* 1993;4:197-250

49. Wojtowicz-Praga SM, Dickson RB, Hawkins MJ: Matrix metalloproteinase inhibitors. *Invest New Drugs* 1997;15:61-75

50. Stetler-Stevenson WG: Dynamics of matrix turnover during pathologic remodeling of the extracellular matrix [comment]. *Am J Pathol* 1996;148:1345-1350

51. Dollery CM, McEwan JR, Henney AM: Matrix metalloproteinases and cardiovascular disease. *Circ Res* 1995;77:863-868

52. Greene J, Wang M, Liu YE, Raymond LA, Rosen C, Shi YE: Molecular cloning and characterization of human tissue inhibitor of metalloproteinase 4. *J Biol Chem* 1996;271:30375-30380

53. Tyagi SC, Kumar SG, Banks J, Fortson W: Co-expression of tissue inhibitor and matrix metalloproteinase in myocardium. *J Mol Cell Cardiol* 1995;27:2177-2189

54. Robert V, Besse S, Sabri A, Silvestre JS, Assayag P, Nguyen VT, Swynghedauw B, Delcayre C: Differential regulation of matrix metalloproteinases associated with aging and hypertension in the rat heart. *Lab Invest* 1997;76:729-738

55. Cleutjens JP, Kandala JC, Guarda E, Guntaka RV, Weber KT: Regulation of collagen degradation in the rat myocardium after infarction. *J Mol Cell Cardiol* 1995;27:1281-1292

56. Apte SS, Hayashi K, Seldin MF, Mattei MG, Hayashi M, Olsen BR: Gene encoding a novel murine tissue inhibitor of metalloproteinases (TIMP), TIMP-3, is expressed in developing mouse epithelia, cartilage, and muscle, and is located on mouse chromosome 10. *Dev Dyn* 1994;200:177-197

57. Leco KJ, Apte SS, Taniguchi GT, Hawkes SP, Khokha R, Schultz GA, Edwards DR: Murine tissue inhibitor of metalloproteinases-4 (TIMP-4): cDNA isolation and expression in adult mouse tissues. *FEBS Lett* 1997;401:213-217

58. Ju H, Dixon IM: Extracellular matrix and cardiovascular diseases. *Can J Cardiol* 1996;12:1259-1267

59. Takahashi S, Barry AC, Factor SM: Collagen degradation in ischaemic rat hearts. *Biochem J* 1990;265:233-241

60. Sato S, Ashraf M, Millard RW, Fujiwara H, Schwartz A: Connective tissue changes in early ischemia of porcine myocardium: an ultrastructural study. *J Mol Cell Cardiol* 1983;15:261-275

61. Carlyle WC, Jacobson AW, Judd DL, Tian B, Chu C, Hauer KM, Hartman MM, McDonald KM: Delayed reperfusion alters matrix metalloproteinase activity and fibronectin mRNA expression in the infarct zone of the ligated rat heart. *J Mol Cell Cardiol* 1997;29:2451-2463

62. Hutchins GM, Bulkley BH: Infarct expansion versus extension: two different complications of acute myocardial infarction. *Am J Cardiol* 1978;41:1127-1132

63. Mukherjee D, Sen S: Alteration of collagen phenotypes in ischemic cardiomyopathy. *J Clin Invest* 1991;88:1141-1146

64. Volders PG, Willems IE, Cleutjens JP, Arends JW, Havenith MG, Daemen MJ: Interstitial collagen is increased in the non-infarcted human myocardium after myocardial infarction. *J Mol Cell Cardiol* 1993;25:1317-1323

65. Cleutjens JP, Verluyten MJ, Smits JF, Daemen MJ: Collagen remodeling after myocardial infarction in the rat heart. *Am J Pathol* 1995;147:325-338

66. McCormick RJ, Musch TI, Bergman BC, Thomas DP: Regional differences in LV collagen accumulation and mature cross- linking after myocardial infarction in rats. *Am J Physiol* 1994;266:H354-H359

67. Reiser K, McCormick RJ, Rucker RB: Enzymatic and nonenzymatic cross-linking of collagen and elastin. *FASEB J* 1992;6:2439-2449

68. Norton GR, Tsotetsi J, Trifunovic B, Hartford C, Candy GP, Woodiwiss AJ: Myocardial stiffness is attributed to alterations in cross-linked collagen rather than total collagen or phenotypes in spontaneously hypertensive rats. *Circulation* 1997;96:1991-1998

69. Tyagi SC, Kumar S, Glover G: Induction of tissue inhibitor and matrix metalloproteinase by serum in human heart-derived fibroblast and endomyocardial endothelial cells. *J Cell Biochem* 1995;58:360-371

70. Tyagi SC, Kumar S, Voelker DJ, Reddy HK, Janicki JS, Curtis JJ: Differential gene expression of extracellular matrix components in dilated cardiomyopathy. *J Cell Biochem* 1996;63:185-198

71. Tyagi SC, Kumar SG, Haas SJ, Reddy HK, Voelker DJ, Hayden MR, Demmy TL, Schmaltz RA, Curtis JJ: Post-transcriptional regulation of extracellular matrix metalloproteinase in human heart end-stage failure secondary to ischemic cardiomyopathy. *J Mol Cell Cardiol* 1996;28:1415-1428

72. Gunja-Smith Z, Morales AR, Romanelli R, Woessner JF, Jr. Remodeling of human myocardial collagen in idiopathic dilated cardiomyopathy. Role of metalloproteinases and pyridinoline cross-links [see comments]. *Am J Pathol* 1996;148:1639-1648

73. Dostal DE, Baker KM: Biochemistry, molecular biology, and potential roles of the cardiac renin-angiotensin system, in Dhalla NS, Beamish RE, Takeda N, Nagano M (eds): *The Failing Heart*. Philadelphia, Lippincott-Raven Publishers, 1995, pp 275-294

74. Rosendorff C: The renin-angiotensin system and vascular hypertrophy. *J Am Coll Cardiol* 1996;28:803-812

75. Danser AH: Local renin-angiotensin systems. *Mol Cell Biochem* 1996;157:211-216

76. Dzau VJ, Re R: Tissue angiotensin system in cardiovascular medicine. A paradigm shift? [editorial; comment]. *Circulation* 1994;89:493-498

77. von Lutterotti N, Catanzaro DF, Sealey JE, Laragh JH: Renin is not synthesized by cardiac and extrarenal vascular tissues. A review of experimental evidence [see comments]. *Circulation* 1994;89:458-470

78. Sadoshima J, Xu Y, Slayter HS, Izumo S: Autocrine release of angiotensin II mediates stretch-induced hypertrophy of cardiac myocytes *in vitro*. *Cell* 1993;75:977-984

79. Dostal DE, Rothblum KN, Conrad KM, Cooper GR, Baker KM: Detection of angiotensin I and II in cultured rat cardiac myocytes and fibroblasts. *Am J Physiol* 1992;263:C851-C863

80. Danser AH, van Kesteren CA, Bax WA, Tavenier M, Derkx FH, Saxena PR, Schalekamp MA: Prorenin, renin, angiotensinogen, and angiotensin-converting enzyme in normal and failing human hearts. Evidence for renin binding. *Circulation* 1997;96:220-226

81. Dell'Italia LJ, Meng QC, Balcells E, Wei CC, Palmer R, Hageman GR, Durand J, Hankes GH, Oparil S: Compartmentalization of angiotensin II generation in the dog heart. Evidence for independent mechanisms in intravascular and interstitial spaces. *J Clin Invest* 1997;100:253-258

82. van Kats JP, de Lannoy LM, Jan Danser AH, van Meegen JR, Verdouw PD, Schalekamp MA: Angiotensin II type 1 (AT_1) receptor-mediated accumulation of angiotensin II in tissues and its intracellular half-life *in vivo*. *Hypertension* 1997;30:42-49

83. Goodfriend TL, Elliott ME, Catt KJ: Angiotensin receptors and their antagonists. *N Engl J Med* 1996;334:1649-1654

84. Steinberg MI, Wiest SA, Palkowitz AD: Nonpeptide angiotensin II receptor antagonists. *Cardiovasc Drug Rev* 1993;11:312-358

85. Chiu AT, Herblin WF, McCall DE, Ardecky RJ, Carini DJ, Duncia JV, Pease LJ, Wong PC, Wexler RR, Johnson AL: Identification of angiotensin II receptor subtypes. *Biochem Biophys Res Commun* 1989;165:196-203

86. Wong PC, Hart SD, Zaspel AM, Chiu AT, Ardecky RJ, Smith RD, Timmermans PB: Functional studies of nonpeptide angiotensin II receptor subtype-specific ligands: DuP 753 (AII-1) and PD123177 (AII-2). *J Pharmacol Exp Ther* 1990;255:584-592

87. Whitebread S, Mele M, Kamber B, de Gasparo M: Preliminary biochemical characterization of two angiotensin II receptor subtypes. *Biochem Biophys Res Commun* 1989;163:284-291

88. Griendling KK, Lassegue B, Alexander RW: Angiotensin receptors and their therapeutic implications. *Annu Rev Pharmacol Toxicol* 1996;36:281-306

89. Clauser E, Curnow KM, Davies E, Conchon S, Teutsch B, Vianello B, Monnot C, Corvol P: Angiotensin II receptors: protein and gene structures, expression and potential pathological involvements. *Eur J Endocrinol* 1996;134:403-411

90. Shanmugam S, Corvol P, Gasc JM: Angiotensin II type 2 receptor mRNA expression in the developing cardiopulmonary system of the rat. *Hypertension* 1996;28:91-97

91. Oliverio MI, Best CF, Kim HS, Arendshorst WJ, Smithies O, Coffman TM: Angiotensin II responses in AT_{1A} receptor-deficient mice: a role for AT_{1B} receptors in blood pressure regulation. *Am J Physiol* 1997;272:F515-F520

92. Sechi LA, Grady EF, Griffin CA, Kalinyak JE, Schambelan M: Characterization of angiotensin II receptor subtypes in the rat kidney and heart using the non-peptide antagonists DuP 753 and PD 123 177. *J Hypertens* 1991;9(Suppl 6):S224-5

93. Regitz Zagrosek V, Friedel N, Heymann A, Bauer P, Neuss M, Rolfs A, Steffen C, Hildebrandt A, Hetzer R, Fleck E: Regulation, chamber localization, and subtype distribution of angiotensin II receptors in human hearts. *Circulation* 1995;91:1461-1471

94. Asano K, Dutcher DL, Port JD, Minobe WA, Tremmel KD, Roden RL, Bohlmeyer TJ, Bush EW, Jenkin MJ, Abraham WT, Raynolds MV, Zisman LS, Perryman MB, Bristow MR: Selective downregulation of the angiotensin II AT_1-receptor subtype in failing human ventricular myocardium [see comments]. *Circulation* 1997;95:1193-1200

95. Kim NN, Villarreal FJ, Printz MP, Lee AA, Dillmann WH: Trophic effects of angiotensin II on neonatal rat cardiac myocytes are mediated by cardiac fibroblasts. *Am J Physiol* 1995;269:E426-E437

96. Hein L, Meinel L, Pratt RE, Dzau VJ, Kobilka BK: Intracellular trafficking of angiotensin II and its AT_1 and AT_2 receptors: evidence for selective sorting of receptor and ligand. *Mol Endocrinol* 1997;11:1266-1277

97. Yamada T, Horiuchi M, Dzau VJ: Angiotensin II type 2 receptor mediates programmed cell death. *Proc Natl Acad Sci U S A* 1996;93:156-160

98. Stoll M, Steckelings UM, Paul M, Bottari SP, Metzger R, Unger T: The angiotensin AT_2-receptor mediates inhibition of cell proliferation in coronary endothelial cells. *J Clin Invest* 1995;95:651-657

99. Nakajima M, Hutchinson HG, Fujinaga M, Hayashida W, Morishita R, Zhang L, Horiuchi M, Pratt RE, Dzau VJ: The angiotensin II type 2 (AT_2) receptor antagonizes the growth effects of the AT_1 receptor: gain-of-function study using gene transfer. *Proc Natl Acad Sci U S A* 1995;92:10663-10667

100. Ichiki T, Labosky PA, Shiota C, Okuyama S, Imagawa Y, Fogo A, Niimura F, Ichikawa I, Hogan BL, Inagami T: Effects on blood pressure and exploratory behaviour of mice lacking angiotensin II type-2 receptor. *Nature* 1995;377:748-750

101. Hein L, Barsh GS, Pratt RE, Dzau VJ, Kobilka BK: Behavioural and cardiovascular effects of disrupting the angiotensin II type-2 receptor in mice. *Nature* 1995;377:744-747

102. Kijima K, Matsubara H, Murasawa S, Maruyama K, Mori Y, Ohkubo N, Komuro I, Yazaki Y, Iwasaka T, Inada M: Mechanical stretch induces enhanced expression of

angiotensin II receptor subtypes in neonatal rat cardiac myocytes. *Circ Res* 1996;79:887-897

103. Suzuki J, Matsubara H, Urakami M, Inada M: Rat angiotensin II (type 1A) receptor mRNA regulation and subtype expression in myocardial growth and hypertrophy. *Circ Res* 1993;73:439-447

104. Lee YA, Liang CS, Lee MA, Lindpaintner K: Local stress, not systemic factors, regulate gene expression of the cardiac renin-angiotensin system *in vivo*: a comprehensive study of all its components in the dog. *Proc Natl Acad Sci U S A* 1996;93:11035-11040

105. Crozat A, Penhoat A, Saez JM: Processing of angiotensin II (A-II) and (Sar1,Ala8)A-II by cultured bovine adrenocortical cells. *Endocrinology* 1986;118:2312-2318

106. Griendling KK, Delafontaine P, Rittenhouse SE, Gimbrone MA, Jr., Alexander RW: Correlation of receptor sequestration with sustained diacylglycerol accumulation in angiotensin II-stimulated cultured vascular smooth muscle cells. *J Biol Chem* 1987;262:14555-14562

107. Ullian ME, Linas SL: Role of receptor cycling in the regulation of angiotensin II surface receptor number and angiotensin II uptake in rat vascular smooth muscle cells. *J Clin Invest* 1989;84:840-846

108. Penhoat A, Jaillard C, Crozat A, Saez JM: Regulation of angiotensin II receptors and steroidogenic responsiveness in cultured bovine fasciculata and glomerulosa adrenal cells. *Eur J Biochem* 1988;172:247-254

109. Ouali R, Berthelon MC, Begeot M, Saez JM: Angiotensin II receptor subtypes AT_1 and AT_2 are down-regulated by angiotensin II through AT_1 receptor by different mechanisms. *Endocrinology* 1997;138:725-733

110. Ohyama K, Yamano Y, Chaki S, Kondo T, Inagami T: Domains for G-protein coupling in angiotensin II receptor type I: studies by site-directed mutagenesis. *Biochem Biophys Res Commun* 1992;189:677-683

111. Shibata T, Suzuki C, Ohnishi J, Murakami K, Miyazaki H: Identification of regions in the human angiotensin II receptor type 1 responsible for Gi and Gq coupling by mutagenesis study. *Biochem Biophys Res Commun* 1996;218:383-389

112. Sano T, Ohyama K, Yamano Y, Nakagomi Y, Nakazawa S, Kikyo M, Shirai H, Blank JS, Exton JH, Inagami T: A domain for G protein coupling in carboxyl-terminal tail of rat angiotensin II receptor type 1A. *J Biol Chem* 1997;272:23631-23636

113. Neer EJ: Heterotrimeric G proteins: organizers of transmembrane signals. *Cell* 1995;80:249-257

114. Schelling JR, Nkemere N, Konieczkowski M, Martin KA, Dubyak GR: Angiotensin II activates the β1 isoform of phospholipase C in vascular smooth muscle cells. *Am J Physiol* 1997;272:C1558-C1566

115. Nishizuka Y: Intracellular signaling by hydrolysis of phospholipids and activation of protein kinase C. *Science* 1992;258:607-614

116. Yamaguchi K, Ogita K, Nakamura S, Nishizuka Y: The protein kinase C isoforms leading to MAP-kinase activation in CHO cells. *Biochem Biophys Res Commun* 1995;210:639-647

117. Sadoshima J, Izumo S: Molecular characterization of angiotensin II--induced hypertrophy of cardiac myocytes and hyperplasia of cardiac fibroblasts. Critical role of the AT_1 receptor subtype. *Circ Res* 1993;73:413-423

118. Paul K, Ball NA, Dorn GW, 2nd, Walsh RA: Left ventricular stretch stimulates angiotensin II--mediated phosphatidylinositol hydrolysis and protein kinase C epsilon isoform translocation in adult guinea pig hearts [see comments]. *Circ Res* 1997;81:643-650

119. Wakasaki H, Koya D, Schoen FJ, Jirousek MR, Ways DK, Hoit BD, Walsh RA, King GL: Targeted overexpression of protein kinase C β2 isoform in myocardium causes cardiomyopathy. *Proc Natl Acad Sci U S A* 1997;94:9320-9325

120. Bowman JC, Steinberg SF, Jiang T, Geenen DL, Fishman GI, Buttrick PM: Expression of protein kinase C β in the heart causes hypertrophy in adult mice and sudden death in neonates. *J Clin Invest* 1997;100:2189-2195

121. Davis RJ: The mitogen-activated protein kinase signal transduction pathway. *J Biol Chem* 1993;268:14553-14556

122. Schorb W, Conrad KM, Singer HA, Dostal DE, Baker KM: Angiotensin II is a potent stimulator of MAP-kinase activity in neonatal rat cardiac fibroblasts. *J Mol Cell Cardiol* 1995;27:1151-1160

123. Muller JM, Krauss B, Kaltschmidt C, Baeuerle PA, Rupec RA: Hypoxia induces c-fos transcription via a mitogen-activated protein kinase-dependent pathway. *J Biol Chem* 1997;272:23435-23439

124. Zechner D, Thuerauf DJ, Hanford DS, McDonough PM, Glembotski CC: A role for the p38 mitogen-activated protein kinase pathway in myocardial cell growth, sarcomeric organization, and cardiac-specific gene expression. *J Cell Biol* 1997;139:115-127

125. Ishida M, Marrero MB, Schieffer B, Ishida T, Bernstein KE, Berk BC: Angiotensin II activates pp60c-src in vascular smooth muscle cells. *Circ Res* 1995;77:1053-1059

126. Sadoshima J, Izumo S: The heterotrimeric G q protein-coupled angiotensin II receptor activates p21 ras via the tyrosine kinase-Shc-Grb2-Sos pathway in cardiac myocytes. *EMBO J* 1996;15:775-787

127. Marrero MB, Schieffer B, Paxton WG, Heerdt L, Berk BC, Delafontaine P, Bernstein KE: Direct stimulation of Jak/STAT pathway by the angiotensin II AT_1 receptor. *Nature* 1995;375:247-250

128. Kudoh S, Komuro I, Mizuno T, Yamazaki T, Zou Y, Shiojima I, Takekoshi N, Yazaki Y: Angiotensin II stimulates c-Jun NH2-terminal kinase in cultured cardiac myocytes of neonatal rats. *Circ Res* 1997;80:139-146

129. Schieffer B, Paxton WG, Marrero MB, Bernstein KE: Importance of tyrosine phosphorylation in angiotensin II type 1 receptor signaling. *Hypertension* 1996;27:476-480

130. Marrero MB, Schieffer B, Li B, Sun J, Harp JB, Ling BN: Role of Janus kinase/signal transducer and activator of transcription and mitogen-activated protein kinase cascades in angiotensin II- and platelet-derived growth factor-induced vascular smooth muscle cell proliferation. *J Biol Chem* 1997;272:24684-24690

131. Bhat GJ, Thekkumkara TJ, Thomas WG, Conrad KM, Baker KM: Angiotensin II stimulates sis-inducing factor-like DNA binding activity. Evidence that the AT_{1A} receptor activates transcription factor-Stat91 and/or a related protein. *J Biol Chem* 1994;269:31443-31449

132. Ali MS, Sayeski PP, Dirksen LB, Hayzer DJ, Marrero MB, Bernstein KE: Dependence on the motif YIPP for the physical association of Jak2 kinase with the intracellular carboxyl tail of the angiotensin II AT_1 receptor. *J Biol Chem* 1997;272:23382-23388

133. Inagami T: Recent progress in molecular and cell biological studies of angiotensin receptors. *Curr Opin Nephrol Hypertens* 1995;4:47-54

134. Zhang J, Pratt RE: The AT_2 receptor selectively associates with Giα2 and Giα3 in the rat fetus. *J Biol Chem* 1996;271:15026-15033

135. Hayashida W, Horiuchi M, Dzau VJ: Intracellular third loop domain of angiotensin II type-2 receptor. Role in mediating signal transduction and cellular function. *J Biol Chem* 1996;271:21985-21992

136. Massague J: The transforming growth factor-β family. *Annu Rev Cell Biol* 1990;6:597-641

137. Roberts AB, Sporn MB: The transforming growth factor-βs, in Sporn MB, Roberts AB (eds): *Peptide Growth Factors and Their Receptors I.* New York, Springer-Verlag, 1990, pp 420-472

138. Engelmann GL, Boehm KD, Birchenall Roberts MC, Ruscetti FW: Transforming growth factor-β1 in heart development. *Mech Dev* 1992;38:85-97

139. Lee AA, Dillmann WH, McCulloch AD, Villarreal FJ: Angiotensin II stimulates the autocrine production of transforming growth factor-β1 in adult rat cardiac fibroblasts. *J Mol Cell Cardiol* 1995;27:2347-2357

140. MacLellan WR, Brand T, Schneider MD: Transforming growth factor-β in cardiac ontogeny and adaptation. *Circ Res* 1993;73:783-791

141. Flanders KC, Winokur TS, Holder MG, Sporn MB: Hyperthermia induces expression of transforming growth factor-βs in rat cardiac cells *in vitro* and *in vivo*. *J Clin Invest* 1993;92:404-410

142. Chua CC, Diglio CA, Siu BB, Chua BH: Angiotensin II induces TGF-β1 production in rat heart endothelial cells. *Biochim Biophys Acta* 1994;1223:141-147

143. Eghbali M: Cellular origin and distribution of transforming growth factor-β in the normal rat myocardium. *Cell Tissue Res* 1989;256:553-558

144. Takahashi N, Calderone A, Izzo NJ, Jr., Maki TM, Marsh JD, Colucci WS: Hypertrophic stimuli induce transforming growth factor-β1 expression in rat ventricular myocytes. *J Clin Invest* 1994;94:1470-1476

145. Miyazono K, Ichijo H, Heldin CH: Transforming growth factor-β: latent forms, binding proteins and receptors. *Growth Factors* 1993;8:11-22

146. Yamaguchi Y, Mann DM, Ruoslahti E: Negative regulation of transforming growth factor-β by the proteoglycan decorin. *Nature* 1990;346:281-284

147. Isaka Y, Brees DK, Ikegaya K, Kaneda Y, Imai E, Noble NA, Border WA: Gene therapy by skeletal muscle expression of decorin prevents fibrotic disease in rat kidney. *Nat Med* 1996;2:418-423

148. Engelmann GL, Grutkoski PS: Coordinate TGF-β receptor gene expression during rat heart development. *Cell Mol Biol Res* 1994;40:93-104

149. Ross J, Janero DR, Hreniuk D: Identification and biochemical characterization of a heart-muscle cell transforming growth factor β-1 receptor. *Biochem Pharmacol* 1993;46:511-516

150. Ross J, Janero DR, Hreniuk D: Identification and molecular characterization of a high-affinity cardiomyocyte transforming growth factor-β2 receptor. *FEBS Lett* 1993;320:229-234

151. Wrana JL, Attisano L, Wieser R, Ventura F, Massague J: Mechanism of activation of the TGF-β receptor. *Nature* 1994;370:341-347

152. Brand T, Schneider MD: Inactive type II and type I receptors for TGF β are dominant inhibitors of TGF β-dependent transcription. *J Biol Chem* 1995;270:8274-8284

153. Brand T, MacLellan WR, Schneider MD: A dominant-negative receptor for type β transforming growth factors created by deletion of the kinase domain. *J Biol Chem* 1993;268:11500-11503

154. Massague J: TGFβ signaling: receptors, transducers, and Mad proteins. *Cell* 1996;85:947-950

155. Zhang Y, Feng X, We R, Derynck R: Receptor-associated Mad homologues synergize as effectors of the TGF-β response. *Nature* 1996;383:168-172

156. Lagna G, Hata A, Hemmati Brivanlou A, Massague J: Partnership between DPC4 and SMAD proteins in TGF-β signalling pathways. *Nature* 1996;383:832-836

157. Chen X, Rubock MJ, Whitman M: A transcriptional partner for MAD proteins in TGF-β signalling. *Nature* 1996;383:691-696

158. Kim J, Johnson K, Chen HJ, Carroll S, Laughon A: Drosophila Mad binds to DNA and directly mediates activation of vestigial by Decapentaplegic. *Nature* 1997;388:304-308

159. Topper JN, Cai J, Qiu Y, Anderson KR, Xu YY, Deeds JD, Feeley R, Gimeno CJ, Woolf EA, Tayber O, Mays GG, Sampson BA, Schoen FJ, Gimbrone MA, Jr., Falb D: Vascular MADs: two novel MAD-related genes selectively inducible by flow in human vascular endothelium. *Proc Natl Acad Sci U S A* 1997;94:9314-9319

160. Hayashi H, Abdollah S, Qiu Y, Cai J, Xu YY, Grinnell BW, Richardson MA, Topper JN, Gimbrone MA, Jr., Wrana JL, Falb D: The MAD-related protein Smad7 associates with the TGFβ receptor and functions as an antagonist of TGFβ signaling. *Cell* 1997;89:1165-1173

161. Imamura T, Takase M, Nishihara A, Oeda E, Hanai J, Kawabata M, Miyazono K: Smad6 inhibits signalling by the TGF-β superfamily [see comments]. *Nature* 1997;389:622-626

162. Sankar S, Mahooti Brooks N, Centrella M, McCarthy TL, Madri JA: Expression of transforming growth factor type III receptor in vascular endothelial cells increases their responsiveness to transforming growth factor β2. *J Biol Chem* 1995;270:13567-13572

163. Gibbons GH, Pratt RE, Dzau VJ: Vascular smooth muscle cell hypertrophy *vs* hyperplasia. Autocrine transforming growth factor-β1 expression determines growth response to angiotensin II. *J Clin Invest* 1992;90:456-461

164. Antonipillai I, Le TH, Soceneantu L, Horton R: Transforming growth factor-β is a renin secretagogue at picomolar concentrations. *Am J Physiol* 1993;265:F537-41

165. Booz GW, Baker KM: Role of type 1 and type 2 angiotensin receptors in angiotensin II-induced cardiomyocyte hypertrophy. *Hypertension* 1996;28:635-640

166. van Kesteren CA, van Heugten HA, Lamers JM, Saxena PR, Schalekamp MA, Danser AH: Angiotensin II-mediated growth and antigrowth effects in cultured neonatal rat cardiac myocytes and fibroblasts. *J Mol Cell Cardiol* 1997;29:2147-2157

167. Schunkert H, Sadoshima J, Cornelius T, Kagaya Y, Weinberg EO, Izumo S, Riegger G, Lorell BH: Angiotensin II-induced growth responses in isolated adult rat hearts. Evidence for load-independent induction of cardiac protein synthesis by angiotensin II. *Circ Res* 1995;76:489-497

168. Ponicke K, Heinroth Hoffmann I, Becker K, Brodde OE: Trophic effect of angiotensin II in neonatal rat cardiomyocytes: role of endothelin-1 and non-myocyte cells. *Br J Pharmacol* 1997;121:118-124

169. Sil P, Sen S: Angiotensin II and myocyte growth: role of fibroblasts. *Hypertension* 1997;30:209-216

170. Dostal DE, Baker KM: Angiotensin II stimulation of left ventricular hypertrophy in adult rat heart. Mediation by the AT_1 receptor. *Am J Hypertens* 1992;5:276-280

171. Schieffer B, Wirger A, Meybrunn M, Seitz S, Holtz J, Riede UN, Drexler H: Comparative effects of chronic angiotensin-converting enzyme inhibition and angiotensin II type 1 receptor blockade on cardiac remodeling after myocardial infarction in the rat. *Circulation* 1994;89:2273-2282

172. Pfeffer JM, Pfeffer MA, Braunwald E: Influence of chronic captopril therapy on the infarcted left ventricle of the rat. *Circ Res* 1985;57:84-95

173. Wollert KC, Studer R, Doerfer K, Schieffer E, Holubarsch C, Just H, Drexler H: Differential effects of kinins on cardiomyocyte hypertrophy and interstitial collagen matrix in the surviving myocardium after myocardial infarction in the rat. *Circulation* 1997;95:1910-1917

174. Makino N, Hata T, Sugano M, Dixon IM, Yanaga T: Regression of hypertrophy after myocardial infarction is produced by the chronic blockade of angiotensin type 1 receptor in rats. *J Mol Cell Cardiol* 1996;28:507-517

175. Ju H, Dixon IM: Effect of angiotensin II on myocardial collagen gene expression. *Mol Cell Biochem* 1996;163-164:231-237

176. Campbell SE, Janicki JS, Weber KT: Temporal differences in fibroblast proliferation and phenotype expression in response to chronic administration of angiotensin II or aldosterone. *J Mol Cell Cardiol* 1995;27:1545-1560

177. Kim S, Ohta K, Hamaguchi A, Yukimura T, Miura K, Iwao H: Angiotensin II induces cardiac phenotypic modulation and remodeling *in vivo* in rats. *Hypertension* 1995;25:1252-1259

178. Brecher P: Angiotensin II and cardiac fibrosis. *Trends Cardiovasc Med* 1996;6:193-198

179. van Krimpen C, Smits JF, Cleutjens JP, Debets JJ, Schoemaker RG, Struyker Boudier HA, Bosman FT, Daemen MJ: DNA synthesis in the non-infarcted cardiac interstitium after left coronary artery ligation in the rat: effects of captopril. *J Mol Cell Cardiol* 1991;23:1245-1253

180. Smits JF, van Krimpen C, Schoemaker RG, Cleutjens JP, Daemen MJ: Angiotensin II receptor blockade after myocardial infarction in rats: effects on hemodynamics, myocardial DNA synthesis, and interstitial collagen content. *J Cardiovasc Pharmacol* 1992;20:772-778

181. Linz W, Schaper J, Wiemer G, Albus U, Scholkens BA: Ramipril prevents left ventricular hypertrophy with myocardial fibrosis without blood pressure reduction: a one year study in rats. *Br J Pharmacol* 1992;107:970-975

182. Sun Y, Weber KT: Angiotensin II receptor binding following myocardial infarction in the rat. *Cardiovasc Res* 1994;28:1623-1628

183. Nio Y, Matsubara H, Murasawa S, Kanasaki M, Inada M: Regulation of gene transcription of angiotensin II receptor subtypes in myocardial infarction. *J Clin Invest* 1995;95:46-54

184. Liu YH, Yang XP, Sharov VG, Nass O, Sabbah HN, Peterson E, Carretero OA: Effects of angiotensin-converting enzyme inhibitors and angiotensin II type 1 receptor antagonists in rats with heart failure. Role of kinins and angiotensin II type 2 receptors. *J Clin Invest* 1997;99:1926-1935

185. Colucci WS, Braunwald E: Pathophysiology of heart failure, in Braunwald E (ed): *Heart Disease*. Philadelphia, W.B.Saunders Company, 1997, pp 394-420

186. Hirsch AT, Talsness CE, Schunkert H, Paul M, Dzau VJ: Tissue-specific activation of cardiac angiotensin converting enzyme in experimental heart failure. *Circ Res* 1991;69:475-482

187. Yamagishi H, Kim S, Nishikimi T, Takeuchi K, Takeda T: Contribution of cardiac renin-angiotensin system to ventricular remodelling in myocardial-infarcted rats. *J Mol Cell Cardiol* 1993;25:1369-1380

188. Lindpaintner K, Lu W, Neidermajer N, Schieffer B, Just H, Ganten D, Drexler H: Selective activation of cardiac angiotensinogen gene expression in post-infarction ventricular remodeling in the rat. *J Mol Cell Cardiol* 1993;25:133-143

189. Reiss K, Capasso JM, Huang HE, Meggs LG, Li P, Anversa P: ANG II receptors, c-*myc*, and c-*jun* in myocytes after myocardial infarction and ventricular failure. *Am J Physiol* 1993;264:H760-H769

190. Schunkert H, Tang SS, Litwin SE, Diamant D, Riegger G, Dzau VJ, Ingelfinger JR: Regulation of intrarenal and circulating renin-angiotensin systems in severe heart failure in the rat. *Cardiovasc Res* 1993;27:731-735

191. Johnston CI, Mooser V, Sun Y, Fabris B: Changes in cardiac angiotensin converting enzyme after myocardial infarction and hypertrophy in rats. *Clin Exp Pharmacol Physiol* 1991;18:107-110

192. Huang H, Arnal JF, Llorens Cortes C, Challah M, Alhenc Gelas F, Corvol P, Michel JB: Discrepancy between plasma and lung angiotensin-converting enzyme activity in experimental congestive heart failure. A novel aspect of endothelium dysfunction. *Circ Res* 1994;75:454-461

193. Sun Y, Cleutjens JP, Diaz-Arias AA, Weber KT: Cardiac angiotensin converting enzyme and myocardial fibrosis in the heart. *Cardiolvasc Res* 1994;28:1423-1432

194. Passier RC, Smits JF, Verluyten MJ, Studer R, Drexler H, Daemen MJ: Activation of angiotensin-converting enzyme expression in infarct zone following myocardial infarction. *Am J Physiol* 1995;269:H1268-H1276

195. Hokimoto S, Yasue H, Fujimoto K, Yamamoto H, Nakao K, Kaikita K, Sakata R, Miyamoto E: Expression of angiotensin-converting enzyme in remaining viable myocytes of human ventricles after myocardial infarction. *Circulation* 1996;94:1513-1518

196. Lefroy DC, Wharton J, Crake T, Knock GA, Rutherford RA, Suzuki T, Morgan K, Polak J, Poole-Wilson PA: Regional changes in angiotensin II receptor density after experimental myocardial infarction. *J Mol Cell Cardiol* 1996;28:429-440

197. Duncan AM, Burrell LM, Kladis A, Campbell DJ: Angiotensin and bradykinin peptides in rats with myocardial infarction. *Growth Factors* 1997;3:41-52

198. Luchner A, Stevens TL, Borgeson DD, Redfield MM, Bailey JE, Sandberg SM, Heublein DM, Burnett JC, Jr. Angiotensin II in the evolution of experimental heart failure. *Hypertension* 1996;28:472-477

199. Lambert C, Massillon Y, Meloche S: Upregulation of cardiac angiotensin II AT_1 receptors in congenital cardiomyopathic hamsters. *Circ Res* 1995;77:1001-1007

200. Dzau VJ: Tissue renin-angiotensin system in myocardial hypertrophy and failure. *Arch Intern Med* 1993;153:937-942

201. Baker KM, Booz GW, Dostal DE: Cardiac actions of angiotensin II: Role of an intracardiac renin-angiotensin system. *Annu Rev Physiol* 1992;54:227-241

202. Wollert KC, Studer R, von Bulow B, Drexler H: Survival after myocardial infarction in the rat. Role of tissue angiotensin-converting enzyme inhibition. *Circulation* 1994;90:2457-2467

203. AIRE Study Investigators. Effect of ramipril on mortality and morbidity of survivors of acute myocardial infarction with clinical evidence of heart failure. The Acute Infarction Ramipril Efficacy (AIRE) Study Investigators [see comments]. *Lancet* 1993;342:821-828

204. Pfeffer MA, Braunwald E, Moye LA, Basta L, Brown EJ, Jr., Cuddy TE, Davis BR, Geltman EM, Goldman S, Flaker GC, et al: Effect of captopril on mortality and morbidity in patients with left ventricular dysfunction after myocardial infarction. Results of the survival and ventricular enlargement trial. The SAVE Investigators [see comments]. *N Engl J Med* 1992;327:669-677

205. Milavetz JJ, Raya TE, Johnson CS, Morkin E, Goldman S: Survival after myocardial infarction in rats: captopril versus losartan. *J Am Coll Cardiol* 1996;27:714-719

206. Pitt B, Segal R, Martinez FA, Meurers G, Cowley AJ, Thomas I, Deedwania PC, Ney DE, Snavely DB, Chang PI: Randomised trial of losartan versus captopril in patients over 65 with heart failure (Evaluation of Losartan in the Elderly Study, ELITE). *Lancet* 1997;349:747-752

207. Heimer R, Bashey RI, Kyle J, Jimenez SA: TGF-β modulates the synthesis of proteoglycans by myocardial fibroblasts in culture. *J Mol Cell Cardiol* 1995;27:2191-2198

208. Eghbali M, Tomek R, Sukhatme VP, Woods C, Bhambi B: Differential effects of transforming growth factor-β1 and phorbol myristate acetate on cardiac fibroblasts. Regulation of fibrillar collagen mRNAs and expression of early transcription factors. *Circ Res* 1991;69:483-490

209. Ito K, Ryuto M, Ushiro S, Ono M, Sugenoya A, Kuraoka A, Shibata Y, Kuwano M: Expression of tissue-type plasminogen activator and its inhibitor couples with development of capillary network by human microvascular endothelial cells on Matrigel. *J Cell Physiol* 1995;162:213-224

210. Koff A, Ohtsuki M, Polyak K, Roberts JM, Massague J: Negative regulation of G1 in mammalian cells: inhibition of cyclin E-dependent kinase by TGF-β. *Science* 1993;260:536-539

211. Ewen ME, Sluss HK, Whitehouse LL, Livingston DM: TGF β inhibition of Cdk4 synthesis is linked to cell cycle arrest. *Cell* 1993;74:1009-1020

212. Hannon GJ, Beach D: $p^{15INK4B}$ is a potential effector of TGF-β-induced cell cycle arrest [see comments]. *Nature* 1994;371:257-261

213. Datto MB, Li Y, Panus JF, Howe DJ, Xiong Y, Wang XF: Transforming growth factor β induces the cyclin-dependent kinase inhibitor p21 through a p53-independent mechanism. *Proc Natl Acad Sci U S A* 1995;92:5545-5549

214. Long CS: Autocrine and paracrine regulation of myocardial cell growth *in vitro*. *Trends Cardiovasc Med* 1996;6:217-226

215. Sigel A, Douglas JA, Eghbali Webb M: Regulation of mRNA transcripts and DNA synthesis in the rat heart following intravenous injection of transforming growth factor β1. *Mol Cell Biochem* 1994;141:145-151

216. Long CS, Henrich CJ, Simpson PC: A growth factor for cardiac myocytes is produced by cardiac nonmyocytes. *Cell Regul* 1991;2:1081-1095

217. Parker TG, Packer SE, Schneider MD: Peptide growth factors can provoke "fetal" contractile protein gene expression in rat cardiac myocytes. *J Clin Invest* 1990;85:507-514

218. Schluter KD, Zhou XJ, Piper HM: Induction of hypertrophic responsiveness to isoproterenol by TGF-β in adult rat cardiomyocytes. *Am J Physiol* 1995;269:C1311-C1316

219. Miki N, Hamamori Y, Hirata K, Suematsu M, Kawashima S, Akita H, Yokoyama M: Transforming growth factor-β1 potentiated α1-adrenergic and stretch-induced c-fos mRNA expression in rat myocardial cells. *Circ Res* 1994;75:8-14

220. Villarreal FJ, Dillmann WH: Cardiac hypertrophy-induced changes in mRNA levels for TGF-β1, fibronectin, and collagen. *Am J Physiol* 1992;262:H1861-H1866

221. Everett AD, Tufro McReddie A, Fisher A, Gomez RA: Angiotensin receptor regulates cardiac hypertrophy and transforming growth factor-β1 expression. *Hypertension* 1994;23:587-592

222. Li RK, Mickle DA, Weisel RD, Merante F, Luss H, Rao V, Christakis GT, Williams WG: Overexpression of transforming growth factor-β1 and insulin-like growth factor-I in patients with idiopathic hypertrophic cardiomyopathy. *Circulation* 1997;96:874-881

223. Li JM, Brooks G: Differential protein expression and subcellular distribution of TGF β1, β2 and β3 in cardiomyocytes during pressure overload-induced hypertrophy. *J Mol Cell Cardiol* 1997;29:2213-2224

224. Dixon IM, Lee SL, Dhalla NS: Nitrendipine binding in congestive heart failure due to myocardial infarction. *Circ Res* 1990;66:782-788

225. Johns T, N., Olson BJ: Experimental myocardial infarction. I. A method of coronary occlusion in small animals. *Ann Surg* 1954;140:675-682

226. Selye H, Bajusz E, Grasso S, Mendell P: Simple techniques for the sugical occlusion of coronary vessels in the rat. *Angiology* 1960;11:398-407

227. Dixon IM, Hata T, Dhalla NS: Sarcolemmal calcium transport in congestive heart failure due to myocardial infarction in rats. *Am J Physiol* 1992;262:H1387-H1394

228. Fletcher PJ, Pfeffer JM, Pfeffer MA, Braunwald E: Left ventricular diastolic pressure-volume relations in rats with healed myocardial infarction. *Circ Res* 1981;49:618-626

229. Chiariello M, Ambrosio G, Cappelli Bigazzi M, Perrone Filardi P, Brigante F, Sifola C: A biochemical method for the quantitation of myocardial scarring after experimental coronary artery occlusion. *J Mol Cell Cardiol* 1986;18:283-290

230. Polak JM, van Noorden S: An introduction to immunocytochemistry:current techniques and problems. 1984;1-49

231. Ju H, Scammel La Fleur T, Dixon IM: Altered mRNA abundance of calcium transport genes in cardiac myocytes induced by angiotensin II. *J Mol Cell Cardiol* 1996;28:1119-1128

232. Chomczynski P, Sacchi N: Single-step method of RNA isolation by acid guanidinium thiocyanate-phenol-chloroform extraction. *Anal Biochem* 1987;162:156-159

233. Chan YL, Gutell R, Noller HF, Wool IG: The nucleotide sequence of a rat 18 S ribosomal ribonucleic acid gene and a proposal for the secondary structure of 18 S ribosomal ribonucleic acid. *J Biol Chem* 1984;259:224-230

234. Bai Y, Muragaki Y, Obata K, Iwata K, Ooshima A: Immunological properties of monoclonal antibodies to human and rat prolyl 4-hydroxylase. *J Biochem Tokyo* 1986;99:1563-1570

235. Smith PK, Krohn RI, Hermanson GT, Mallia AK, Gartner FH, Provenzano MD, Fujimoto EK, Goeke NM, Olson BJ, Klenk DC: Measurement of protein using bicinchoninic acid [published erratum appears in Anal Biochem 1987 May 15;163(1):279]. *Anal Biochem* 1985;150:76-85

236. Tyagi SC, Matsubara L, Weber KT: Direct extraction and estimation of collagenase(s) activity by zymography in microquantities of rat myocardium and uterus. *Clin Biochem* 1993;26:191-198

237. Raya TE, Gay RG, Lancaster L, Aguirre M, Moffett C, Goldman S: Serial changes in left ventricular relaxation and chamber stiffness after large myocardial infarction in rats. *Circulation* 1988;77:1424-1431

238. Gettys TW, Sheriff Carter K, Moomaw J, Taylor IL, Raymond JR: Characterization and use of crude α -subunit preparations for quantitative immunoblotting of G proteins. *Anal Biochem* 1994;220:82-91

239. Wahl MI, Jones GA, Nishibe S, Rhee SG, Carpenter G: Growth factor stimulation of phospholipase C-γ1 activity. Comparative properties of control and activated enzymes. *J Biol Chem* 1992;267:10447-10456

240. Chilvers ER, Batty IH, Challiss RA, Barnes PJ, Nahorski SR: Determination of mass changes in phosphatidylinositol 4,5-bisphosphate and evidence for agonist-stimulated metabolism of inositol 1,4,5-trisphosphate in airway smooth muscle. *Biochem J* 1991;275:373-379

241. Tanaka Y, Kashiwagi A, Ogawa T, Abe N, Asahina T, Ikebuchi M, Takagi Y, Shigeta Y: Effect of verapamil on cardiac protein kinase C activity in diabetic rats. *Eur J Pharmacol* 1991;200:353-356

242. Xiang H, McNeill JH: Protein kinase C activity is altered in diabetic rat hearts. *Biochem Biophys Res Commun* 1992;187:703-710

243. Danielpour D: Improved sandwich enzyme-linked immunosorbent assays for transforming growth factor β1. *J Immunol Methods* 1993;158:17-25

244. Fisher SA, Periasamy M: Collagen synthesis inhibitors disrupt embryonic cardiocyte myofibrillogenesis and alter the expression of cardiac specific genes *in vitro*. *J Mol Cell Cardiol* 1994;26:721-731

245. Knowlton AA, Connelly CM, Romo GM, Mamuya W, Apstein CS, Brecher P: Rapid expression of fibronectin in the rabbit heart after myocardial infarction with and without reperfusion. *J Clin Invest* 1992;89:1060-1068

246. Pfeffer JM, Pfeffer MA, Fletcher PJ, Braunwald E: Ventricular performance in rats with myocardial infarction and failure. *Am J Med* 1984;76:99-103

247. Geenen DL, Malhotra A, Scheuer J: Regional variation in rat cardiac myosin isoenzymes and ATPase activity after infarction. *Am J Physiol* 1989;256:H745-H750

248. Anversa P, Olivetti G, Capasso JM: Cellular basis of ventricular remodeling after myocardial infarction. *Am J Cardiol* 1991;68:7D-16D

249. Inoue K, Kusachi S, Niiya K, Kajikawa Y, Tsuji T: Sequential changes in the distribution of type I and III collagens in the infarct zone: immunohistochemical study of experimental myocardial infarction in the rat. *Coron Artery Dis* 1995;6:153-158

250. Conrad CH, Brooks WW, Hayes JA, Sen S, Robinson KG, Bing OH: Myocardial fibrosis and stiffness with hypertrophy and heart failure in the spontaneously hypertensive rat. *Circulation* 1995;91:161-170

251. Butt RP, Bishop JE: Mechanical load enhances the stimulatory effect of serum growth factors on cardiac fibroblast procollagen synthesis. *J Mol Cell Cardiol* 1997;29:1141-1151

252. Crawford DC, Chobanian AV, Brecher P: Angiotensin II induces fibronectin expression associated with cardiac fibrosis in the rat. *Circ Res* 1994;74:727-739

253. Eleftheriades EG, Ferguson AG, Spragia ML, Samarel AM: Prolyl hydroxylation regulates intracellular procollagen degradation in cultured rat cardiac fibroblasts. *J Mol Cell Cardiol* 1995;27:1459-1473

254. Michel JB, Lattion AL, Salzmann JL, Cerol ML, Philippe M, Camilleri JP, Corvol P: Hormonal and cardiac effects of converting enzyme inhibition in rat myocardial infarction. *Circ Res* 1988;62:641-650

255. Booz GW, Baker KM: Molecular signalling mechanisms controlling growth and function of cardiac fibroblasts. *Cardiovasc Res* 1995;30:537-543

256. Meggs LG, Coupet J, Huang H, Cheng W, Li P, Capasso JM, Homcy CJ, Anversa P: Regulation of angiotensin II receptors on ventricular myocytes after myocardial infarction in rats. *Circ Res* 1993;72:1149-1162

257. Capasso JM, Li P, Meggs LG, Herman MV, Anversa P: Efficacy of angiotensin-converting enzyme inhibition and AT_1 receptor blockade on cardiac pump performance after myocardial infarction in rats. *J Cardiovasc Pharmacol* 1994;23:584-593

258. Hanatani A, Yoshiyama M, Kim S, Omura T, Toda I, Akioka K, Teragaki M, Takeuchi K, Iwao H, Takeda T: Inhibition by angiotensin II type 1 receptor antagonist of cardiac phenotypic modulation after myocardial infarction. *J Mol Cell Cardiol* 1995;27:1905-1914

259. Kim S, Ohta K, Hamaguchi A, Omura T, Yukimura T, Miura K, Inada Y, Ishimura Y, Chatani F, Iwao H: Angiotensin II type I receptor antagonist inhibits the gene expression of transforming growth factor-β1 and extracellular matrix in cardiac and vascular tissues of hypertensive rats. *J Pharmacol Exp Ther* 1995;273:509-515

260. Mays PK, McAnulty RJ, Campa JS, Laurent GJ: Age-related changes in collagen synthesis and degradation in rat tissues. Importance of degradation of newly synthesized collagen in regulating collagen production. *Biochem J* 1991;276:307-313

261. Shi B, Heavner JE, McMahon KK, Spallholz JE: Dynamic changes in $G\alpha_{i-2}$ levels in rat hearts associated with impaired heart function after myocardial infarction. *Am J Physiol* 1995;269:H1073-H1079

262. Brodde OE, Michel MC, Zerkowski HR: Signal transduction mechanisms controlling cardiac contractility and their alterations in chronic heart failure. *Cardiovasc Res* 1995;30:570-584

263. LaMorte VJ, Thorburn J, Absher D, Spiegel A, Brown JH, Chien KR, Feramisco JR, Knowlton KU: Gq- and ras-dependent pathways mediate hypertrophy of neonatal rat ventricular myocytes following α1-adrenergic stimulation. *J Biol Chem* 1994;269:13490-13496

264. Sakai S, Miyauchi T, Kobayashi M, Yamaguchi I, Goto K, Sugishita Y: Inhibition of myocardial endothelin pathway improves long-term survival in heart failure. *Nature* 1996;384:353-355

265. Eguchi S, Hirata Y, Imai T, Marumo F: Endothelin receptor subtypes are coupled to adenylate cyclase via different guanyl nucleotide-binding proteins in vasculature. *Endocrinology* 1993;132:524-529

266. Sokolovsky M: Functional coupling between endothelin receptors and multiple G-proteins in rat heart myocytes. *Receptors Channels* 1993;1:295-304

267. Sun Y, Weber KT: Cells expressing angiotensin II receptors in fibrous tissue of rat heart. *Cardiovasc Res* 1996;31:518-525

268. Dhalla NS, Dixon IM, Rupp H, Barwinsky J: Experimental congestive heart failure due to myocardial infarction: sarcolemmal receptors and cation transporters. *Basic Res Cardiol* 1991;86(Suppl 3):13-23

269. Strathmann M, Simon MI: G protein diversity: a distinct class of α subunits is present in vertebrates and invertebrates. *Proc Natl Acad Sci U S A* 1990;87:9113-9117

270. Eichhorn EJ, Bristow MR: Medical therapy can improve the biological properties of the chronically failing heart. A new era in the treatment of heart failure. *Circulation* 1996;94:2285-2296

271. Nash JA, Hammond HK, Saffitz JE: Subcellular compartmentalization of Gsα in cardiac myocytes and its redistribution in heart failure. *Am J Physiol* 1996;271:H2209-H2217

272. Hansen CA, Schroering AG, Robishaw JD: Subunit expression of signal transducing G proteins in cardiac tissue: implications for phospholipase C-β regulation. *J Mol Cell Cardiol* 1995;27:471-484

273. Sappino AP, Schurch W, Gabbiani G: Differentiation repertoire of fibroblastic cells: expression of cytoskeletal proteins as marker of phenotypic modulations. *Lab Invest* 1990;63:144-161

274. Sun Y, Weber KT: Angiotensin converting enzyme and myofibroblasts during tissue repair in the rat heart. *J Mol Cell Cardiol* 1996;28:851-858

275. Willems IE, Havenith MG, De Mey JG, Daemen MJ: The α-smooth muscle actin-positive cells in healing human myocardial scars. *Am J Pathol* 1994;145:868-875

276. D'Angelo DD, Sakata Y, Lorenz JN, Boivin GP, Walsh RA, Liggett SB, Dorn II GW: Transgenic Gαq overexpression induces cardiac contractile failure in mice. *Proc Natl Acad Sci USA* 1997;94:8121-8126

277. Blank JL, Ross AH, Exton JH: Purification and characterization of two G-proteins that activate the β1 isozyme of phosphoinositide-specific phospholipase C. Identification as members of the Gq class. *J Biol Chem* 1991;266:18206-18216

278. Jhon DY, Lee HH, Park D, Lee CW, Lee KH, Yoo OJ, Rhee SG: Cloning, sequencing, purification, and Gq-dependent activation of phospholipase C-β3. *J Biol Chem* 1993;268:6654-6661

279. Chareonthaitawee P, Christian TF, Hirose K, Gibbons RJ, Rumberger JA: Relation of initial infarct size to extent of left ventricular remodeling in the year after acute myocardial infarction. *J Am Coll Cardiol* 1995;25:567-573

280. Holmes JW, Nunez JA, Covell JW: Functional implications of myocardial scar structure. *Am J Physiol* 1997;272:H2123-H2130

281. Jugdutt BI, Joljart MJ, Khan MI: Rate of collagen deposition during healing and ventricular remodeling after myocardial infarction in rat and dog models. *Circulation* 1996;94:94-101

282. Villarreal FJ, Lee AA, Dillmann WH, Giordano FJ: Adenovirus-mediated overexpression of human transforming growth factor-β1 in rat cardiac fibroblasts, myocytes and smooth muscle cells. *J Mol Cell Cardiol* 1996;28:735-742

283. Hall FL, Benya PD, Padilla SR, Carbonaro Hall D, Williams R, Buckley S, Warburton D: Transforming growth factor-β type-II receptor signalling: intrinsic/associated casein kinase activity, receptor interactions and functional effects of blocking antibodies. *Biochem J* 1996;316:303-310

284. Mucsi I, Goldberg HJ: Dominant-negative SMAD-3 interferes with transcriptional activation by multiple agonists. *Biochem Biophys Res Commun* 1997;232:517-521

285. Liu X, Sun Y, Constantinescu SN, Karam E, Weinberg RA, Lodish HF: Transforming growth factor β-induced phosphorylation of Smad3 is required for growth inhibition and transcriptional induction in epithelial cells. *Proc Natl Acad Sci USA* 1997;94:10669-10674

286. Chari RS, Price DT, Sue SR, Meyers WC, Jirtle RL: Down-regulation of transforming growth factor β receptor type I, II, and III during liver regeneration. *Am J Surg* 1995;169:126-131

287. Centrella M, Ji C, Casinghino S, McCarthy TL: Rapid flux in transforming growth factor-β receptors on bone cells. *J Biol Chem* 1996;271:18616-18622

288. Takeuchi Y, Nakayama K, Matsumoto T: Differentiation and cell surface expression of transforming growth factor-β receptors are regulated by interaction with matrix collagen in murine osteoblastic cells. *J Biol Chem* 1996;271:3938-3944

IMAGE EVALUATION
TEST TARGET (QA-3)

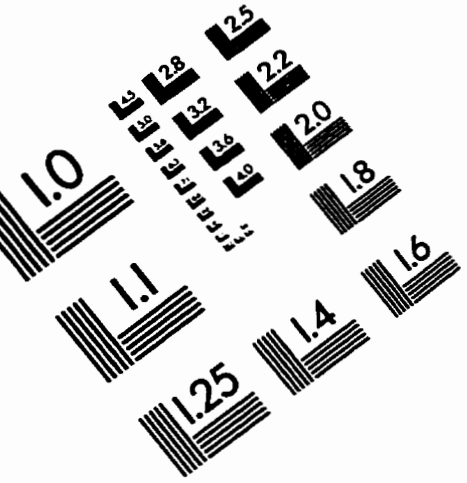

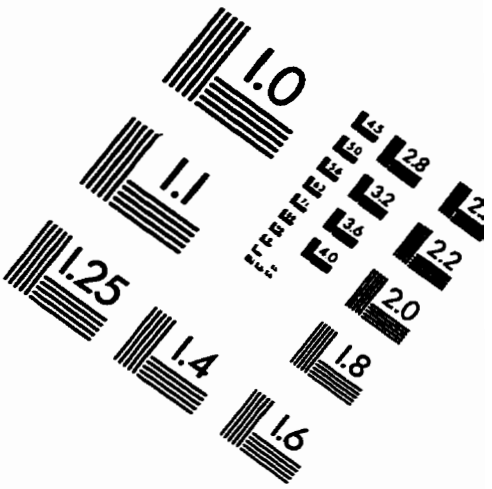

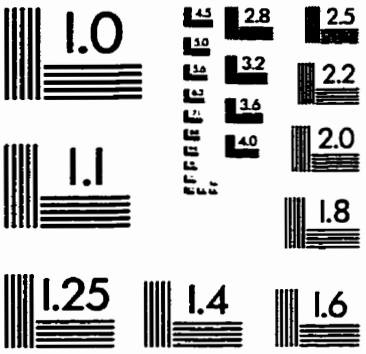

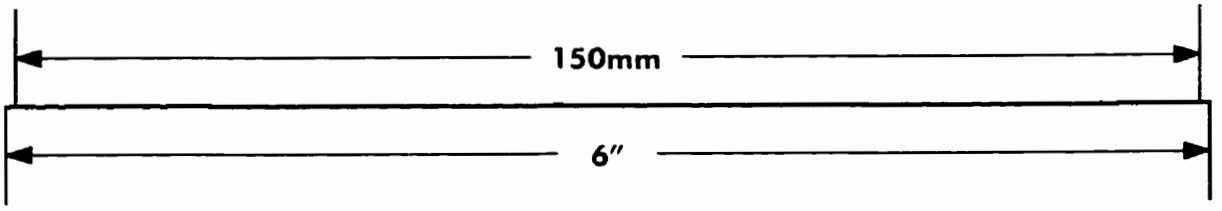

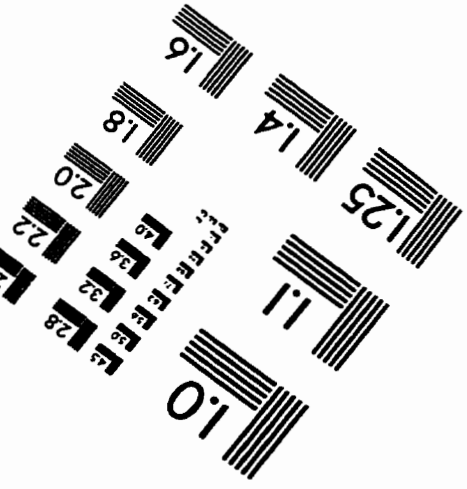

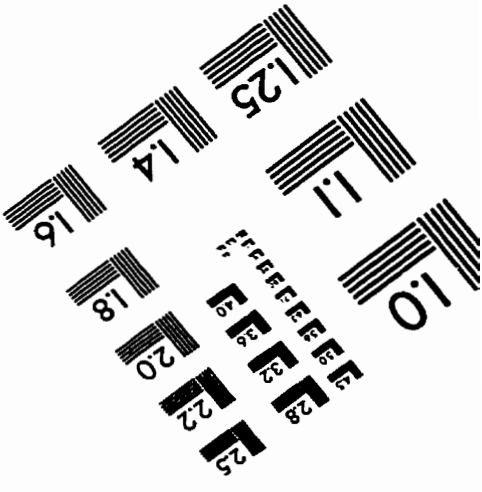

APPLIED IMAGE, Inc
1653 East Main Street
Rochester, NY 14609 USA
Phone: 716/482-0300
Fax: 716/288-5989

© 1993, Applied Image, Inc., All Rights Reserved